UiT
THE ARCTIC
UNIVERSITY
OF NORWAY

Faculty of Science and Technology
Department of Mathematics and Statistics

Modelling high intensity laser pulse propagation in air using the modified Korteweg-de Vries equation

Bjarne Rørnes

MAT-3941 Master thesis in Applied Mathematics, May 2018

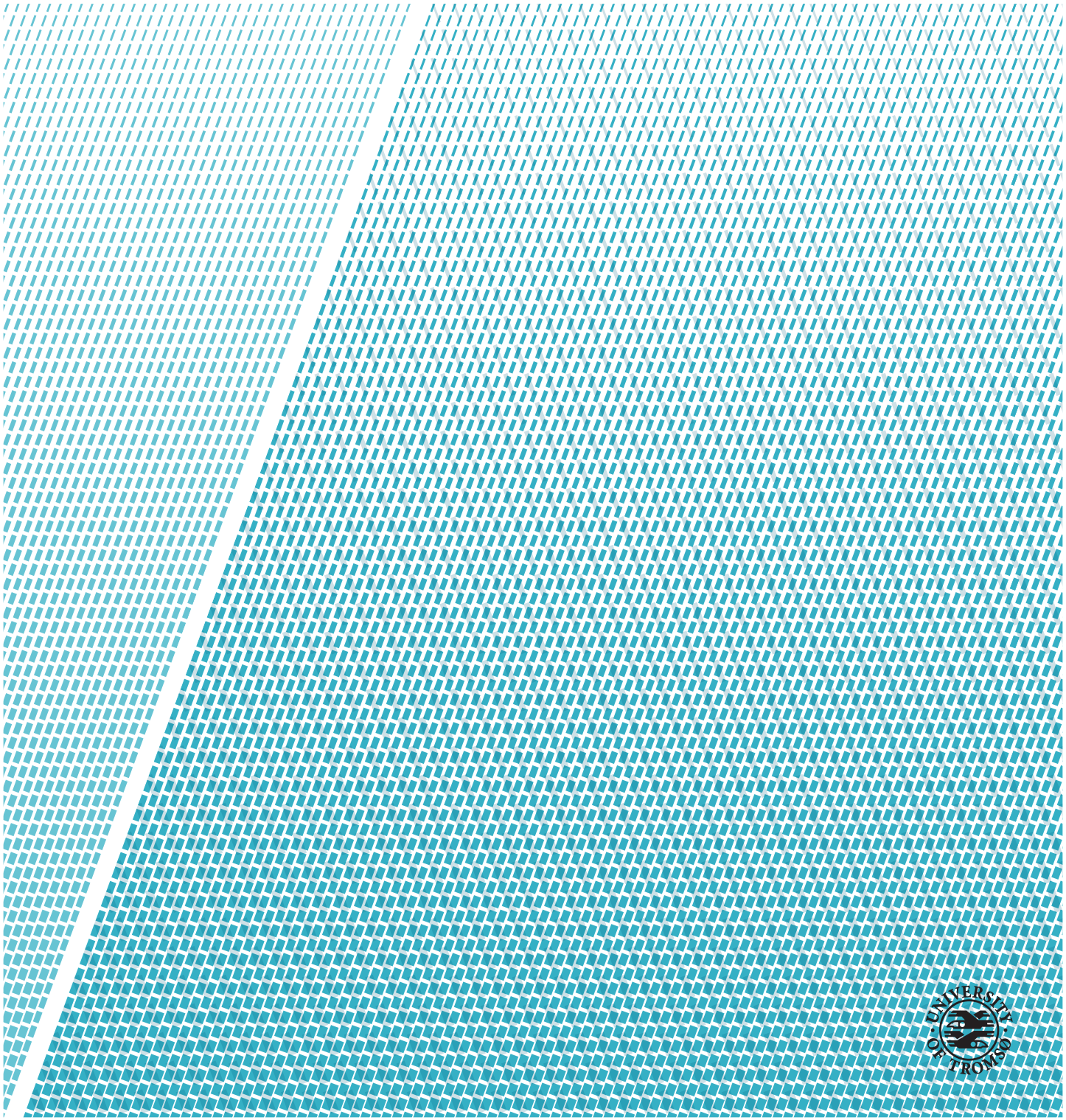

Til Malin og Elias

Abstract

Ultrafast laser pulse experiments and applications are entering a phase that challenges the validity of mathematical models utilised to model longer pulses in nonlinear optics. This thesis aims to propose a possible mathematical model for high intensity laser pulse propagation in air through a multiple scales expansion of Maxwell's equations and discuss a method on how to solve the corresponding differential equation, known as the modified Korteweg-de Vries equation

$$u_t + 6u^2 u_x - \epsilon^2 u_{xxx} = 0$$

where $\epsilon \ll 1$, corresponding to the small dispersion regime. This equation is solvable using a technique named the scattering transform and due to the smallness of the parameter ϵ, the equation can be solved asymptotically and thus simplifying the solution process. The method is based on using the asymptotic WKB approximation for the forward scattering problem and reformulating the inverse scattering as a Riemann-Hilbert problem.

Both analytical steps and numerical procedures needed to use the method is discussed and implemented. An example calculation using a particular initial condition is performed and some challenges using the method for more general initial conditions are discussed.

Acknowledgements

First I would like to thank my supervisor professor Per Jakobsen for all his support and help. All our discussions and conversations, both relevant and irrelevant for this thesis, have been interesting and inspiring to me. Without you and the interesting topic you found this thesis would not have happened. Also thanks to Helge Johansen who has been of great help in all formal and practical matters during my time at the Department of Mathematics and Statistics.

Thanks to all that have contributed during the work on this thesis. Fredrikke and Erlend for keeping me supplied with good food, drink and company. Linda for offering to prof read my English, unfortunately I did not fini. To Morgan for carrying my kayak back while I had to go finish writing this thesis, you were probably a bit annoyed.

Last but not least thanks to my friends and family for support during my studies, perhaps wondering what exactly I've been doing - now you can read for yourself.

Contents

List of Figures

1 Introduction

Ultrafast laser pulse experiments and applications are entering a phase that challenges the validity of physical models utilized for longer pulses in nonlinear optics. Due to technological advances precise control of high intensity ultrashort pulses has become possible and this high energy regime is termed extreme nonlinear optics. The high energies and short timescales means that the physical assumptions made when deriving the commonly used models for laser pulse propagation are no longer valid [18]. The nonlinear Schrödinger(NLS) equation has been the standard equation used to model phenomena in the field, but it proved unable to predict experimental results when pushed to the more extreme regimes. In this thesis we will first propose the modified Korteweg-de Vries(mKdV) equation as a possible model for high intensity laser pulse propagation for wavelengths in the mid infrared domain.

$$u_t + 6u^2u_x - \epsilon^2 u_{xxx} = 0 \tag{1.1}$$

Further, through the Miura transformation [21] the solutions to the mKdV equation can be found by solving the standard Korteweg-de Vries(KdV) equation

$$u_t - 6uu_x + \epsilon^2 u_{xxx} = 0 \tag{1.2}$$

While both the mKdV and the KdV equations are solvable, studying the KdV equation is simpler than the mKdV and after we propose the mKdV equation as a mathematical model, we will focus on solving the KdV equation. One of the earliest studies where the KdV equation was mentioned was through the work

of Dutch scientists Diederik Korteweg and Gustav de Vries in their 1895 article concerning water waves in a rectangular channel [19]. Since it have been shown to be a general evolution equation for a number of physical phenomena with both dispersive and nonlinar behaviour [1]. Further progress was made by the discovery of the soliton solution to the equation by Zabusky and Kruskal [28] in 1965. Two years after the discovery of the soliton a solution to the KdV as an initial value problem method was discovered by Gardner, Greene, Kruskal and Miura in their article 'Method for solving the Korteweg-de Vries equation' [9]. Simply stated, the method involved calculating the reflection coefficient for the initial potential, transforming this into another space using an integral equation and time evolve in the transformed space before it is an inverse transformation is applied. Because of the key idea of calculating a reflection coefficient, the method was called the inverse scattering transform(IST). After this a number of people worked to find if this was a special case only valid for the KdV or if there existed other equations solvable using the IST. From the work of Lax, Zakrov and Shabat it was in 1971 found that the nonlinear Schrödinger equation was also solvable using the same method and later the results of Ablowitz, Kaup, Newell and Segur [2] showed that both the KdV and the NLS belonged to a class of equations solvable by the inverse scattering transform. This class of equations was named integrable or exactly solvable and the solution method was described as a described as a generalization [22] of the Fourier transform for linear equations. Despite the theoretically success in the IST still challenges exists today, explicit calculations of the steps outlined for the inverse scattering are often very hard or impossible and numerical calculations are likewise demanding. Some special cases of initial potentials the KdV has been solved explicit using IST. Specifically some potentials leads to a reflection coefficient equal to zero which again leads to a simplification in the integral transform, allowing for exact calculations. These potentials all corresponds potentials wells $u(x,0) < 0$ while our purposed model leads to solving the KdV with a positive initial potential $u(x,0) > 0$, a bump function with a single maximum. Calculating the needed reflection coefficient for the KdV equation involves solving the time independent Schrödinger equation(TISE) using the initial potential $u(x,0)$ [1], and from quantum mechanics it is a known result [11] [8] that solving the TISE with $u(x,0) < 0$ or $u(x,0) > 0$ leads to quite different physical and mathematical results, the first to bound eigenstates and discrete eigenvalues, while the latter to scattering states and a continuous spectrum. Solving the corresponding integral transform proved difficult both analytically and numerically. After Shabat in 1976 [25] made a remarkable reformation of the IST into a Riemann-Hilbert(RH) problem progress was later made in the so-called dispersionless limit of the the KdV, where the dispersion term $\epsilon^2 u_{xxx}$ is small compared to the nonlinear term $6uu_x$. RH problems are the study of differential equations in the complex planes, and a number of mathematical problems can be studied as RH problems [20]. In the small dispersion regime asymptotic calculations of the reflection coefficient can be

made using the approximate WKB multiple scales method [5]. Through the work of many of the leading researchers on the field, the study of the IST as a RH problem for the dispersionless limit culminated in 1997 though the work of P.Deift, S. Venakides and X. Shou in their article 'New results in small dispersion KdV by an extension of the steepest descent method for Riemann-Hilbert problems [7]. Here the authors purposed a systematic approach to solving the corresponding RH problem by, amongst other, using the WKB approximation and by introducing a phase function as a change of variable. The starting point solving our purposed model will be the procedure from [7], as the model is in the small dispersion regime. An outline for this thesis is as follows

- In Chapter 2 we derive the mKdV equation using the method of multiple scales on Maxwell's equations, and propose this as an model for high intensity laser pulse propagation in air.

- Chapter 3 we present the results by Deift et al [7], proposing an asymptotic solution method for the KdV equation. In addition we perform the some practical calculations necessary to use the procedure and discuss some implications of using the method for our class of potentials.

- Chapter 4 discusses numerical methods needed to use the method described in chapter 3 and numerical results are compared to analytical when possible. A worked example for a specific initial condition is presented.

- Chapter 5 summarises and discusses the results from chapters 2,3 and 4.

- The last chapter is an appendix containing some supplementary calculations and theory.

As an aid in the symbolic calculations in this thesis, for the most part computing integrals, the computer algebra system Mathematica [13] is used.

2

High intensity laser pulse propagation

Using techniques from the field of nonlinear optics we will in this section derive an equation we propose is valid as a model for high intensity laser pulse propagation in the mid infrared region(wavelengths approximately $5\mu m - 50\mu m$ [24]). Mathematical models for laser pulse propagation is usually derived with either Maxwell's equations or the wave equation as a starting point [18] and simplified using physical and mathematical approximations, depending on the physics of the problem trying to model. Our approach will be first, starting with the macroscopic Maxwell's equations and reduce the problem into a scalar partial differential equation using the method of multiple scales. This PDE will turn out to be the modified Korteweg-de Vries equation. Starting with Maxwell's equation, denote the electric $\boldsymbol{E}$ and magnetic field $\boldsymbol{B}$ in space and time. In addition, the fields $\boldsymbol{D}$, $\boldsymbol{H}$ are the electric and magnetic induction. Maxwell's equation in MKS units are cited from [23]

$$\begin{aligned} \partial_t \boldsymbol{B} + \boldsymbol{\nabla} \times \boldsymbol{E} &= 0 \\ \partial_t \boldsymbol{D} - \boldsymbol{\nabla} \times \boldsymbol{H} &= -\boldsymbol{j} \\ \nabla \cdot \boldsymbol{D} &= \rho \\ \nabla \cdot \boldsymbol{B} &= 0 \end{aligned} \tag{2.1}$$

where ρ and $\boldsymbol{j}$ are the electric charge and current densities. Our first simplification is to assume that any free charges or currents have an negligible effect

on the system, setting $\boldsymbol{j} = 0$ and $\rho = 0$

$$\partial_t \boldsymbol{B} + \boldsymbol{\nabla} \times \boldsymbol{E} = 0 \tag{2.2}$$
$$\partial_t \boldsymbol{D} - \boldsymbol{\nabla} \times \boldsymbol{H} = 0 \tag{2.3}$$
$$\nabla \cdot \boldsymbol{D} = 0 \tag{2.4}$$
$$\nabla \cdot \boldsymbol{B} = 0 \tag{2.5}$$

the fields $\boldsymbol{H}$ and $\boldsymbol{D}$ can be written in terms of the magnetic and electric field by the relations

$$\eta \boldsymbol{H} = \boldsymbol{B} \tag{2.6}$$
$$\boldsymbol{D} = \epsilon_0 \boldsymbol{E} + \boldsymbol{P} \tag{2.7}$$

where ϵ_0 is the standard vacuum permittivity and η is the vacuum permeability. From [23] we have both that in the optical mid-infrared frequency η can be set as a constant equal $\epsilon_0^{-1} c^2$, and the polarization term $\boldsymbol{P}$ in (2.7) can be divided into a linear part $\boldsymbol{P}_L$ and a non-linear part $\boldsymbol{P}_{NL}$ and can in this regime be approximated as

$$\boldsymbol{P}_L = \epsilon_0 \int_{-\infty}^{t} dt' \chi(t - t') \boldsymbol{E}(\boldsymbol{x}, t) \tag{2.8}$$
$$\boldsymbol{P}_{NL} = \epsilon_0 \eta \boldsymbol{E} \cdot \boldsymbol{E}^2 \tag{2.9}$$

Where χ is the electric susceptibility. Observe that the integral (2.8) is integrated from all previous times before t, meaning that this term depends on what has happened before. In optics this is called temporal dispersion and causes difficulties in solving the system (2.2) - (2.5) as a standard initial value problem. The approach we will take to get around this is to derive approximations to Maxwell's equations using the method of multiple scales. Taking the Fourier transform of (2.8)

$$\begin{aligned}
\boldsymbol{P}_L &= \epsilon_0 \int_{-\infty}^{t} dt' \chi(t - t') \boldsymbol{E}(\boldsymbol{x}, t) \\
&= \epsilon_0 \int_{-\infty}^{\infty} d\omega \widehat{\chi}(\omega) \widehat{\boldsymbol{E}}(\boldsymbol{x}, \omega) \exp(-i\omega t) \\
&= \epsilon_0 \int_{-\infty}^{\infty} d\omega \left[\sum_{n=0}^{\infty} \frac{\widehat{\chi}^n(0)}{n!} \omega^n \right] \widehat{\boldsymbol{E}}(\boldsymbol{x}, \omega) \exp(-i\omega t) \\
&= \epsilon_0 \sum_{n=0}^{\infty} \frac{\widehat{\chi}^n(0)}{n!} \left[\int_{-\infty}^{\infty} d\omega \omega^n \widehat{\boldsymbol{E}}(\boldsymbol{x}, \omega) \exp(-i\omega t) \right] \\
&= \epsilon_0 \sum_{n=0}^{\infty} \frac{\widehat{\chi}^n(0)}{n!} \left[\int_{-\infty}^{\infty} d\omega (i\partial_t)^n \widehat{\boldsymbol{E}}(\boldsymbol{x}, \omega) \exp(-i\omega t) \right] \\
&= \epsilon_0 \widehat{\chi}(i\partial_t) \boldsymbol{E}(\boldsymbol{x}, t)
\end{aligned} \tag{2.10}$$

The non-linear polarization term is generated by what is called the Kerr effect and can be approximated by the term (2.9) [18], simply stated a model for a change in the refractive index when an electric field is applied to a dielectric medium, in this case air, and standard for modelling in the field of non-linear optics. Inserting (2.6), (2.7), (2.9) and (2.10) into the system (2.2)-(2.5)

$$\partial_t \boldsymbol{B} + \boldsymbol{\nabla} \times \boldsymbol{E} = 0 \tag{2.11}$$
$$\partial_t \boldsymbol{E} - c^2 \boldsymbol{\nabla} \times \boldsymbol{B} = -\epsilon^2 \partial_t \widehat{\chi}(i\partial_t)\boldsymbol{E} - \epsilon^2 \eta \partial_t \boldsymbol{E}^2 \boldsymbol{E} \tag{2.12}$$
$$\nabla \cdot \boldsymbol{E} = -\epsilon^2 \widehat{\chi}(i\partial_t)\nabla \cdot \boldsymbol{E} - \epsilon^2 \eta \nabla \cdot (\boldsymbol{E}^2 \boldsymbol{E}) \tag{2.13}$$
$$\nabla \cdot \boldsymbol{B} = 0 \tag{2.14}$$

where we have inserted the parameter ϵ^2 into the LHS of equations (2.12) and (2.13). This parameter is called a formal perturbation parameter and in accordance with the multiple scales method described in [23][14]. Next we will assume that the optical pulse we are trying to model propagates in a given direction, we set it along the z-axis. Thus in the expansion the (x, y) coordinates will be treated different than the z coordinate. Inspired by this introduce the moving frame of reference

$$\theta = z - ct$$
$$\tau = z$$

which gives differentials

$$\partial_z = \partial_\theta + \partial_\tau$$
$$\partial_t = -c\partial_\theta \tag{2.15}$$

If we insert these into (2.11)-(2.14) and write each equation into its component form in x, y, z we get three equations from each of the first two and one equation for each of the last

$$-c\partial_\theta B_x - \partial_\theta E_y = -\partial_y E_z + \partial_\tau E_y \tag{2.16}$$
$$-c\partial_\theta B_y + \partial_\theta E_x = \partial_x E_z - \partial_\tau E_x$$
$$-c\partial_\theta B_z = -\partial_x E_y + \partial_y E_x$$
$$-c\partial_\theta E_x + c^2 \partial_\theta B_y = -c^2 \partial_\tau B_y + c^2 \partial_y B_z + \epsilon^2 c \partial_\theta \widehat{\chi}(-ic\partial_\theta) E_x + \epsilon^2 c\eta \partial_\theta (\boldsymbol{E}^2 E_x)$$
$$-c\partial_\theta E_y + c^2 \partial_\theta B_x = c^2 \partial_\tau B_x - c^2 \partial_y B_x + \epsilon^2 c \partial_\theta \widehat{\chi}(-ic\partial_\theta) E_y + \epsilon^2 c\eta \partial_\theta (\boldsymbol{E}^2 E_y)$$
$$-c\partial_\theta E_z = c^2 \partial_x B_y - c^2 \partial_y B_x + \epsilon^2 c \partial_\theta \widehat{\chi}(-ic\partial_\theta) E_z + \epsilon^2 c\eta \partial_\theta (\boldsymbol{E}^2 E_z)$$
$$\partial_\theta B_z = -\partial_\tau B_z - \partial_x B_x - \partial_y B_y$$
$$\partial_\theta E_z = -\partial_\tau E_z - \partial - \partial_\tau E_z - \partial_x E_x - \partial_y E_y - \epsilon^2 \widehat{\chi}(-ic\partial_\theta) \left[\partial_x E_x + \partial_y E_y + \partial_\theta E_z \partial_\tau E_z\right]$$
$$- \epsilon^2 \eta \left[\partial_x (\boldsymbol{E}^2 E_x) + \partial_y (\boldsymbol{E}^2 E_y) + \partial_\theta (\boldsymbol{E}^2 E_z) + \partial_\tau (\boldsymbol{E}^2 E_z)\right]$$

Now we proceed to use the method of multiple scales on system (2.16) by introducing the following expansions

$$\begin{aligned}
\boldsymbol{E}(\theta, \boldsymbol{x}_1, \tau) &= \boldsymbol{e}(\theta, \boldsymbol{x}_1, \tau_1, \tau_2..)|_{\boldsymbol{x}_1=\epsilon\boldsymbol{x}, \tau_j=\epsilon^j\tau} \\
\boldsymbol{B}(\theta, \boldsymbol{x}_1, \tau) &= \boldsymbol{b}(\theta, \boldsymbol{x}_1, \tau_1, \tau_2..)|_{\boldsymbol{x}_1=\epsilon\boldsymbol{x}, \tau_j=\epsilon^j\tau} \\
\boldsymbol{e} &= \boldsymbol{e}_0 + \epsilon\boldsymbol{e}_1 + \epsilon^2\boldsymbol{e}_2 + .. \\
\boldsymbol{b} &= \boldsymbol{b}_0 + \epsilon\boldsymbol{b}_1 + \epsilon^2\boldsymbol{b}_2 + .. \\
\partial_{\boldsymbol{x}} &= \epsilon\partial_{\boldsymbol{x}_1} \\
\partial_\tau &= \epsilon\partial_{\tau_1} + \epsilon^2\partial\tau_2 + ..
\end{aligned} \tag{2.17}$$

where $\boldsymbol{x} = (x, y)$ and $\boldsymbol{x}_1 = (x_1, y_1)$ are the physical and multiple scale transverse coordinates. Using this schema means that we are looking for solutions that along the z-axis is a paraxial wave with an unconstrained shape but we assume that it is slowly varying. This is a physical assumption based on knowledge from other pulse propagating systems. We insert (2.17) into (2.16) and expand up to order two in ϵ. Doing this results in quite a bit of algebra, so we write the first equation out in detail and for the rest we just give the result.

$$\begin{aligned}
&- c\partial_\theta B_x - \partial_\theta E_y = -\partial_y E_z + \partial_\tau E_y \\
LHS: &- c\partial_\theta(b_{x0} + \epsilon b_{x1} + \epsilon^2 b_{x2}) - \partial_\theta(e_{y0} + \epsilon e_{y1} + \epsilon^2 e_{y2}) \\
RHS: &- \epsilon\partial_{y_1}(e_{z0} + \epsilon e_{z1}) + (\epsilon\partial_{\tau_1} + \epsilon^2\partial_{\tau_2})(e_{y0} + \epsilon e_{y1}) \\
\epsilon^0: & \\
&- c\partial_\theta b_{x0} - \partial_\theta e_{y0} = 0 \\
\epsilon^1: & \\
&- c\partial_\theta b_{x1} - \partial_\theta e_{y2} = -\partial_y e_{z0} + \partial_{\tau_1} e_{y0} \\
\epsilon^2: & \\
&- c\partial_\theta b_{x2} - \partial_\theta e_{y2} = -\partial_y e_{z1} + \partial_{\tau_1} e_{y1} + \partial_{\tau_2} e_{y0}
\end{aligned} \tag{2.18}$$

these are the equations up to order two for the first equation. Doing the same for the rest gives us the following three systems for order zero, one and two. For order ϵ^0

$$\begin{aligned}
c\partial_\theta b_{x0} + \partial_\theta e_{y0} &= 0 \\
-c\partial_\theta b_{x0} + \partial_\theta e_{y0} &= 0 \\
c\partial_\theta b_{z0} &= 0 \\
-c\partial_\theta b_{y0} + \partial_\theta e_{x0} &= 0 \\
c\partial_\theta b_{x0} + \partial_\theta e_{y0} &= 0 \\
\partial_\theta e_{z0} &= 0 \\
\partial_\theta b_{z0} &= 0 \\
\partial_\theta e_{z0} &= 0
\end{aligned} \tag{2.19}$$

At order ϵ^1

$$\begin{aligned}
c\partial_\theta b_{x1} + \partial_\theta e_{y1} &= \partial_{y1} e_{z0} - \partial_{\tau_1} e_{y0} \\
-c\partial_\theta b_{x1} + \partial_\theta e_{y1} &= \partial_{x1} e_{z0} - \partial_{\tau_1} e_{x0} \\
c\partial_\theta b_{z1} &= \partial_{x1} e_{y0} - \partial_{y1} e_{x0} \\
-c\partial_\theta b_{y1} + \partial_\theta e_{x1} &= c\partial_{\tau_1} b_{y0} - c\partial_{y1} b_{z0} \\
c\partial_\theta b_{x1} + \partial_\theta e_{y1} &= -c\partial_{\tau_1} b_{x0} + c\partial_{x1} b_{z0} \\
\partial_\theta e_{z1} &= -c\partial_{x1} b_{y0} + c\partial_{y1} b_{x0} \\
\partial_\theta b_{z1} &= -\partial_{\tau_1} b_{z0} - \partial_{x1} b_{x0} - b_{y0} \\
\partial_\theta e_{z1} &= -\partial_{\tau_1} e_{z0} - \partial_{x1} e_{x0} - \partial_{y1} e_{y0}
\end{aligned} \tag{2.20}$$

and order ϵ^2

$$\begin{aligned}
c\partial_\theta b_{x2} + \partial_\theta e_{y2} &= -\partial_y e_{z1} + \partial_{\tau_1} e_{y1} + \partial_{\tau_2} e_{y0} \\
-c\partial_\theta b_{x2} + \partial_\theta e_{y2} &= \partial_{x1} e_{z1} - \partial_{\tau_1} e_{x1} - \partial_{\tau_2} e_{x0} \\
c\partial_\theta b_{z2} &= \partial_{x1} e_{y1} - \partial_{y1} e_{x1} \\
-c\partial_\theta b_{y2} + \partial_\theta e_{x2} &= c\partial_{\tau_1} b_{y1} + c\partial_{\tau_2} b_{y0} - c\partial_{y1} b_{z1} \\
&\quad - \partial_\theta \widehat{\chi}(-ic\partial_\theta) e_{y0} - \eta\partial_\theta(\boldsymbol{e}_0^2 e_{x0}) \\
c\partial_\theta b_{x2} + \partial_\theta e_{y2} &= -c\partial_{\tau_1} b_{x1} - c\partial_{\tau_2} b_{x0} + c\partial_{x1} b_{z1} \\
&\quad - \partial_\theta \widehat{\chi}(-ic\partial_\theta) e_{y0} - \eta\partial_\theta(\boldsymbol{e}_0^2 e_{y0}) \\
\partial_\theta e_{z2} &= -c\partial_{x1} b_{y1} + c\partial_{y1} b_{x1} \\
&\quad - \partial_\theta \widehat{\chi}(-ic\partial_\theta) e_{z0} - \eta\partial_\theta(\boldsymbol{e}_0^2 e_{z0}) \\
\partial_\theta b_{z2} &= -c\partial_{\tau_1} b_{z1} - c\partial_{\tau_2} b_{z0} - c\partial_{x1} b_{x1} - c\partial_{y1} b_{y1} \\
\partial_\theta e_{z2} &= -\partial_{\tau_1} e_{z1} - \partial_{\tau_2} e_{z0} - \partial_{x1} e_{x1} - \partial_{y1} e_{y1} \\
&\quad - \widehat{\chi}(-ic\partial_\theta) e_{z0} - \eta\partial_\theta(\boldsymbol{e}_0^2 e_{z0})
\end{aligned} \tag{2.21}$$

We observe that the left side of each order have the same structure and that the right hand side contains unknowns that we can find using the solutions from the order below. We also see that the system are singular, there are four pairs of equations at each order which have the same left side but different right hand side. This means in order to use this we must find conditions for when we can solve these systems. The conditions we find will give us equations for the leading order functions e_{x0} and e_{y0}. The left hand side of these four solvability conditions are

$$\begin{aligned}
c\partial_\theta b_{xn} + \partial_\theta e_{yn} \\
-c\partial_\theta b_{yn} + \partial_\theta e_{xn} \\
c\partial_\theta b_{zn} \\
\partial_\theta e_{zn}
\end{aligned} \tag{2.22}$$

When we proceed to solve the perturbation system we must ensure that the right hand sides are consistent with these in order for us to find a solution. We start by solving the first system (2.19), the general solution is

$$\begin{aligned} cb_{x0} &= -e_{y0}(\theta, \boldsymbol{x}_1, \tau_1, \tau_2..) + \alpha(\boldsymbol{x}_1, \tau_1, \tau_2..) \\ cb_{x0} &= e_{x0}(\theta, \boldsymbol{x}_1, \tau_1, \tau_2..) + \beta(\boldsymbol{x}_1, \tau_1, \tau_2..) \\ e_{z0} &= \iota(\boldsymbol{x}_1, \tau_1, \tau_2..) \\ b_{z0} &= \kappa(\boldsymbol{x}_1, \tau_1, \tau_2..) \end{aligned} \tag{2.23}$$

if we remember our definition (2.15) we see that the time variable is contained in θ and that only e_{y0} and e_{x0} in the above equations depends on θ, meaning that the four terms α, β, ι and κ are solutions to a static field already present from the beginning. If we assume that there are no pre-existing electric field we can set all these to zero. We then get the solution to the first order equations

$$\begin{aligned} cb_{x0} &= -e_{y0}(\theta, \boldsymbol{x}_1, \tau_1, \tau_2..) \\ cb_{x0} &= e_{x0}(\theta, \boldsymbol{x}_1, \tau_1, \tau_2..) \\ e_{z0} &= 0 \\ b_{z0} &= 0 \end{aligned} \tag{2.24}$$

We proceed by inserting (2.24) into the first order system in ϵ^1 (2.20)

$$\begin{aligned} c\partial_\theta b_{x1} + \partial_\theta e_{y1} &= -\partial_{\tau_1} e_{y0} \\ -c\partial_\theta b_{x1} + \partial_\theta e_{y1} &= -\partial_{\tau_1} e_{x0} \\ c\partial_\theta b_{z1} &= \partial_{x1} e_{y0} - \partial_{y1} e_{x0} \\ -c\partial_\theta b_{y1} + \partial_\theta e_{x1} &= \partial_{\tau_1} e_{x0} \\ c\partial_\theta b_{x1} + \partial_\theta e_{y1} &= \partial_{\tau_1} e_{y0} \\ \partial_\theta e_{z1} &= -\partial_{x1} e_{x0} - \partial_{y1} e_{y0} \\ \partial_\theta b_{z1} &= \partial_{x1} e_{y0} - \partial_{y1} e_{x0} \\ \partial_\theta e_{z1} &= -\partial_{x1} e_{x0} - \partial_{y1} e_{y0} \end{aligned} \tag{2.25}$$

We see that equations 3,6,7 and 8 are consistent, but 1,2,4 and 5 are not. The inconsistent equations gives us

$$\begin{aligned} c\partial_\theta b_{x1} + \partial_\theta e_{y1} &= -\partial_{\tau_1} e_{y0} \\ -c\partial_\theta b_{x1} + \partial_\theta e_{y1} &= -\partial_{\tau_1} e_{x0} \\ -c\partial_\theta b_{y1} + \partial_\theta e_{x1} &= \partial_{\tau_1} e_{x0} \\ c\partial_\theta b_{x1} + \partial_\theta e_{y1} &= \partial_{\tau_1} e_{y0} \end{aligned} \tag{2.26}$$

We could here use the Fredholm Alternative to find when this system is solvable, but we simply observe that we must have

$$\partial_{\tau_1} e_{y0} = \partial_{\tau_1} e_{x0} = 0 \tag{2.27}$$

in order for us to have a solution. Using this we write the system (2.25) as

$$\begin{aligned} c\partial_\theta b_{x1} + \partial_\theta e_{y1} &= 0 \\ c\partial_\theta b_{z1} &= \partial_{x1} e_{y0} - \partial_{y1} e_{x0} \\ -c\partial_\theta b_{y1} + \partial_\theta e_{x1} &= 0 \\ \partial_\theta e_{z1} &= -\partial_{x1} e_{x0} - \partial_{y1} e_{y0} \end{aligned} \tag{2.28}$$

According to [23] and [14] we do not solve for a general solution to the expansions beyond order ϵ^0, but only solve for a special solution to (2.28)

$$\begin{aligned} e_{x1} = e_{y1} = b_{x1} = b_{y1} &= 0 \\ \partial_\theta e_{z1} &= -\partial_{x1} e_{x0} - \partial_{y1} e_{y0} \\ c\partial_\theta b_{z1} &= \partial_{x1} e_{y0} - \partial_{y1} e_{x0} \end{aligned} \tag{2.29}$$

We proceed by inserting (2.24) and (2.29) into the second order system (2.21).

$$\begin{aligned} c\partial_\theta b_{x2} + \partial_\theta e_{y2} &= \partial_{y1} e_{z1} - \partial_{\tau_2} e_{y0} \\ -c\partial_\theta b_{y2} + \partial_\theta e_{x2} &= \partial_{x1} e_{z1} - \partial_{\tau_2} e_{x0} \\ c\partial_\theta b_{z2} &= 0 \\ -c\partial_\theta b_{y2} + \partial_\theta e_{x2} &= \partial_{\tau_2} e_{x0} - c\partial_{y1} b_{z1} \\ &\quad - \partial_\theta \widehat{\chi}(-ic\partial_\theta) e_{x0} - \eta\partial\theta(\boldsymbol{e}_0^2 e_{x0}) \\ c\partial_\theta \partial_{b2} + \partial_\theta e_{y2} &= \partial_{\tau_2} e_{y0} + c\partial_{x1} b_{z1} \\ &\quad - \partial_\theta \widehat{\chi}(-ic\partial_\theta) - \eta\partial_\theta(\boldsymbol{e}_0^2 e_{y0}) \\ \partial_\theta e_{z2} &= 0 \\ c\partial_\theta b_{z2} &= 0 \\ \partial_\theta e_{z2} &= 0 \end{aligned} \tag{2.30}$$

In the above equation there are four pairs of solvability conditions, equations 3 and 7 is identical and automatically satisfied. The same is true for equations 6 and 8. Hence in order for the system to have a solution equations 1 and 5 must be consistent, and equations 2 and 4. If we combine these four equation into two, we get the following equations for the solvability of the system

$$\begin{aligned} 2\partial_{\tau_2} e_{x0} &= \partial_{x_1} e_{z1} + c\partial_{y_1} b_{z1} + \partial_\theta \widehat{\chi}(-ic\partial_\theta) e_{x0} + \eta\partial_\theta(\boldsymbol{e}_0^2 e_{x0}) \\ 2\partial_{\tau_2} e_{y0} &= -\partial_{x_1} e_{z1} + c\partial_{y_1} b_{z1} + \partial_\theta \widehat{\chi}(-ic\partial_\theta) e_{y0} + \eta\partial_\theta(\boldsymbol{e}_0^2 e_{y0}) \end{aligned} \tag{2.31}$$

We are not going further than order two in ϵ so we do not need a special solution to these equations. Now we differentiate these with respect to θ and get

$$\begin{aligned} 2\partial_{\theta\tau_2} e_{x0} &= \partial_{x_1 x_1} e_{x0} + \partial_{y_1 y_1} e_{x1} + \partial_{\theta\theta} \widehat{\chi}(-ic\partial_\theta) e_{x0} + \eta\partial_{\theta\theta}(\boldsymbol{e}_0^2 e_{x0}) \\ 2\partial_{\theta\tau_2} e_{y0} &= \partial_{x_1 x_1} e_{y0} + \partial_{y_1 y_1} e_{y1} + \partial_{\theta\theta} \widehat{\chi}(-ic\partial_\theta) e_{y0} + \eta\partial_{\theta\theta}(\boldsymbol{e}_0^2 e_{y0}) \end{aligned} \tag{2.32}$$

If we now use (2.17) to return to the variables $(\tau, \theta, \boldsymbol{x})$ we get

$$\begin{aligned} 2\partial_{\theta\tau_2} E_{x0} &= \nabla_\perp E_{x0} + \varepsilon^2 \partial_{\theta\theta} \widehat{\chi}(-ic\partial_\theta) E_{x0} + \varepsilon^2 \eta \partial_{\theta\theta}(\boldsymbol{E}_0^2 E_{x0}) \\ 2\partial_{\theta\tau_2} E_{x0} &= \nabla_\perp E_{y0} + \varepsilon^2 \partial_{\theta\theta} \widehat{\chi}(-ic\partial_\theta) E_{y0} + \varepsilon^2 \eta \partial_{\theta\theta}(\boldsymbol{E}_0^2 E_{y0}) \end{aligned} \tag{2.33}$$

If we assume that the physical situation corresponds to linear polarization we can set $E_{x0} = E_{y0}$ and we reduce the system (2.33) to the scalar equation

$$2\partial_{\theta\tau} E = \nabla_\perp E + \partial_{\theta\theta} \widehat{\chi}(-ic\partial_\theta) E + \eta \partial_{\theta\theta} E^3 \tag{2.34}$$

In the domain we assume that the dispersion can be approximated by a quadratic [18]

$$\widehat{\chi}(\xi) \approx a + b\xi^2 \tag{2.35}$$

then we have

$$\partial_{\theta\theta} \widehat{\chi}(\xi) E = a\partial_{\theta\theta} E - bc^2 \partial_{\theta\theta\theta\theta} E \tag{2.36}$$

which leads to the equation

$$2\partial_{\theta\tau} E = \nabla_\perp E + a\partial_{\theta\theta} E - bc^2 \partial_{\theta\theta\theta\theta} E + \eta \partial_{\theta\theta} E^3 \tag{2.37}$$

Up to this point the approximations we have done has been in accordance with standard methods used in nonlinear optics. To proceed we have to forsake this for a moment and make some not so well justified steps. These steps are made based on [15], we could say that we are interested in cases where the following assumptions are valid. Let A be the cross-sectional area of a filament on the propagation axis and define

$$e = \int_A dSE \tag{2.38}$$

Integrating (2.37) over this cross-section

$$2\partial_{\theta\tau} e - a\partial_{\theta\theta} e + c^2 b \partial_{\theta\theta\theta\theta} e - \eta \partial_{\theta\theta} \int_A dSE^3 = \int_{\partial A} dl\boldsymbol{n} \cdot \nabla e \tag{2.39}$$

Now we assume that most of the electric field is on the axis we can approximate the last term on the LHS

$$2\partial_{\theta\tau} e - a\partial_{\theta\theta} e + c^2 b \partial_{\theta\theta\theta\theta} e - \eta f A^2 \partial_{\theta\theta} e^3 = \int_{\partial A} dl\boldsymbol{n} \cdot \nabla e \tag{2.40}$$

where f is a number and represents the error in making this approximation. The next step is to assume that the RHS is approximately zero. This is not a well justified step either, but we assume that the flux average and cancel, making RHS approximately zero. Then we get the homogeneous equation

$$2\partial_{\theta\tau} e - a\partial_{\theta\theta} e + c^2 b \partial_{\theta\theta\theta\theta} e - \eta f A^2 \partial_{\theta\theta} e^3 = 0 \tag{2.41}$$

Since all terms contain a ∂_θ term we integrate the above equation

$$\begin{aligned} 2\partial_\tau e - a\partial_\theta e + c^2 b\partial_{\theta\theta\theta} e - \eta f A^2 \partial_\theta e^3 &= D \\ 2\partial_\tau e - a\partial_\theta e + c^2 b\partial_{\theta\theta\theta} e - \eta f A^2 \partial_\theta e^3 &= 0 \end{aligned} \tag{2.42}$$

The D is a constant, plane wave solution that we will disregard and set equal to zero. If we make the change of variable $\theta \longrightarrow \theta + d\tau$ we can remove the travelling linear term $a\partial_\theta$

$$\partial_\tau e - 3\beta e^2 \partial_\theta e + \alpha \partial_{\theta\theta\theta} e = 0 \tag{2.43}$$

where $\alpha = \frac{1}{2} bc^2$ and $\beta = \frac{1}{2}\eta f A^2$. By scaling and a change in notation we write it into a form more suitable to work with

$$m_t - 6m^2 m_x + \epsilon^2 m_{xxx} = 0 \tag{2.44}$$

The above equation is the modified Korteweg-de Vries equation. The standard KdV equation is

$$u_t - 6uu_x + \epsilon^2 u_{xxx} = 0 \tag{2.45}$$

Now introduce the transformation $u = m^2 + \epsilon m_x$ and insert into (2.45)

$$\begin{aligned} u_t - 6uu_x + \epsilon^2 u_{xxx} &= (2mm_t + \epsilon m_{xt}) \\ &\quad - 6(2m^3 m_x + \epsilon m^2 m_{xx} + 2\epsilon m m_{xx}^2 + \epsilon^2 m_x m_{xx}) \qquad (2.46) \\ &\quad + \epsilon^2 (6m_x m_{xx} + 2mm_{xxx} + \epsilon m_{xxxx}) \\ &= \epsilon(m_{xt} - 6m^2 m_{xx} - 12m m_x^2 + \epsilon^2 m_{xxxx}) \\ &\quad + (2mm_t - 12m^3 m_x + 2\epsilon^2 m m_{xxx}) \\ &= (2m + \epsilon\partial_x)(m_t - 6m^2 m_x + \epsilon^2 m_{xxx}) \qquad (2.47) \end{aligned}$$

The transformation used in the above equation is the Miura transformation [21] and connects the KdV equation (2.45) to the mKdV equation (2.44). Solutions to the mKdV can thus be found by solving the KdV equation and then using the Miura transformation [1]. Equation (2.45) is simpler to work with than (2.44) and solving this equation will be the focus for the rest of this thesis. The KdV equation has both a nonlinear term $6uu_x$ and a dispersive term $\epsilon^2 u_{xxx}$, we want to solve the equation using a method that assumes that $\epsilon \longrightarrow 0$. This can be justified since the dispersion is small in air, thus $\epsilon \ll 1$, allowing us to solve the equation asymptotically. We will solve (2.45) as an initial value problem so finally we impose a generic start condition $u(x, 0) = u_0(x)$ giving the final form of the problem

$$\begin{aligned} u_t - 6uu_x + \epsilon^2 u_{xxx} &= 0 \\ u(x, 0) &= u_0(x) \end{aligned} \tag{2.48}$$

The shape of the initial condition $u_0(x)$, also called the potential, is determined by what physical situation one wants to model. For example, a potential $u_0(x) < 0$ would represent a situation where light is 'trapped' and there are no reflection or transmission. A potential $u_0(x) > 0$ represents to the opposite, all light is either transmitted or reflected. We will consider the latter, an initial potential of bump shape $u_0 > 0$, this corresponds to the case discussed in the solution method we will follow.

Finally, it should be noted that solving (2.48) could give us qualitative insight into the physics, but does not in its current form directly represent the same electric field as a solution obtained from Maxwell's equation. This concludes our derivation of the model, the rest of this thesis will be focused on solving (2.48) in the limit $\epsilon \to 0$.

3

Korteweg-de Vries equation and the Riemann-Hilbert approach to inverse scattering transform

In chapter 2 we proposed, using the method of multiple scales, the Korteweg-de Vries equation (2.45) as a model for high intensity short optical pulses. In this and the remaining chapters of this thesis we are interested in solving the KdV equation as an initial value problem. As mentioned in the introduction this equation belongs to a class of partial differential equations solvable using a technique called the inverse scattering transform(IST). We will consider

Figure 3.1: Illustration of the Inverse Scattering Transform(IST)

an initial condition $u_0(x)$ that have the properties described in definition (1). The requirement that u_0 must decay to zero sufficiently fast is a necessary condition to be able to use the IST [1], therefore no addition restriction specific for our purposes. The remaining requirements on u_0 are present to simplify calculations, but one could for example consider an u_0 with a whole period, opposed to the half period potential we will work with. Informally the inverse scattering transform can by described in the following way: if you know what you send out and can register what comes back, then it should be possible to reconstruct what happened far away. Mathematically the idea is to first transform the initial potential by direct scattering, employ time evolution in the transformed space and then transform back into the time and space domain by inverse scattering, see figure (3.1). In this sense the structure of IST is similar to that of the Fourier transform for solving linear differential equations and because of this the method has been seen as a non-linear analogue to the Fourier transform. Our problem can be summarised in the equation (3.1), where u_0 satisfies definition (1).

$$\begin{aligned} u_t - 6uu_x + \epsilon^2 u_{xxx} &= 0 \\ u(x,0) &= u_0(x) \end{aligned} \tag{3.1}$$

In this chapter we will use the reformulation of the IST problem made by Shabat [25], where the inverse transform is solved as a Riemann-Hilbert problem instead of solving integral equations as done in its original form. See section B for a brief introduction to RH problems. A further development was made by Deift, Venakides and Zhou [7], where by using the WKB approximation to calculate the forward scattering problem, an explicit solution to the RH problem could be found, thus giving a method to find the solution to the KdV equation. By using the WKB approximation we are in the regime where $\epsilon \to 0$, known as the small dispersion limit of the KdV, where the nonlinear $6uu_x$ term dominates. In this chapter we will present the steps proposed by Deift et al. in [7] to solve the KdV and make some calculations needed to use the procedure in practice. However, we will not go into all theoretical details as some of these are complicated and better treated in a more purely theoretical setting, see for example [27]. Our first objective is to solve the forward scattering problem for our potential, corresponding to computing the WKB approximation for the Schrödinger equation with two turning points. After we can proceed to describe the steps in the solution process, and the last two sections in this chapter examines some practical consequences using the procedure.

Definition 1. *The initial potential $u_0(x)$ is required to satisfy the following requirements(see figure (3.2))*

- *Even function with single maximum point, located at $x = 0$ and with height normalized to unity*
- *Continuous and strictly monotonic decreasing from maximum point*
- *Asymptotic behaviour $u_0(x) \sim 1 - a|x|^n$ in limit $x \longrightarrow 0^{\pm}$, where n is either 1(linear) or 2(parabolic) and $a > 0$*
- *Either compact support $[-s, s]$ with $s > 0$ or non-compact support with asymptotic behaviour $u_0(x) \sim x^{-p}, |x| \longrightarrow \infty$, where $p \geq 2$*
- *$u_0(\pm s) = 0$(compact support) or $\lim_{x \to \pm\infty} u_0(x) = 0$(non-compact support)*

The potential $u_0(x)$ are the initial condition for the KdV equation, but we are interested using the mKdV equation as a model. Thus, the initial potential m_0 we use for the mKdV must result in that the requirements for u_0 in definition (1) is satisfied when using the transformation

$$u_0 = m_0^2 + \epsilon m_{0x} \tag{3.2}$$

If the operation m_{0x} does not result in any pathological behaviour we can approximate the transformations as follows

$$u_0 \approx m_0^2 \tag{3.3}$$

as $\epsilon \longrightarrow 0$. A possible behaviour that invalidates this would be if the derivative operator results in multiplying with a big numerical value e.g. $m_0 = \exp(-\gamma x^2)$ where γ is very large. We see now if we use the same requirements for m_0 where the potentials are positive, even, decaying and so fourth, the transformation m^2 preserves the properties we need, thus results in a u_0 that also satisfies definition (1).

3.1 WKB-approximation for a potential with two turning points

To use the procedure purposed in [7] we need to calculate the solution to the following differential equation

$$\epsilon^2 \varphi''(x) + (\lambda^2 - u_0(x))\varphi(x) = 0 \tag{3.4}$$

$$\varphi \sim T(\lambda) \exp(-\frac{i\lambda x}{\epsilon}) \qquad x \longrightarrow -\infty \tag{3.5}$$

$$\varphi \sim R(\lambda) \exp(\frac{i\lambda x}{\epsilon}) + \exp(-\frac{i\lambda x}{\epsilon}) \qquad x \longrightarrow \infty \tag{3.6}$$

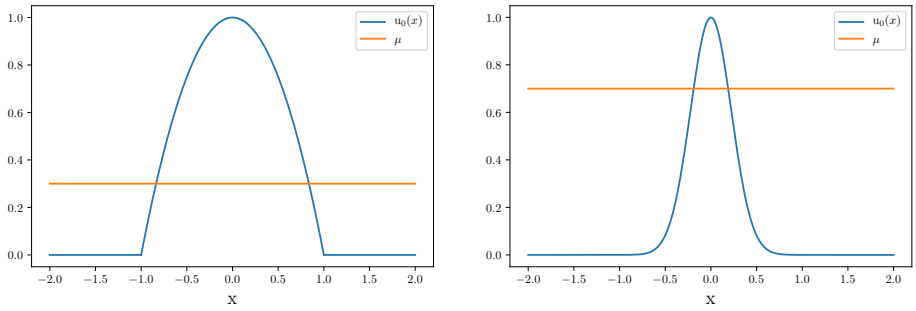

(a) Compact Support **(b)** Non Compact Support

Figure 3.2: General shapes of potentials

This is part of the forward scattering problem and our aim is to solve for the quantities $R(\lambda)$ and $T(\lambda)$ which are the reflection and transmission coefficient for the Schrödinger equation (3.4). An asymptotic solution to the Schrödinger equation that is valid when $\epsilon \to 0$ can be found using the WKB approximation [5], we will use this for the two turning point problem. We make the following definitions

$$\begin{aligned} \theta &= \frac{i\lambda x}{\epsilon} \\ \tau &= \lambda^2 - u_0 \\ x_+ &= |u_0^{-1}(\lambda^2)| \\ x_- &= -x_+ \end{aligned} \tag{3.7}$$

From elementary theory on differential equations we have that the solution to (3.4) depend on the sign of $\lambda^2 - u_0(x)$ and by examining figure (3.2) it is clear that (3.4) have two turning points in $0 < \lambda^2 < 1$ and we have three different regions for the WKB approximation

$$x < x_- :$$
$$\varphi \sim \frac{A_-}{\tau^{1/4}} \exp\left(\frac{i}{\epsilon}\int_{x_-}^{x} d\eta\sqrt{\tau}\right) + \frac{B_-}{\tau^{1/4}} \exp\left(-\frac{i}{\epsilon}\int_{x_-}^{x} d\eta\sqrt{\tau}\right) \tag{3.8}$$

$$x_- < x < x_+$$
$$\varphi \sim \frac{A_0}{(-\tau)^{1/4}} \exp\left(\frac{1}{\epsilon}\int_{x_-}^{x} d\eta\sqrt{-\tau}\right) + \frac{B_0}{(-\tau)^{1/4}} \exp\left(-\frac{1}{\epsilon}\int_{x_-}^{x} d\eta\sqrt{-\tau}\right) \tag{3.9}$$

$$x_+ < x :$$
$$\varphi \sim \frac{A_+}{\tau^{1/4}} \exp\left(\frac{i}{\epsilon}\int_{x_+}^{x} d\eta\sqrt{\tau}\right) + \frac{B_+}{\tau^{1/4}} \exp\left(-\frac{i}{\epsilon}\int_{x_+}^{x} d\eta\sqrt{\tau}\right) \tag{3.10}$$

We have

$$\int_{x_-}^{x} d\eta\sqrt{\tau} = \int_{x_-}^{x} d\eta \left[\sqrt{\tau} - \lambda + \lambda\right] = \int_{x_-}^{x} d\eta(\sqrt{\tau} - \lambda) + \lambda(x - x_-)$$
$$= \gamma_- + \lambda x \tag{3.11}$$

where

$$\gamma_- = \int_{x_-}^{x} d\eta(\sqrt{\tau} - \lambda) - \lambda x_- \tag{3.12}$$

We then can write (3.8) as

$$\frac{A_-}{\tau^{1/4}} \exp(\frac{i}{\epsilon}\gamma_-) \exp(\theta) + \frac{B_-}{\tau^{1/4}} \exp(-\frac{i}{\epsilon}\gamma_-) \exp(-\theta) \tag{3.13}$$

Now we can compare the last expression with the asymptotic boundary condition (3.5)

$$\frac{A_-}{\tau^{1/4}} \exp(\frac{i}{\epsilon}\gamma_-) \exp(\theta) = 0 \tag{3.14}$$

$$\frac{B_-}{\tau^{1/4}} \exp(-\frac{i}{\epsilon}\gamma_-) \exp(-\theta) = T(\lambda) \exp(-\frac{i\lambda x}{\epsilon}) \tag{3.15}$$

this gives

$$A_- = 0 \tag{3.16}$$

$$B_- = T\tau^{1/4} \exp(\frac{i}{\epsilon}\gamma_-) \tag{3.17}$$

By performing the same method for $x \longrightarrow \infty$ we have

$$\int_{x_+}^{x} d\eta\sqrt{\tau} = \int_{x_+}^{x} d\eta \left[\sqrt{\tau} - \lambda + \lambda\right] = \int_{x_+}^{x} d\eta(\sqrt{\tau} - \lambda) + \lambda(x - x_+)$$
$$= \gamma_+ + \lambda x \tag{3.18}$$

where

$$\gamma_+ = \int_{x_+}^{x} d\eta(\sqrt{\tau} - \lambda) - \lambda x_+ \tag{3.19}$$

Inserting this into (3.10)

$$\frac{A_+}{\tau^{1/4}} \exp(\frac{i}{\epsilon}\gamma_+) \exp(\theta) + \frac{B_+}{\tau^{1/4}} \exp(-\frac{i}{\epsilon}\gamma_+) \exp(-\theta) \tag{3.20}$$

And by comparing for large x we get

$$A_+ = R\tau^{1/4} \exp(-\frac{i}{\epsilon}\gamma_+)$$
$$B_+ = \tau^{1/4} \exp(\frac{i}{\epsilon}\gamma_+) \tag{3.21}$$

At the points x_- and x_+ the WKB approximation is singular since $\tau(x_\pm) = 0$. This means that at these points we can not use equations (3.8)-(3.10) directly. Instead, we linearise the potential u_0 at the singular points $x_\pm$ and solve the equation (3.4). Then we connect the exact solution with asymptotic solutions on both sides of the singular points to obtain connections for all three regions. Around the singular points we assume that the potential can be linearised, starting at x_-

$$\begin{aligned} u_0(x_- + x) &\sim u_0(x_-) + u_0'(x_-)x \\ &= \lambda^2 + \alpha x \end{aligned} \tag{3.22}$$

where $\alpha > 0$. We get the equation

$$\begin{aligned} \epsilon^2\varphi'' - \alpha x\varphi = 0 \\ \varphi = C_- Ai((\frac{\alpha}{\epsilon^2})^{1/3}x) + D_- Bi((\frac{\alpha}{\epsilon^2})^{1/3}x) \end{aligned} \tag{3.23}$$

where $Ai(z)$ and $Bi(z)$ are the Airy functions, see the appendix section C.1. Both these functions have asymptotic expansions for large positive and negative arguments and by using these we can match the inner solution with the outer WKB solutions. Starting with the region to the left of x_- and using the asymptotic forms (C.2),(C.3) we get an expression for (3.23)

$$\varphi \sim \frac{C_-\epsilon^{1/6}}{2\sqrt{\pi}\alpha^{1/12}x^{1/4}} \exp(-\frac{2}{3}\frac{\sqrt{\alpha}}{\epsilon}x^{3/2}) + \frac{D_-\epsilon^{1/6}}{\sqrt{\pi}\alpha^{1/12}x^{1/4}} \exp(\frac{2}{3}\frac{\sqrt{\alpha}}{\epsilon}x^{3/2}) \tag{3.24}$$

By using the same linearisation around x_- we get from the WKB formula (3.9)

$$\varphi \sim \frac{A_0}{(\alpha x)^{1/4}} \exp(\frac{3}{2}\frac{\sqrt{\alpha}}{\epsilon}x^{3/2}) + \frac{B_0}{(\alpha x)^{1/4}} \exp(-\frac{3}{2}\frac{\sqrt{\alpha}}{\epsilon}x^{3/2}) \tag{3.25}$$

We can now compare (3.24) and (3.25)

$$\begin{aligned} \frac{C_-\epsilon^{1/6}}{2\sqrt{\pi}\alpha^{1/12}x^{1/4}} &= \frac{B_0}{(\alpha x)^{1/4}} \\ \frac{D_-\epsilon^{1/6}}{\sqrt{\pi}\alpha^{1/12}x^{1/4}} &= \frac{A_0}{(\alpha x)^{1/4}} \end{aligned} \tag{3.26}$$

This gives

$$\begin{aligned} A_0 &= \frac{D_-(\epsilon\alpha)^{1/6}}{\sqrt{\pi}} \\ B_0 &= \frac{C_-(\epsilon\alpha)^{1/6}}{2\sqrt{\pi}} \end{aligned} \tag{3.27}$$

We now repeat the process for negative arguments, using the asymptotic expansions (C.4) and (C.5). Equation (3.23) becomes

$$\begin{aligned}
&\frac{C_-\epsilon^{1/6}}{\sqrt{\pi}\alpha^{1/12}|x|^{1/4}}\sin(\frac{2}{3}\frac{\sqrt{\alpha}}{\epsilon}|x|^{3/2}+\frac{\pi}{4})+\frac{D_-\epsilon^{1/6}}{\sqrt{\pi}\alpha^{1/12}|x|^{1/4}}\cos(\frac{2}{3}\frac{\sqrt{\alpha}}{\epsilon}|x|^{3/2}+\frac{\pi}{4})\\
&=C_-\beta\sin(\omega+\frac{\pi}{4})+D_-\beta\cos(\omega+\frac{\pi}{4})\\
&=C_-\beta\left[\frac{\exp(i\omega)\exp(i\frac{\pi}{4})-\exp(-i\omega)\exp(-i\frac{\pi}{4})}{2i}\right]\\
&+D_-\beta\left[\frac{\exp(i\omega)\exp(i\frac{\pi}{4})+\exp(-i\omega)\exp(-i\frac{\pi}{4})}{2}\right]\\
&=\beta\exp(i\omega)\exp(i\frac{\pi}{4})\left[\frac{D_-}{2}+\frac{C_-}{2i}\right]+\beta\exp(-i\omega)\exp(-i\frac{\pi}{4})\left[\frac{D_-}{2}-\frac{C_-}{2i}\right]
\end{aligned} \tag{3.28}$$

where $\beta=\frac{\epsilon^{1/6}}{\sqrt{\pi}\alpha^{1/12}|x|^{1/4}}$ and

$$\omega=\frac{2}{3}\frac{\sqrt{\alpha}}{\epsilon}|x|^{3/2} \tag{3.29}$$

Similar we we find the expansion (3.8) in this region

$$\frac{A_-}{\alpha^{1/4}|x|^{1/4}}\exp(-i\omega)+\frac{B_-}{\alpha^{1/4}|x|^{1/4}}\exp(i\omega) \tag{3.30}$$

By comparing these two equations we get

$$A_-=\frac{(\alpha\epsilon)^{1/6}}{\sqrt{\pi}}\left[\frac{D_-}{2}-\frac{C_-}{2i}\right]\exp(-i\frac{\pi}{4}) \tag{3.31}$$

$$B_-=\frac{(\alpha\epsilon)^{1/6}}{\sqrt{\pi}}\left[\frac{D_-}{2}+\frac{C_-}{2i}\right]\exp(i\frac{\pi}{4}) \tag{3.32}$$

and by using (3.27) we get

$$A_-=\left[\frac{A_0}{2}-\frac{B_0}{i}\right]\exp(-i\frac{\pi}{4}) \tag{3.33}$$

$$B_-=\left[\frac{A_0}{2}+\frac{B_0}{i}\right]\exp(i\frac{\pi}{4}) \tag{3.34}$$

This is the connection between the WKB solutions and the inner solution around x_-. We now do the same procedure around x_+. We linearise around x_+

$$u_0(x_++x)=\lambda^2+u_0'(x_+)x=\lambda^2-\alpha x \tag{3.35}$$

Solving the Schrödinger equation (3.4) with the linearised potential

$$\varphi \sim C_+ Ai((-\frac{\alpha}{\epsilon^2})^{1/3}x) + D_+ Bi((-\frac{\alpha}{\epsilon^2})^{1/3}x) \tag{3.36}$$

By using the asymptotic expansions on the left of x_+ we get

$$\begin{aligned}\varphi &\sim C_+\beta \sin(\omega + \frac{\pi}{4}) + D_+\beta\cos(\omega+\frac{\pi}{4}) \\ &= \beta\exp(i\omega)\exp(i\frac{\pi}{4})\left[\frac{D_+}{2} + \frac{C_+}{2i}\right] + \beta\exp(-i\omega)\exp(-i\frac{\pi}{4})\left[\frac{D_+}{2} - \frac{C_+}{2i}\right]\end{aligned} \tag{3.37}$$

We must compare this with the two expansions (3.9) and (3.10). Starting with (3.10) we compute the integral part using the linearised potential $u_0 = \alpha^2 - \alpha x$

$$\varphi \sim \frac{A_+}{(\alpha x)^{1/4}}\exp(i\omega) + \frac{B_+}{(\alpha x)^{1/4}}\exp(-i\omega) \tag{3.38}$$

Comparing (3.37) and (3.38) we get the connection between these two solutions

$$\begin{aligned}A_+ &= \frac{(\alpha\epsilon)^{1/6}}{\sqrt{\pi}}\left[\frac{D_+}{2} + \frac{C_+}{2i}\right]\exp(i\frac{\pi}{4}) \\ B_+ &= \frac{(\alpha\epsilon)^{1/6}}{\sqrt{\pi}}\left[\frac{D_+}{2} - \frac{C_+}{2i}\right]\exp(-i\frac{\pi}{4})\end{aligned} \tag{3.39}$$

Next we look at the region at the left of x_+, using equations (3.36) and (C.2),(C.3)

$$\varphi \sim \frac{C_+\epsilon^{1/6}}{2\sqrt{\pi}\alpha^{1/4}(-x)^{1/4}}\exp(-\frac{2}{3}\frac{\sqrt{\alpha}}{\epsilon}(-x)^{3/2}) + \frac{D_+\epsilon^{1/6}}{2\sqrt{\pi}\alpha^{1/4}(-x)^{1/4}}\exp(\frac{2}{3}\frac{\sqrt{\alpha}}{\epsilon}(-x)^{3/2}) \tag{3.40}$$

the WKB-approximation in this region is given by (3.9) and by first computing the integral part

$$\begin{aligned}\int_{x_-}^{x} d\eta\sqrt{-\tau} &= \int_{x_-}^{x_+} d\eta\sqrt{-\tau} + \frac{2}{3}\sqrt{\alpha}(-x)^{3/2} \\ &= \chi - \frac{2}{3}\sqrt{\alpha}(-x)^{3/2}\end{aligned} \tag{3.41}$$

We insert it into (3.9)

$$\varphi \sim \frac{A_0}{\alpha^{1/4}(-x)^{1/4}}\exp(\frac{1}{\epsilon}\chi)\exp(-\frac{2}{3}\frac{\sqrt{\alpha}}{\epsilon}(-x)^{3/2}) + \frac{B_0}{\alpha^{1/4}(-x)^{1/4}}\exp(\frac{1}{\epsilon}\chi)\exp(\frac{2}{3}\frac{\sqrt{\alpha}}{\epsilon}(-x)^{3/2}) \tag{3.42}$$

Now the expressions containing A_0, B_0 and C_+, D_+ can be compared

$$C_+ = \frac{A_0 2\sqrt{\pi}}{(\alpha\epsilon)^{1/6}} \exp(\frac{1}{\epsilon}\chi)$$
$$D_+ = \frac{B_0\sqrt{\pi}}{(\alpha\epsilon)^{1/6}} \exp(-\frac{1}{\epsilon}\chi) \tag{3.43}$$

And by inserting these into (3.39)

$$A_+ = \left[\frac{B_0}{2}\exp(-\frac{1}{\epsilon}\chi) + \frac{A_0}{i}\exp(\frac{1}{\epsilon}\chi)\right]\exp(i\frac{\pi}{4})$$
$$B_+ = \left[\frac{B_0}{2}\exp(\frac{1}{\epsilon}\chi) - \frac{A_0}{i}\exp(-\frac{1}{\epsilon}\chi)\right]\exp(-i\frac{\pi}{4}) \tag{3.44}$$

To summarise, we have the following results in addition to the two above equations

$$A_- = 0 \tag{3.45}$$
$$B_- = T\tau^{1/4}\exp(\frac{i}{\epsilon}\gamma_-) \tag{3.46}$$
$$A_+ = R\tau^{1/4}\exp(-\frac{i}{\epsilon}\gamma_+) \tag{3.47}$$
$$B_+ = \tau^{1/4}\exp(\frac{i}{\epsilon}\gamma_+) \tag{3.48}$$
$$A_- = \left[\frac{A_0}{2} - \frac{B_0}{i}\right]\exp(-i\frac{\pi}{4}) \tag{3.49}$$
$$B_- = \left[\frac{A_0}{2} + \frac{B_0}{i}\right]\exp(i\frac{\pi}{4}) \tag{3.50}$$

To find connections between the reflection and transmissions coefficients we need to solve this as a linear system, first by rewriting all into matrix form

$$\begin{bmatrix}A_-\\B_-\end{bmatrix} = \begin{bmatrix}0 & 0\\0 & \tau^{1/4}\exp(\frac{i}{\epsilon}\gamma_-)\end{bmatrix}\begin{bmatrix}0\\T\end{bmatrix}$$
$$= \begin{bmatrix}0 & 0\\0 & \kappa\end{bmatrix}\begin{bmatrix}0\\T\end{bmatrix}$$
$$= K\begin{bmatrix}0\\T\end{bmatrix} \tag{3.51}$$

And

$$\begin{bmatrix}A_+\\B_+\end{bmatrix} = \begin{bmatrix}\tau^{1/4}\exp(-\frac{i}{\epsilon}\gamma_+) & 0\\0 & \tau^{1/4}\exp(\frac{i}{\epsilon}\gamma_+)\end{bmatrix}\begin{bmatrix}R\\1\end{bmatrix}$$
$$= \begin{bmatrix}h & 0\\0 & h^*\end{bmatrix}\begin{bmatrix}R\\1\end{bmatrix}$$
$$= H\begin{bmatrix}R\\1\end{bmatrix} \tag{3.52}$$

And

$$\begin{aligned}\begin{bmatrix}A_+\\B_+\end{bmatrix} &= \begin{bmatrix}-i\exp(i\frac{\pi}{4})\exp(\frac{1}{\epsilon}\chi) & \frac{1}{2}\exp(i\frac{\pi}{4})\exp(-\frac{1}{\epsilon}\chi)\\ i\exp(-i\frac{\pi}{4})\exp(\frac{1}{\epsilon}\chi) & \frac{1}{2}\exp(-i\frac{\pi}{4})\exp(-\frac{1}{\epsilon}\chi)\end{bmatrix}\begin{bmatrix}A_0\\B_0\end{bmatrix}\\ &= \begin{bmatrix}\exp(i\frac{\pi}{4}) & 0\\ 0 & \exp(-i\frac{\pi}{4})\end{bmatrix}\begin{bmatrix}-i\exp(\frac{1}{\epsilon}\chi) & \frac{1}{2}\exp(-\frac{1}{\epsilon}\chi)\\ i\exp(\frac{1}{\epsilon}\chi) & \frac{1}{2}\exp(-\frac{1}{\epsilon}\chi)\end{bmatrix}\begin{bmatrix}A_0\\B_0\end{bmatrix}\\ &= \begin{bmatrix}a & 0\\ 0 & a^*\end{bmatrix}\begin{bmatrix}-ic & \frac{1}{2}c^{-1}\\ ic & \frac{1}{2}c^{-1}\end{bmatrix}\begin{bmatrix}A_0\\B_0\end{bmatrix}\\ &= PM\begin{bmatrix}A_0\\B_0\end{bmatrix}\end{aligned} \tag{3.53}$$

And

$$\begin{aligned}\begin{bmatrix}A_-\\B_-\end{bmatrix} &= \begin{bmatrix}\exp(-i\frac{\pi}{4}) & 0\\ 0 & \exp(i\frac{\pi}{4})\end{bmatrix}\begin{bmatrix}\frac{1}{2} & i\\ \frac{1}{2} & -i\end{bmatrix}\begin{bmatrix}A_0\\B_0\end{bmatrix}\\ &= \begin{bmatrix}a & 0\\ 0 & a^*\end{bmatrix}\begin{bmatrix}\frac{1}{2} & i\\ \frac{1}{2} & -i\end{bmatrix}\begin{bmatrix}A_0\\B_0\end{bmatrix}\\ &= P^*N\begin{bmatrix}A_0\\B_0\end{bmatrix}\end{aligned} \tag{3.54}$$

Now a chain can be written if we observe that

$$\begin{aligned}K\begin{bmatrix}0\\T\end{bmatrix} &\to \begin{bmatrix}A_-\\B_-\end{bmatrix}\\ (P^*N)^{-1}K\begin{bmatrix}0\\T\end{bmatrix} &\to (P^*N)^{-1}\begin{bmatrix}A_-\\B_-\end{bmatrix} = \begin{bmatrix}A_0\\B_0\end{bmatrix}\\ PM(P^*N)^{-1}K\begin{bmatrix}0\\T\end{bmatrix} &\to PM\begin{bmatrix}A_0\\B_0\end{bmatrix} = \begin{bmatrix}A_+\\B_+\end{bmatrix}\\ H^{-1}PM(P^*N)^{-1}K\begin{bmatrix}0\\T\end{bmatrix} &\to H^{-1}\begin{bmatrix}A_+\\B_+\end{bmatrix} = \begin{bmatrix}R\\1\end{bmatrix}\end{aligned} \tag{3.55}$$

We start simplifying by calculating

$$\begin{aligned}(P^*N)^{-1} &= \begin{bmatrix}\exp(i\frac{\pi}{4}) & \exp(-i\frac{\pi}{4})\\ -\frac{i}{2}\exp(i\frac{\pi}{4}) & \frac{i}{2}\exp(-i\frac{\pi}{4})\end{bmatrix}\\ &= \begin{bmatrix}a & a^*\\ b^* & b\end{bmatrix}\end{aligned} \tag{3.56}$$

and

$$\begin{aligned}(PM)(P^*N)^{-1} &= \begin{bmatrix}c+\frac{1}{2}ab^*c^{-1} & -ic+\frac{1}{2}abc^{-1}\\ ic+\frac{1}{2}a^*b^*c^{-1} & c+\frac{1}{2}a^*bc^{-1}\end{bmatrix}\\ &= \begin{bmatrix}\mu & \nu\\ \nu^* & \mu^*\end{bmatrix}\end{aligned} \tag{3.57}$$

Finally we multiply by K and H^{-1}

$$\begin{aligned} H^{-1}(PM)(P^*N)^{-1}K &= \frac{1}{\tau^{1/4}}\begin{bmatrix} h^* & 0 \\ 0 & h \end{bmatrix}\begin{bmatrix} \mu & \nu \\ \nu^* & \mu^* \end{bmatrix}\begin{bmatrix} 0 & 0 \\ 0 & \kappa \end{bmatrix} \\ &= \frac{1}{\tau^{1/4}}\begin{bmatrix} 0 & h^*\nu\kappa \\ 0 & h\mu^*\kappa \end{bmatrix} \end{aligned} \tag{3.58}$$

This gives us equations for R and T

$$\begin{bmatrix} R \\ 1 \end{bmatrix} = \frac{1}{\tau^{1/4}}\begin{bmatrix} 0 & h^*\nu\kappa \\ 0 & h\mu^*\kappa \end{bmatrix}\begin{bmatrix} 0 \\ T \end{bmatrix} \tag{3.59}$$

Solving these gives

$$\begin{aligned} T &= \frac{\tau^{1/4}}{h\mu^*\kappa} \\ R &= \frac{h^*\nu}{h\mu^*} \end{aligned} \tag{3.60}$$

Further we see that in the limit $\epsilon \to 0$

$$\begin{aligned} &\mu \sim c \\ &\nu \sim -ic, \epsilon \to 0 \end{aligned} \tag{3.61}$$

Using this gives for the reflection coefficient

$$\begin{aligned} R(\lambda) \sim -i\frac{h^*}{h} &= -i\exp(-i\frac{2}{\epsilon}\gamma_+) \\ &= -i\exp\left[-i\frac{2}{\epsilon}(\lambda x_+ + \int_{x_-}^{x_+} d\eta(\lambda - \sqrt{\lambda^2 - u_0(\eta)}))\right] \end{aligned} \tag{3.62}$$

We are interested in the squared norm of T and we then get in the limit $\epsilon \to 0$

$$\begin{aligned} |T(\lambda)|^2 \sim \frac{1}{|c|^2} &= \exp\left[-\frac{2}{\epsilon}\chi\right] \\ &= \exp\left[-\frac{2}{\epsilon}\int_{x_-}^{x_+} d\eta(\sqrt{-\tau(\eta)}\right] \\ &= \exp\left[-\frac{2}{\epsilon}\int_{x_-}^{x_+} d\eta\sqrt{u_0(\eta) - \lambda^2}\right] \end{aligned} \tag{3.63}$$

We now have expressions for reflection and transmission coefficients for $0 < \lambda^2 < 1$, but what about $\lambda^2 > 1$? In this region there are no turning points and we use the WKB-approximation on form (3.9)

$$\varphi \sim \frac{A}{\tau^{1/4}}\exp(i\frac{1}{\epsilon}\gamma_-)\exp(\theta) + \frac{B}{\tau^{1/4}}\exp(-i\frac{1}{\epsilon}\gamma_-)\exp(-\theta) \tag{3.64}$$

By first employing the boundary condition at $x \longrightarrow -\infty$ and then when $x \longrightarrow \infty$ we get the result

$$\begin{aligned} R(\lambda) &= 0 \\ T(\lambda) &= 1 \end{aligned} \tag{3.65}$$

when the eigenvalues $\lambda^2 > 1$. For simplicity we have used λ^2 in these calculations, but to use the same notation as in the reference we let $\lambda^2 \longrightarrow \lambda$ and we redefine γ_+ and χ. Our expressions then become

$$\begin{aligned} R(\lambda) &\sim -i \exp\left[-i\frac{2}{\epsilon}(\lambda^{1/2}x_+(\lambda) + \int_{x_-}^{\infty} d\eta(\lambda^{1/2} - \sqrt{\lambda^{1/2} - u_0(\eta)}))\right] \\ &= -i \exp\left[-i\frac{2}{\epsilon}\rho(\lambda)\right] \end{aligned} \tag{3.66}$$

and

$$\begin{aligned} T(\lambda) &\sim \exp\left[-\frac{2}{\epsilon}\int_{x_-}^{x_+} d\eta\sqrt{u_0(\eta) - \lambda}\right] \\ &= \exp\left[-\frac{2}{\epsilon}\tau(\lambda)\right] \end{aligned} \tag{3.67}$$

where we have (re)-defined ρ and τ

$$\rho(\lambda) := \lambda^{1/2}x_+(\lambda) + \int_{x_-}^{\infty} d\eta(\lambda^{1/2} - \sqrt{\lambda^{1/2} - u_0(\eta)}) \tag{3.68}$$

$$\tau(\lambda) := \int_{x_-}^{x_+} d\eta\sqrt{u_0(\eta) - \lambda} \tag{3.69}$$

3.2 Burger's equation and breaking time

Before we start solving the KdV equation it is of interest to study equation (3.1) when we set $\epsilon = 0$

$$u_t - 6uu_x = 0 \tag{3.70}$$

The equation above is called the inviscid Burger's equation and is known to develop a shock at a specific time t^*. Denote this as the breaking time and for times greater than t^*, the solution to (3.70) become multivalued. Studying (3.70) in our context is important for at least two reasons, first because we get insight into what the term $\epsilon^2 u_{xxx}$ does to the equation. The second reason is a technical one that will be described in later sections, simply stated the

method we will use solve the KdV equation before t^* in one particular way and after t^* another. To find the breaking time of (3.70) we use the method of characteristics

$$\begin{aligned}\frac{dt}{ds} &= 1, t(0,\eta) = 0\\ \frac{dx}{ds} &= -6u, x(0,\eta) = \eta\\ \frac{du}{ds} &= 0, u(0,\eta) = u_0(\eta)\end{aligned} \tag{3.71}$$

the solution for $x(\eta)$ is

$$x = -6u_0(\eta)t + \eta \tag{3.72}$$

if we look at two curves

$$-6u_0(\eta_0)t + \eta_0 = -6u_0(\eta_1)t + \eta_1 \tag{3.73}$$

if these curves intersect then the solution is multivalued, and if we can find the minimum time this happens we have the breaking time

$$t = -\frac{\eta_1 - \eta_0}{6(u_0(\eta_1) - u_0(\eta_0))} \tag{3.74}$$

we have the minimal time t^*

$$\begin{aligned}t^* &= -\frac{1}{min_{(\eta_0,\eta_1)\in\mathcal{R}}\frac{1}{\eta_1-\eta_0}6\int_{\eta_0}^{\eta_1} d\eta u_0'}\\ &= -\frac{1}{min_{\eta\in\mathcal{R}}6u_0'(\eta)}\end{aligned} \tag{3.75}$$

In addition to this, using (3.72) and setting $\eta = 0$ we get the following result

$$x^* = -6u_0(0)t + 0 = -6t \tag{3.76}$$

The point x^* corresponds to the position of the maximum of $u(x,t)$ before breaking.

3.3 Inverse Scattering Transform as a Riemann-Hilbert problem

We will now present the steps needed to solve the KdV equation in the small dispersion limit using the Riemann-Hilbert approach that Shabat introduced

[25] and later culminated in the work of Deift et al. [7] and the following description is mainly based on the latter. The first step, already performed, is to perform forward scattering and obtained expressions for the reflection coefficient R and transmission coefficient T. From the theory of IST for the KdV equation is correspond to solving the Schrödinger eigenvalue problem

$$-\epsilon^2\varphi'' + u_0(x)\varphi = \lambda\varphi \tag{3.77}$$

with appropriate boundary value conditions, exactly the problem we solved in section 3.1. Here λ is the eigenvalue and will become the independent variable that we use in the solution process, while the space and time variables (x, t) will be treated as parameters. The next step is to define the scattering matrix $\boldsymbol{G}$

$$\boldsymbol{G} = \begin{cases} \sigma_1 & \text{if } \lambda < 0 \\ \begin{bmatrix} 1 - |R|^2 & -\bar{R}\exp(-\frac{2i}{\epsilon}\alpha) \\ R\exp(\frac{2i}{\epsilon}\alpha) & 1 \end{bmatrix} & \text{if } \lambda > 0 \end{cases} \tag{3.78}$$

Here σ_1 denotes the Pauli matrix $\sigma_1 = \begin{bmatrix} 0 & 1 \\ 1 & 0 \end{bmatrix}$, R is the reflection coefficient, the quantity $T = 1 - |R|^2$ is the transmission coefficient and

$$\alpha = 4t\lambda^{3/2} + x\lambda^{1/2} \tag{3.79}$$

The redefinition of the scattering problem into a Riemann-Hilbert problem done by Shabat in [25] is to find a row vector-valued function $\boldsymbol{m}(\lambda) = (m_1, m_2)$ analytic for $\lambda \in \mathbb{C}\backslash\mathbb{R}$

$$\boldsymbol{m_+} = \boldsymbol{m_-}\boldsymbol{G} \tag{3.80}$$

with asymptotic behaviour

$$\boldsymbol{m} \to (1, 1),\ \lambda \to \infty \tag{3.81}$$

The limiting functions are defined as $\boldsymbol{m}_\pm = \lim_{\delta\to 0} \boldsymbol{m}(\lambda \pm i\delta; x, t, \epsilon)$. Equation (3.80) is a vector Riemann-Hilbert problem, with jump function $\boldsymbol{m}$. From the reference, the solution to $u(x, t)$ is at this point

$$u(x, t; \epsilon) = -2i\epsilon\partial_x m_{11}(x, t; \epsilon) \tag{3.82}$$

where

$$m_1(\lambda; x, t, \epsilon) = 1 + \frac{m_{11}}{\lambda^{1/2}} + O(\frac{1}{\lambda}), \lambda \to \infty \tag{3.83}$$

There are two main simplifying ideas in the proposed solution process, the first being using the WKB approximation to solve for the reflection coefficient, the second is to introduce a change of variable named the phase function.

Starting with the former, the differential equation (3.4) solved in section 3.1 is the forward scattering problem for the KdV equation where u_0 and satisfies definition (1). We insert the calculated approximations for R (3.66) and T (3.67) into equation (3.78)

$$\boldsymbol{G} = \begin{cases} \begin{bmatrix} 0 & 1 \\ 1 & 0 \end{bmatrix} & \text{if } \lambda < 0 \\ \begin{bmatrix} \exp(-\frac{2}{\epsilon}\tau) & -i\exp(\frac{2i}{\epsilon}(\rho-\alpha)) \\ -i\exp(\frac{2i}{\epsilon}(\alpha-\rho)) & 1 \end{bmatrix} & \text{if } 0 < \lambda < 1 \\ \begin{bmatrix} 1 & 0 \\ 0 & 1 \end{bmatrix} & \text{if } \lambda > 1 \end{cases} \tag{3.84}$$

where the last matrix is introduced when the results from the WKB approximation for $\lambda > 1$ is used. The problem is now reduced to a problem on the interval $(-\infty, 1]$ in λ, since the third matrix in (3.84) is the identity. The second step is to introduce a change of variable $\boldsymbol{m}$

$$\boldsymbol{m}^{(1)} = \boldsymbol{m}\begin{bmatrix} \exp(\frac{i}{\epsilon}g(\lambda)) & 0 \\ 0 & \exp(-\frac{i}{\epsilon}g(\lambda)) \end{bmatrix} \tag{3.85}$$

The function $g(\lambda)$ is called the phase function. The phase function is a complex function, analytic when not on the cut $\lambda = (-\infty, 1]$.

$$g(\lambda; x, t) = \frac{g_1(x,t)}{\lambda^{1/2}} + O(\frac{1}{\lambda}), \lambda \to \infty \tag{3.86}$$

By inverting (3.85) and inserting into $\boldsymbol{G}$ we get the modified jump matrix

$$\boldsymbol{G}^{(1)} = \begin{cases} \begin{bmatrix} 0 & \exp(-\frac{i}{\epsilon}(g_+ + g_-)) \\ \exp(\frac{i}{\epsilon}(g_+ + g_-)) & 0 \end{bmatrix} & \text{if } \lambda < 0 \\ \begin{bmatrix} \exp(\frac{1}{\epsilon}(ig_+ - ig_- - 2\tau)) & -i\exp(\frac{i}{\epsilon}(-g_+ - g_- + 2\rho - 2\alpha)) \\ -i\exp(\frac{i}{\epsilon}(g_+ + g_- + 2\alpha - 2\rho)) & \exp(-\frac{i}{\epsilon}(g_+ - g_-)) \end{bmatrix} & \text{if } 0 < \lambda < 1 \\ \begin{bmatrix} \exp(\frac{i}{\epsilon}(g_+ - g_-)) & 0 \\ 0 & \exp(\frac{i}{\epsilon}(g_+ - g_-)) \end{bmatrix} & \text{if } \lambda > 1 \end{cases} \tag{3.87}$$

In order to satisfy the jump condition when $\lambda < 0$ and the identity matrix when $\lambda > 1$ in (3.84) two requirements on g is necessary

$$g_+(\lambda) + g_-(\lambda) = 0, \lambda \in (-\infty, 0) \tag{3.88}$$
$$g_+(\lambda) - g_-(\lambda) = 0, \lambda \in (1, \infty) \tag{3.89}$$

After this change of variable the solution $u(x,t)$ is now given by

$$u(x,t;\epsilon) = -2i\epsilon\partial_x m_{11}^{(1)} - 2\partial_x g_1(x,t) \tag{3.90}$$

Let us assume that for every (x,t) we can make certain requirements on the phase function g for $\lambda \in (0,1)$, we will later briefly mention why exactly these requirements are made. First we pose that there exists $N+1$ number of partitions $(\alpha_j(\lambda), \beta_j(\lambda))$ in $\lambda \in (0,1)$, where $0 \leq j \leq n$. We also require that $\beta_0 < \alpha_1 < \beta_1 \ldots < \beta_N$. If we are in the region between two intervals, e.g. (α_1, β_1) we demand that the phase function satisfies the following

$$\begin{aligned} -\tau < \frac{1}{2i}(g_+ - g_-) < 0 \\ h' = 0 \\ h = \Omega_j \end{aligned} \tag{3.91}$$

where Ω_j is a constant of integration. On the other hand if we are not in this interval, $\lambda \in (0,1) - \cup(\alpha_j, \beta_j)$, we require one of the two following cases

$$\begin{aligned} -\tau = \frac{1}{2i}(g_+ - g_-) \\ h' < 0 \end{aligned} \tag{3.92}$$

or

$$\begin{aligned} g_+ - g_- = 0 \\ h' > 0 \end{aligned} \tag{3.93}$$

Now observe that the conditions (3.92), (3.91) and (3.93) gives rise to two scalar Riemann-Hilbert problems, one for g and one for ∂g

$$\partial g_+ + \partial g_- = 0, \ \lambda < 0 \tag{3.94}$$

$$\partial g_+ + \partial g_- + 2\partial\alpha - 2\partial\rho = 0, \ \lambda \in \cup(\alpha_j, \beta_j) \tag{3.95}$$

$$\partial g_+ - \partial g_- = 0, \ \lambda > 1 \tag{3.96}$$

And ∂g should satisfy one of the following conditions

$$\text{A)} \ -2i\partial\tau = \partial g_+ - \partial g_- \tag{3.97}$$

or

$$\text{B)} \quad 0 = \partial g_+ - \partial g_-, \ \lambda \in (0,1) - \cup(\alpha_j, \beta_j) \tag{3.98}$$

The RH problem for g is

$$g_+ + g_- = 0, \ \lambda < 0 \tag{3.99}$$

$$g_+ + g_- + 2\alpha - 2\rho = \Omega_j, \ \lambda \in \cup(\alpha_j, \beta_j) \tag{3.100}$$

$$g_+ - g_- = 0, \ \lambda > 1 \tag{3.101}$$

And g should satisfy one of the following conditions

$$\text{A)} \ -2i\tau = g_+ - g_- \tag{3.102}$$

or

$$\text{B)} \quad 0 = g_+ - g_-, \ \lambda \in (0,1) - \cup(\alpha_j, \beta_j) \tag{3.103}$$

It is more clear that these are RH problems if we, for example for ∂g, rewrite in the form

$$\partial g_+ = k\partial g_- + f \tag{3.104}$$

where the jump function is

$$k = \begin{cases} -1 & \lambda < 0 \\ -1 & \lambda \in (\alpha_j, \beta_j) \\ 1 & o.w \end{cases} \tag{3.105}$$

and the inhomogeneous term f

$$f = \begin{cases} 0 & \lambda < 0 \\ 2\partial\rho - 2\partial\alpha, & \lambda \in (\alpha_j, \beta_j) \\ -2i\tau' \vee 0 & \lambda \in (0,1) - \cup(\alpha_j, \beta_j) \\ 0 & \lambda > 1 \end{cases} \tag{3.106}$$

A similar rewriting can be done for the RH problem for g. In the appendix section B we derived the general solution to scalar RH problems

$$\Psi(z) = X(z)\left[\int_{-\infty}^{\infty} dt \frac{1}{2\pi i}\frac{h(t)}{X^+(t)(t-z)} + P(z)\right] \tag{3.107}$$

where $X(z)$ are the solution to the homogeneous problem

$$X(z) = \frac{1}{2\pi i}\int_{-\infty}^{\infty} dt \frac{\phi(t)}{t-z} \tag{3.108}$$

The jump function (3.105), with an unspecified number of partitions (α_j, β_j) gives rise to the following homogeneous solution X of the RH problem, consider the function

$$X(\lambda)^2 = (\lambda - \beta_0)\prod_{j=1}^{N}(\lambda - \alpha_j)(\lambda - \beta_j) \tag{3.109}$$

Can X be a solution to a RH problem, if a particular branch is taken? Let us write X as

$$X = \exp\left[\frac{1}{2}\log\left((\lambda - \beta_0)\prod_{j=1}^{N}(\lambda - \alpha_j)(\lambda - \beta_j)\right)\right] \tag{3.110}$$

what shape must it then take to satisfy the jump condition (3.105)? The cases $\lambda < 0$ and $\lambda \in (\alpha_j, \beta_j)$ has identical jump condition so let us first examine these two cases, we have $\lambda < \beta_0, \alpha_j, \beta_j$ so we pick

$$X = \left[(\beta_0 - \lambda)\prod_{j=1}^{N}(\alpha_j - \lambda)(\beta_j - \lambda)\right]^{1/2} \tag{3.111}$$

then using (3.110) we can find the limiting functions X_+ and X_- as follows

$$\begin{aligned} X_+ &= \lim_{\theta \to \frac{\pi}{2}} \exp\left[\frac{1}{2}\log\left((\beta_0 - \lambda)\prod_{j=1}^{N}(\alpha_j - \lambda)(\beta_j - \lambda)\right) + i\theta\right] \\ &= i\left[(\beta_0 - \lambda)\prod_{j=1}^{N}(\alpha_j - \lambda)(\beta_j - \lambda)\right]^{1/2} \end{aligned} \tag{3.112}$$

using the same method but taking the limit $\theta \to -\frac{\pi}{2}$ gives

$$X_- = -i\left[(\beta_0 - \lambda)\prod_{j=1}^{N}(\alpha_j - \lambda)(\beta_j - \lambda)\right]^{1/2} \tag{3.113}$$

thus for both these cases we have $X_+ = -X_-$. Hence, X is a solution to a RH problem and is a solution to our problem. By taking different branches of (3.109) we can find solutions to the types of problems we require solutions to. We will denote the homogeneous solutions X in the following calculations, but depending on the scalar RH problem the explicit form might differ from case to case. Now we can write down the solution to the RH problem (3.104) using the formula (3.107)

$$g'(\lambda) = X(\lambda)\left[\int_{\cup I_j}\frac{d\mu}{2\pi i}\frac{2\rho'(\mu) - 2\alpha'(\mu)}{X_+(\mu)(\mu - \lambda)} + \int_{(0,E)-\cup I_j}\frac{d\mu}{2\pi i}\frac{-2i\tau'(\mu)}{X_+(\mu)(\mu - \lambda)} + P(\lambda)\right] \tag{3.114}$$

where E is either 1 (case A) or β_N (case B). From the theory we have that as $\lambda \to \infty$ the phase function must satisfy the asymptotic condition

$$\lim_{\lambda \to \infty} g(\lambda) \sim \frac{1}{\lambda^{1/2}} \tag{3.115}$$

implying $\lim_{\lambda\to\infty} g'(\lambda) \sim \frac{1}{\lambda^{3/2}}$. This leads to $P = 0$ and the following equation

$$\int_{\cup I_j} d\lambda\lambda^k \frac{2\rho'(\lambda) - 2\alpha'(\lambda)}{X_+(\lambda)} + \int_{(0,1)-\cup I_j} d\lambda\lambda^k \frac{-2i\tau'(\lambda)}{X_+(\lambda)} = 0, k = 0, \ldots, N \tag{3.116}$$

This gives N equations for $N + 1$ equations, an addition equation is needed to determine all unknowns. If $g'_\pm$ are both continuous for $\lambda > 0$ we can integrate

around each partition $(\alpha_j, \beta_j), 1 \leq j \leq N$, leading to

$$\begin{aligned}\oint_{I_j} d\lambda g'(\lambda) &= \lim_{\delta\to 0^+} \int_{\alpha_j-\delta}^{\beta_j+\delta} d\lambda \partial g_+ + \lim_{\delta\to 0^+} \int_{\alpha_j-\delta}^{\beta_j+\delta} d\lambda \partial g_- \\ &= \lim_{\delta\to 0^+} \int_{\alpha_j-\delta}^{\beta_j+\delta} d\lambda \left[\partial g_+ - \partial g_-\right] \\ &= \lim_{\delta\to 0^+} \left[g_+ - g_-\right]_{\lambda=\alpha_j-\delta}^{\beta_j+\delta}\end{aligned} \tag{3.117}$$

Now, using the RH problem for g gives for the partitions (α_j, β_j)

$$\lim_{\delta\to 0^+} \int_{\alpha_j-\delta}^{\beta_j+\delta} d\lambda \left[\partial g_+ - \partial g_-\right] = -2i \left[\tau(\beta_j) - \tau(\alpha_j)\right], 1 \leq j \leq N \tag{3.118}$$

Now we have $N + 1$ equations for the unknown quantities α_j, β_j. We are interested in using this method in practice and want to develop the equations further. For a given potential u_0 one could try to go through the whole process and analyse the different cases exact, corresponding to analysing a number of inequalities and calculating integrals. We will take a different, perhaps more crude, approach by simply developing the equations for the simplest cases and later ask if these are enough for the initial potentials we consider. The simplest case is if we set $N = 0, \beta_0 = 0$, this is equivalent to the trivial case $u = 0$ and no further work is needed. Next one could set $N = 0, \beta_0 \neq 0$, from the theory it is suggested that this is valid for times $0 \leq t \leq t^*$ and for $x \in (-s, s)$, where t^* is the breaking time derived in section 3.2. For potentials of compact support the solution before t^* outside the support is zero. After breaking we assume that there will be at least one addition phase $N = 1, \beta_0 \neq 0$ and solve for the additional quantities (α_1, β_1), valid for $t^* < t < T$ and β_0 is valid in $x \in (x0, s)$, (α_1, β_1) for $x_0 < x < x_1$, where T, x_0 and x_1 may or may not be finite, yet to be determined. If this is not sufficient one would have to set $N = 2, 3, 4\ldots$ until all time and space are covered.

3.3.1 Phase before breaking, $N = 0, \beta_0 \neq 0$

Starting with developing the phase before breaking we have one unknown β_0, hence we need one equation to determine this quantity. The equation valid for this case is (3.116), and with $N = 0$ we can write down the homogeneous solution X using formula (3.109)

$$X(\lambda) = (\lambda - \beta_0)^{1/2} \tag{3.119}$$

By repeating the limiting process for the upper branch we get $X_+ = i(\beta_0 - \lambda)^{1/2}$. For this case we have two separate cases A (3.97) or B (3.98) and starting with

case B we have

$$\begin{aligned} g'(\lambda) &= \frac{1}{2\pi i}(\lambda-\beta_0)^{1/2}\int_0^{\beta_0} d\mu \frac{2\rho'(\mu)-2\alpha'(\mu)}{(\mu-\beta_0)^{1/2}(\mu-\lambda)} \\ &= -\frac{1}{2\pi}(\lambda-\beta_0)^{1/2}\int_0^{\beta_0} d\mu \frac{2\rho'(\mu)-2\alpha'(\mu)}{(\beta_0-\mu)^{1/2}(\mu-\lambda)} \end{aligned}$$

Using condition (3.116) we get the equation

$$\begin{aligned} \int_0^{\beta_0} d\lambda \frac{2\rho'(\lambda)-2\alpha'(\lambda)}{(\beta_0-\lambda)^{1/2}} &= 0 \\ \int_0^{\beta_0} d\lambda \frac{2\rho'(\lambda)}{(\beta_0-\lambda)^{1/2}} &= \int_0^{\beta_0} d\lambda \frac{2\alpha'(\lambda)}{(\beta_0-\lambda)^{1/2}} \\ C(\beta_0) &= 6tA(\beta_0)+xB(\beta_0) \end{aligned} \tag{3.120}$$

While ρ' is dependent on the initial potential u_0, the formula for α is not, thus we differentiate α and see if we can make any analytical simplifications. Differentiating α gives

$$\begin{aligned} \alpha' &= \frac{d}{d\lambda}(4t\lambda^{3/2}+x\lambda^{1/2}) \\ &= 6t\lambda^{1/2}+\frac{1}{2}\frac{x}{\lambda^{1/2}} \end{aligned} \tag{3.121}$$

Inserting α' into (3.120) we can compute the RHS exact

$$\begin{aligned} 6tA(\beta_0)+xB(\beta_0) &= 6t\int_0^{\beta_0} d\lambda \frac{2\lambda^{1/2}}{(\beta_0-\lambda)^{1/2}} \\ &\quad + x\int_0^{\beta_0} d\lambda \frac{1}{\lambda^{1/2}(\beta_0-\lambda)^{1/2}} \\ &= 6t\pi\beta_0 + x\pi \end{aligned} \tag{3.122}$$

To make any further progress, analytical or numerical, the quantity ρ' must be computed. Thus we leave the equation for β_0, case B, in the following form

$$6t\pi\beta_0 + x\pi = C(\beta_0) \tag{3.123}$$

where C is the integral

$$C(\beta_0) = \int_0^{\beta_0} d\lambda \frac{2\rho'(\lambda)}{(\beta_0-\lambda)^{1/2}} \tag{3.124}$$

For case A we get the following equation for the phase function (3.97)

$$\begin{aligned} g'(\lambda) &= \frac{1}{2\pi i}X(\lambda)\int_0^{\beta_0} d\mu \frac{2\rho'(\mu) - 2\alpha'(\mu)}{X(\lambda)_+(\mu-\lambda)} \\ &+ \frac{1}{2\pi i}X(\lambda)\int_{\beta_0}^{1} d\mu \frac{-2i\tau'(\mu)}{X(\lambda)_+(\mu-\lambda)} \\ &= -\frac{1}{2\pi}(\lambda-\beta_0)^{1/2}\int_0^{\beta_0} d\mu \frac{2\rho'(\mu) - 2\alpha'(\mu)}{(\beta_0-\mu)^{1/2}(\mu-\lambda)} \\ &- \frac{1}{2\pi}(\lambda-\beta_0)^{1/2}\int_{\beta_0}^{1} d\mu \frac{2\tau'(\mu)}{(\mu-\beta_0)^{1/2}(\mu-\lambda)} \end{aligned} \tag{3.125}$$

Using the asymptotic condition (3.116) we get

$$\int_0^{\beta_0} d\lambda \frac{2\rho' - 2\alpha'}{(\beta_0-\lambda)^{1/2}} + \int_{\beta_0}^{1} d\lambda \frac{2\tau'}{(\lambda-\beta_0)^{1/2}} = 0 \tag{3.126}$$

The difference between this case and case B is the integral involving τ', also dependent on the initial potential u_0 and we can not make any further analytical simplifications past the ones performed for case B, reusing these gives

$$6t\pi\beta_0 + x\pi = C(\beta_0) - D(\beta_0) \tag{3.127}$$

where

$$D(\beta_0) = \int_{\beta_0}^{1} d\lambda \frac{2\tau'}{(\lambda-\beta_0)^{1/2}} \tag{3.128}$$

Equations (3.123) and (3.127) determines β_0. An important question is which of these equations is valid for a particular (x,t), and from [7] we have that both equations is valid for times up to breaking t^*. In section 3.2 we calculated the maximum point x^* of $u(x,t), t < t^*$ to be $x^* = -6t$. Based on what is obtained from actual calculations, we propose that equation (3.123) is valid for $x > x^*$ and equation (3.127) valid for $x < x^*$.

After breaking we need another phase in order to find solutions for all x, but that does not mean the above calculation only applies before breaking time. After breaking this phase connects smoothly with the second phase $\beta_0(x_0) = \beta_1(x_0)$ and is determined by the upper branch determined by equation (3.123) and valid for $x \in (x_0, s)$.

3.3.2 First phase after breaking, $N = 1, \beta_0 \neq 0$

Now consider a region where we need one subinterval e.g. $N = 1, \beta_0 \neq 0$. The equation for β_0 in this phase is the same as for the upper branch of β_0 for

$t < t^*$, hence we reuse equation (3.123), and we only need to develop equations determining (α_1, β_1). Since there is two unknowns we will need to use both equations (3.116) and (3.117). First we need an solution to the homogeneous problem, a natural choice would be

$$X(\lambda) = \lambda^{1/2}(\lambda - \alpha_1)^{1/2}(\lambda - \beta_1)^{1/2} \tag{3.129}$$

However, if we proceed with this equation eventually we will end up with a system of equations that is unsolvable. Therefore we instead try the following branch

$$X(\lambda) = \lambda^{-1/2}(\lambda - \alpha_1)^{1/2}(\lambda - \beta_1)^{1/2} \tag{3.130}$$

It is not trivial to determine in advance which of the branches of X is the correct choice, trail and error might be the most efficient method. Proceeding by finding the limiting functions X_+, if $\lambda < \alpha_1 < \beta_1$ we have

$$\begin{aligned} X_+ &= \lim_{\delta \to 0^+} X(\lambda + i\delta) \\ &= \lim_{\delta \to 0^+} \frac{(\lambda + i\delta - \alpha_1)^{1/2}(\lambda + i\delta - \beta_1)^{1/2}}{(\lambda + i\delta)^{1/2}} \\ &= i^2\lambda^{-1/2}(\alpha_1 - \lambda)^{1/2}(\beta_1 - \lambda)^{1/2} = -\lambda^{-1/2}(\alpha_1 - \lambda)^{1/2}(\beta_1 - \lambda)^{1/2} \end{aligned} \tag{3.131}$$

Similar we have when $\alpha_1 < \lambda < \beta_1$

$$\begin{aligned} X_+ &= \lim_{\delta \to 0^+} X(\lambda + i\delta) \\ &= i\lambda^{-1/2}(\lambda - \alpha_1)^{1/2}(\beta_1 - \lambda)^{1/2} \end{aligned} \tag{3.132}$$

Summarised results for X_+ is

$$X_+(\lambda) = \begin{cases} -\lambda^{-1/2}(\alpha_1 - \lambda)^{1/2}(\beta_1 - \lambda)^{1/2}, \lambda < \alpha_1 < \beta_1 \\ i\lambda^{-1/2}(\lambda - \alpha_1)^{1/2}(\beta_1 - \lambda)^{1/2}, \alpha_1 < \lambda < \beta_1 \end{cases} \tag{3.133}$$

The phase function g' is given by

$$\begin{aligned}
\frac{g'(\lambda)}{X(\lambda)} &= \left[\int_0^{\alpha_1} \frac{d\mu}{2\pi i}\frac{-2i\tau'(\mu)}{X_+(\mu)(\mu-\lambda)} + \int_{\alpha_1}^{\beta_1} d\mu \frac{1}{2\pi i}\frac{2\rho'(\mu)-2\alpha'(\mu)}{X_+(\mu)(\mu-\lambda)}\right] \\
&= \int_0^{\alpha_1} \frac{d\mu}{\pi}\frac{\tau'(\mu)}{\mu^{-1/2}(\mu-\alpha_1)^{1/2}(\mu-\beta_1)^{1/2}(\mu-\lambda)} \\
&- \int_{\alpha_1}^{\beta_1} \frac{d\mu}{\pi}\frac{\rho'(\mu)-\alpha'(\mu)}{\mu^{-1/2}(\mu-\alpha_1)^{1/2}(\beta_1-\mu)^{1/2}(\mu-\lambda)} \\
&= \int_0^{\alpha_1} \frac{d\mu}{\pi}\frac{\tau'(\mu)}{\mu^{-1/2}(\mu-\alpha_1)^{1/2}(\mu-\beta_1)^{1/2}(\mu-\lambda)} \\
&- \int_{\alpha_1}^{\beta_1} \frac{d\mu}{\pi}\frac{\rho'(\mu)}{\mu^{-1/2}(\mu-\alpha_1)^{1/2}(\beta_1-\mu)^{1/2}(\mu-\lambda)} \\
&+ \frac{6t}{\pi}\int_{\alpha_1}^{\beta_1} d\mu \frac{\mu}{(\mu-\alpha_1)^{1/2}(\beta_1-\mu)^{1/2}(\mu-\lambda)} \\
&+ \frac{x}{2\pi}\int_{\alpha_1}^{\beta_1} d\mu \frac{1}{(\mu-\alpha_1)^{1/2}(\beta_1-\mu)^{1/2}(\mu-\lambda)} \\
&= H_1 - H_2 + \frac{6t}{\pi}H_3 + \frac{x}{2\pi}H_4
\end{aligned} \tag{3.134}$$

The two integrals H_3 and H_4 can be computed as Cauchy integrals

$$\begin{aligned}
H_3 &= P.V_\lambda \int_{\alpha_1}^{\beta_1} d\mu \frac{\mu}{(\mu-\alpha_1)^{1/2}(\beta_1-\mu)^{1/2}(\mu-\lambda)} \\
&= \pi
\end{aligned} \tag{3.135}$$

and

$$\begin{aligned}
H_4 &= P.V_\lambda \int_{\alpha_1}^{\beta_1} d\mu \frac{1}{(\mu-\alpha_1)^{1/2}(\beta_1-\mu)^{1/2}(\mu-\lambda)} \\
&= 0
\end{aligned} \tag{3.136}$$

The first equation determining (α_1, β_1) is found using (3.116) and (3.134)

$$\begin{aligned}
0 &= \int_0^{\alpha_1} d\mu \frac{-2\tau'(\mu)}{\mu^{-1/2}(\alpha_1-\mu)^{1/2}(\beta_1-\mu)^{1/2}} \\
&+ \int_{\alpha_1}^{\beta_1} d\mu \frac{2\rho'(\mu)-2\alpha'(\mu)}{\mu^{-1/2}(\mu-\alpha_1)^{1/2}(\beta_1-\mu)^{1/2}} \\
&= F_1 + F_2 + C_0
\end{aligned} \tag{3.137}$$

where F_1,F_2 denotes the integral involving τ', ρ' and C_0 the α' integral. As for the $N = 0, \beta_0 \neq 0$ case, the integral C_0 can be simplified

$$\begin{aligned} C_0 &= -\int_{\alpha_1}^{\beta_1} d\mu \frac{2\alpha'(\mu)}{\mu^{-1/2}(\mu-\alpha_1)^{1/2}(\beta_1-\mu)^{1/2}} \\ &= -12t\int_{\alpha_1}^{\beta_1} d\mu \frac{\mu}{(\mu-\alpha_1)^{1/2}(\beta_1-\mu)^{1/2}} - x\int_{\alpha_1}^{\beta_1} d\mu \frac{1}{(\mu-\alpha_1)^{1/2}(\beta_1-\mu)^{1/2}} \\ &= -6t\pi(\alpha_1+\beta_1) - \pi x \end{aligned} \tag{3.138}$$

Our first equation is therefore

$$6t\pi(\alpha_1+\beta_1) + \pi x = F_1 + F_2 \tag{3.139}$$

where

$$\begin{aligned} F_1 &= \int_0^{\alpha_1} d\mu \frac{-2\tau'(\mu)}{\mu^{-1/2}(\alpha_1-\mu)^{1/2}(\beta_1-\mu)^{1/2}} \\ F_2 &= \int_{\alpha_1}^{\beta_1} d\mu \frac{2\rho'(\mu)}{\mu^{-1/2}(\mu-\alpha_1)^{1/2}(\beta_1-\mu)^{1/2}} \end{aligned} \tag{3.140}$$

The second equation is obtained using equation (3.117), where we replace $\tau(\beta_1)$ with zero, according to the theory.

$$\int_{\alpha_1}^{\beta_1} d\mu \left[g'_+(\mu) - g'_-(\mu)\right] = 2i\tau(\alpha_1) \tag{3.141}$$

From equation (3.134) we have the phase function

$$g'(\lambda) = \lambda^{-1/2}(\lambda-\alpha_1)^{1/2}(\lambda-\beta_1)^{1/2}\left[H_1 - H_2 + 6t\right] \tag{3.142}$$

Finding the limiting functions g_+ and g_- then gives

$$\begin{aligned} g'_+(\mu) - g'_-(\mu) &= iX\left[2H_1 - 2H_2 + 12t\right] \\ &= iX\Bigg[\frac{2}{\pi}\int_0^{\alpha_1} ds \frac{s^{1/2}\tau'(s)}{(s-\alpha_1)^{1/2}(s-\beta_1)^{1/2}(s-\mu)} \\ &\quad - \frac{2}{\pi}P.V_\mu \int_{\alpha_1}^{\beta_1} ds \frac{s^{1/2}\rho'(s)}{(s-\alpha_1)^{1/2}(\beta_1-s)^{1/2}(s-\mu)} \\ &\quad + 12t\Bigg] \end{aligned} \tag{3.143}$$

Inserting into equation (3.141) gives the following equation containing iterated integrals

$$\frac{2}{\pi}\int_{\alpha_1}^{\beta_1} d\mu \frac{(\mu-\alpha_1)^{1/2}(\beta_1-\mu)^{1/2}}{\mu^{1/2}} \int_0^{\alpha_1} ds \frac{s^{1/2}\tau'(s)}{(s-\alpha_1)^{1/2}(s-\beta_1)^{1/2}(s-\mu)}$$
$$-\frac{2}{\pi}\int_{\alpha_1}^{\beta_1} d\mu \frac{(\mu-\alpha_1)^{1/2}(\beta_1-\mu)^{1/2}}{\mu^{1/2}} P.V_\mu \int_{\alpha_1}^{\beta_1} ds \frac{s^{1/2}\rho'(s)}{(s-\alpha_1)^{1/2}(\beta_1-s)^{1/2}(s-\mu)}$$
$$+12t\int_{\alpha_1}^{\beta_1} d\mu \frac{(\mu-\alpha_1)^{1/2}(\beta_1-\mu)^{1/2}}{\mu^{1/2}} = 2\tau(\alpha_1) \tag{3.144}$$

It is actually possible to make some analytical simplifications here, starting with the last term

$$\int_{\alpha_1}^{\beta_1} d\mu \frac{(\mu-\alpha_1)^{1/2}(\beta_1-\mu)^{1/2}}{\mu^{1/2}} = \frac{2}{3}\beta_1^{3/2}\gamma^{1/2}\left[(1+\gamma)E(1-\frac{1}{\gamma}) - 2K(1-\frac{1}{\gamma})\right] \tag{3.145}$$

where we have defined $\gamma = \frac{\alpha_1}{\beta_1}$. To simplify notation we set

$$S(\gamma) = \frac{2}{3}\gamma^{1/2}\left[(1+\gamma)E(1-\frac{1}{\gamma}) - 2K(1-\frac{1}{\gamma})\right] \tag{3.146}$$

Where symbols E and K are the complete elliptic integrals of first and second kind. Next consider the first term in (3.144), by a change of integration order we have

$$\frac{2}{\pi}\int_{\alpha_1}^{\beta_1} d\mu \frac{(\mu-\alpha_1)^{1/2}(\beta_1-\mu)^{1/2}}{\mu^{1/2}} \int_0^{\alpha_1} ds \frac{s^{1/2}\tau'(s)}{(\alpha_1-s)^{1/2}(\beta_1-s)^{1/2}(s-\mu)} =$$
$$\frac{2}{\pi}\int_0^{\alpha_1} ds \frac{s^{1/2}\tau'(s)}{(\alpha_1-s)^{1/2}(\beta_1-s)^{1/2}} \int_{\alpha_1}^{\beta_1} d\mu \frac{(\mu-\alpha_1)^{1/2}(\beta_1-\mu)^{1/2}}{\mu^{1/2}(s-\mu)} \tag{3.147}$$

Introduce the change of variables $s = \beta_1\eta$, $\mu = \beta_1\xi$

$$\frac{2}{\pi}\beta_1\int_0^{\gamma} d\eta \frac{\eta^{1/2}\tau'(\beta_1\eta)}{(\gamma-\eta)^{1/2}(1-\eta)^{1/2}} \int_\gamma^1 d\xi \frac{(\xi-\gamma)^{1/2}(1-\xi)^{1/2}}{\xi^{1/2}(\eta-\xi)} \tag{3.148}$$

Now the last integral can be computed

$$\int_\gamma^1 d\xi \frac{(\xi-\gamma)^{1/2}(1-\xi)^{1/2}}{\xi^{1/2}(\eta-\xi)} =$$
$$\frac{2}{\gamma^{1/2}}\left[\gamma E(1-\frac{1}{\gamma}) - (1+\gamma-\eta)K(1-\frac{1}{\gamma}) + (1-\eta)\Pi(\frac{\gamma-1}{\gamma-\eta}, 1-\frac{1}{\gamma})\right] \tag{3.149}$$

where Π is the complete elliptic integral of the third kind. Note that there are slight differences in how Π is defined by various authors, see section C.2 for

details. Set $\theta = 1 - \frac{1}{\gamma}$, and we define

$$G(\eta,\gamma) = \frac{4}{\pi}\frac{\eta^{1/2}}{\gamma^{1/2}(\gamma-\eta)^{1/2}(1-\eta)^{1/2}}\left[\gamma E(\theta) - (1+\gamma-\eta)K(\theta) + (1-\eta)\Pi(\frac{\gamma-1}{\gamma-\eta},\theta)\right] \tag{3.150}$$

Thus, we can write the first term in (3.144) compactly as

$$\beta_1 \int_0^\gamma d\eta G(\eta,\gamma)\tau'(\beta_1\eta) \tag{3.151}$$

By the same change of variables and interchanging the integration order we get a similar results for the second term in (3.144)

$$\begin{aligned} &PV_\eta \int_\gamma^1 d\xi \frac{(\xi-\gamma)^{1/2}(1-\xi)^{1/2}}{\xi^{1/2}(\eta-\xi)} = \\ &= 2\gamma^{1/2}\left[E(\theta) - K(\theta)\right] + \frac{2}{\gamma^{1/2}}(\eta-1)\Pi(1-\frac{\eta}{\gamma},\theta) \end{aligned} \tag{3.152}$$

Using this we can write the third term as

$$H(\eta,\gamma) = \frac{2\eta^{1/2}}{\pi(\eta-\gamma)^{1/2}(1-\eta)^{1/2}}\left[2\gamma^{1/2}\left\{E(\theta) - K(\theta)\right\} + \frac{2}{\gamma^{1/2}}(\eta-1)\Pi(1-\frac{\eta}{\gamma},\theta)\right] \tag{3.153}$$

Thus this term takes the form

$$\beta_1 \int_\gamma^1 d\eta H(\eta,\gamma)\rho'(\beta_1\eta) \tag{3.154}$$

Collecting the results from equations (3.154),(3.145),(3.151) to form our second equation determining (α_1,β_1), and using (3.139) we get the 2×2 system of equations

$$\begin{aligned} 6t(\alpha_1+\beta_1) + x &= -\frac{2}{\pi}\int_0^{\alpha_1} d\mu \frac{\mu^{1/2}\tau'(\mu)}{(\alpha_1-\mu)^{1/2}(\beta_1-\mu)^{1/2}} + \frac{2}{\pi}\int_{\alpha_1}^{\beta_1} d\mu \frac{\mu^{1/2}\rho'(\mu)}{(\mu-\alpha_1)^{1/2}(\beta_1-\mu)^{1/2}} \\ 2\tau'(\alpha_1) &= 12t\beta_1^{3/2}S(\gamma) + \beta_1\int_0^\gamma d\eta G(\eta,\gamma)\tau'(\beta_1\eta) - \beta_1\int_\gamma^1 d\eta H(\eta,\gamma)\rho'(\beta_1\eta) \end{aligned} \tag{3.155}$$

Solving the system (3.155) will in practice be a numerical task, to be able to solve all the integrals exact for a given u_0 seems unlikely. However, the reduction from iterated integrals reduces the numerical work considerable. Now equations is developed for the β_0 phase and the phase (α_1,β_1) and an important question is for which(if any) these two phases are sufficient. This will be addressed in a later section, for now we will assume that these will be

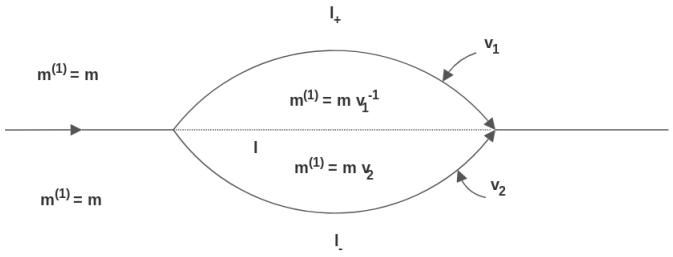

Figure 3.3: Illustration of contour deformation

enough for the potentials we consider.

When we introduced the phase function g a number of requirements it had to satisfy was made, but no justification on why these requirements was introduced was not. While the complete answer is fairly advanced, we can give an outline of the argument. First consider a generic vector RH problem with a jump condition v that can factorized into two invertible matrices

$$\boldsymbol{n}_+ = \boldsymbol{n}_- v_2 v_1 \tag{3.156}$$

We still use the arc $\lambda \in (-\infty, 1)$,denote this as l, but in general this can be arbitrary. Since both v_2 and v_1 are invertible we have

$$\boldsymbol{n}_+ v_1^{-1} = \boldsymbol{n}_- v_2 \tag{3.157}$$

By analytical continuation and a change of variables the above problem can be formulated as two new RH problems, see figure (3.3)

$$\boldsymbol{n}_+^{(1)} = \boldsymbol{n}_-^{(1)} v_1, \qquad z \in l_\oplus \tag{3.158}$$
$$\boldsymbol{n}_+^{(1)} = \boldsymbol{n}_-^{(1)} v_2, \qquad z \in l_\ominus \tag{3.159}$$

Let us now examine the the three cases (3.91),(3.92) and (3.93).

3.3.3 Case I: $i\,[g_+ - g_-] = 2\tau$ and $h' < 0$

Consider an interval (a, b) where this condition holds, the middle matrix in (3.87) reduces to

$$v^{(1)} = \begin{bmatrix} 1 & -i\exp(-\frac{i}{\epsilon}h) \\ -i\exp(\frac{i}{\epsilon}h)) & \exp(-\frac{2}{\epsilon}\tau) \end{bmatrix} \tag{3.160}$$

From the equation (3.69) determining τ and the requirements (1) made on the initial potential u_0 it is clear that $\tau > 0, \lambda \in (0, 1)$, hence as $\epsilon \to 0^+$ this

reduces to

$$v^{(1)} = \begin{bmatrix} 1 & -i\exp(-\frac{i}{\epsilon}h) \\ -i\exp(\frac{i}{\epsilon}h)) & 0 \end{bmatrix} \tag{3.161}$$

This matrix can be factorized in the following way

$$v^{(1)} = v_2 v_1 = \begin{bmatrix} 1 & 0 \\ -i\exp(\frac{i}{\epsilon}h)) & 1 \end{bmatrix} \begin{bmatrix} 1 & -i\exp(-\frac{i}{\epsilon}h) \\ 0 & 1 \end{bmatrix} \tag{3.162}$$

The point is, from [7], when v_1 is inverted and the conditions on h is used, both v_1^{-1} and v_2 reduces to zero. Thus there is no jump, meaning that on this interval we have $\boldsymbol{m}_+ = \boldsymbol{m}_-$ and we can remove the intervals (a, b) from $(-\infty, 1)$.

3.3.4 Case II: $[g_+ - g_-] = 0$ and $h' > 0$

For this case the middle matrix in (3.87) reduces to

$$v^{(1)} = \begin{bmatrix} 1 & -i\exp(-\frac{i}{\epsilon}h) \\ -i\exp(\frac{i}{\epsilon}h)) & \exp(-\frac{2i}{\epsilon}\tau) \end{bmatrix} \tag{3.163}$$

tau is still positive and as $\epsilon \to 0$

$$v^{(1)} = \begin{bmatrix} 1 & -i\exp(-\frac{i}{\epsilon}h) \\ -i\exp(\frac{i}{\epsilon}h)) & 0 \end{bmatrix} \tag{3.164}$$

This matrix can be factorized in the following way

$$v^{(1)} = v_2 v_1 = \begin{bmatrix} 1 & 0 \\ -i\exp(\frac{i}{\epsilon}h)) & 1 \end{bmatrix} \begin{bmatrix} 1 & -i\exp(-\frac{i}{\epsilon}h) \\ 0 & 1 \end{bmatrix} \tag{3.165}$$

Then the same argument as for case II is used and the intervals where this holds can also be removed.

3.3.5 Case III: $-2\tau < -i\,[g_+ - g_-] < 0$ and $h' = 0$

$$\begin{bmatrix} 0 & -i\exp(-\frac{i}{\epsilon}h) \\ -i\exp(\frac{i}{\epsilon}h)) & 0 \end{bmatrix} \tag{3.166}$$

This case is the region we can not remove and where we have (α_j, β_j). These regions give a RH problem that can be solved exactly, and the reason why the problem is partitioned up into the three cases.

Now that equations for the two first phases have been developed we proceed to describe how to construct a solution using these. Before breaking $t < t^*$ the solution is simply β_0. After breaking, the solution to the final RH problem, after the limit $\epsilon \to 0^+$ is taken, is given in [7]

$$u(x,t,\epsilon) \sim \sum_{j=0}^{N}(\alpha_j + \beta_j) + 2q_{N-1} - 2\epsilon^2 \partial_{xx} \log(\Theta(\frac{\Omega}{2\pi\epsilon}, \Phi)) \tag{3.167}$$

where the remaining unknowns are q_{N-1}, Ω and Φ. The function Θ is the known Riemann-Theta(also known as Siegel-Theta) function

$$\Theta(\Omega, \Phi) = \sum_n \exp\left[i\pi(n\Omega n + 2n\Phi)\right] \tag{3.168}$$

The quantity Ω is the same as Ω_j in the scalar RH problem for g, equations (3.99)-(3.101). For $j = 0$ this is set to zero, thus we only need to calculate $\Omega_1, ..., \Omega_N$, corresponding to $(\alpha_1, \beta_1), ..., (\alpha_N, \beta_N)$. To be able to solve for a given Ω_j we write the general solution to equations (3.99)-(3.101), for the case (α_j, β_j)

$$g(\lambda) = X(\lambda)\left[\int_{\cup I_j} \frac{d\mu}{2\pi i}\frac{2\rho(\mu) - 2\alpha(\mu) - \Omega_j}{X_+(\mu)(\mu - \lambda)} + \int_{(0,E)-\cup I_j} \frac{d\mu}{2\pi i}\frac{-2i\tau(\mu)}{X_+(\mu)(\mu - \lambda)}\right] \tag{3.169}$$

By the same argument as for g', the condition $g \sim \frac{1}{\lambda^{1/2}}, \lambda \to \infty$ leads to

$$\left[\int_{\cup I_j} \frac{d\mu}{2\pi i}\frac{2\rho(\mu) - 2\alpha(\mu) - \Omega_j}{X_+(\mu)} + \int_{(0,E)-\cup I_j} \frac{d\mu}{2\pi i}\frac{-2i\tau(\mu)}{X_+(\mu)}\right] = 0$$

$$\int_{\cup I_j} \frac{d\mu}{2\pi i}\frac{\Omega_j}{X_+(\mu)} = A + B \tag{3.170}$$

Where A and B are the integrals containing ρ, α (A) and τ (B). For these intervals we have required that $h = \Omega$ and constant in μ, thus we can solve for Ω_j

$$\Omega_j \int_{\cup I_j} \frac{d\mu}{2\pi i}\frac{1}{X_+} = A + B$$

$$\Omega_j = \left[\int_{\cup I_j} \frac{d\mu}{2\pi i}\frac{1}{X_+}\right]^{-1}(A + B) \tag{3.171}$$

One important detail is that the homogeneous solution X when calculating g need not be the same as X for g', but we must have that the derivate of g is equal to the phase function for g'. This must be examined for a specific potential u_0.

What further complicates the situation is that a new homogeneous solution is required for every new subinterval, and the analytical work increases in complexity. If we consider the case with one subinterval i.g. (α_1, β_1), numerical results suggests that for potentials we consider(satisfies definition (1)) we must use

$$X = \lambda^{1/2}(\lambda - \alpha_1)^{1/2}(\lambda - \beta_1)^{1/2} \tag{3.172}$$

when calculating g and for g' we must use

$$X = \lambda^{-1/2}(\lambda - \alpha_1)^{1/2}(\lambda - \beta_1)^{1/2} \tag{3.173}$$

If we accept this we can make some simplifications in solving for Ω_1, first we have

$$\begin{aligned}\int_{\alpha_1}^{\beta_1} \frac{d\mu}{2\pi i}\frac{1}{X_+} &= -\int_{\alpha_1}^{\beta_1} \frac{d\mu}{2\pi}\frac{1}{\mu^{1/2}(\mu-\alpha_1)^{1/2}(\mu-\beta_1)^{1/2}} \\ &= -\frac{K(1-\gamma)}{\pi\alpha^{1/2}}\end{aligned} \tag{3.174}$$

The term containing α can also be analytical computed

$$\begin{aligned}\int_{\alpha_1}^{\beta_1} \frac{d\mu}{2\pi i}\frac{-2\alpha(\mu)}{X_+} &= \frac{1}{\pi}\int_{\alpha_1}^{\beta_1} d\mu \frac{4t\mu^{3/2} + x\mu^{1/2}}{\mu^{1/2}(\mu-\alpha_1)^{1/2}(\mu-\beta_1)^{1/2}} \\ &= \frac{4t}{\pi}\int_{\alpha_1}^{\beta_1} d\mu \frac{\mu^{3/2}}{\mu^{1/2}(\mu-\alpha_1)^{1/2}(\mu-\beta_1)^{1/2}} \\ &+ \frac{x}{\pi}\int_{\alpha_1}^{\beta_1} d\mu \frac{1}{\mu^{1/2}(\mu-\alpha_1)^{1/2}(\mu-\beta_1)^{1/2}} \\ &= 2t(\alpha_1+\beta_1) + x\end{aligned} \tag{3.175}$$

Thus Ω_1 can be written as

$$\begin{aligned}\Omega_1 = -\frac{K(1-\gamma)}{\pi\alpha^{1/2}}\Bigg[2t(\alpha_1+\beta_1) + x - \frac{1}{\pi}\int_{\alpha_1}^{\beta_1} d\mu \frac{\rho(\mu)}{\mu^{1/2}(\mu-\alpha_1)^{1/2}(\beta_1-\mu)^{1/2}} \\ + \frac{1}{\pi}\int_{\alpha_1}^{\beta_1} d\mu \frac{\tau(\mu)}{\mu^{1/2}(\mu-\alpha_1)^{1/2}(\beta_1-\mu)^{1/2}}\Bigg]\end{aligned} \tag{3.176}$$

To get the final form of Ω_1, the remaining integrals must be computing either analytical or numerical, depending on ρ and τ. Also needed in the solution (3.167) is the quantities q_{N-1}. These quantities occurs when going from the solution for u (3.90) to the solution (3.167), and related to the Riemann surface for the homogeneous solution X. From the method, the meromorphic differentials for the Riemann surface is

$$\frac{q}{X}d\lambda = \frac{\lambda^N + q_{N-1}\lambda^{N-1} + \ldots + q_0}{X}d\lambda \tag{3.177}$$

The unknown quantities q can be determined by

$$\int_{a_j} \frac{q}{X} d\lambda = 0, j = 1, ..., N \tag{3.178}$$

Where a_j is closed curves around the intervals (α_j, β_j), traversed counter clockwise. If we use the homogeneous solution we can compute this for $j = 1$, setting $N = 1$ in (3.178)

$$\begin{aligned}
\int_{a_1} d\lambda \frac{\lambda - q_0}{\lambda^{1/2}(\lambda - \alpha_1)^{1/2}(\lambda - \beta_1)^{1/2}} &= 0 \\
\int_{\beta_1}^{\alpha_1} d\lambda \frac{\lambda - q_0}{\lambda^{1/2}(\lambda - \alpha_1)^{1/2}(\lambda - \beta_1)^{1/2}} &= 0 \\
q_0 = -\alpha_1 \frac{E(1 - \frac{\beta_1}{\alpha_1})}{K(1 - \frac{\beta_1}{\alpha_1})} &
\end{aligned} \tag{3.179}$$

The remaining unknown in (3.167) is Φ, the period matrix for Ω. This is computed by first introducing a basis for the holomorphic differential for the Riemann surface of X

$$\omega_i = \frac{p_i(\lambda)}{X} d\lambda \tag{3.180}$$

where p_i are polynomials of degree $N - 1$ and determined by

$$\int_{a_j} \omega_i = \delta_{ij} \tag{3.181}$$

where a_j is the same curves as above. After p_i is determined using the above equation the period matrix can be calculated by

$$\Psi_j = -\int_{b_i} \omega_i \tag{3.182}$$

where b_i are curves connecting β_0 with α_j. As before we make explicit calculations for the first phase $j = 1, N = 1$

$$\begin{aligned}
\int_{a_j} \omega_1 &= 1 \\
\int_{\beta_1}^{\alpha_1} d\lambda \frac{p_1}{\lambda^{1/2}(\lambda - \alpha_1)^{1/2}(\lambda - \beta_1)^{1/2}} & \\
p_1 = \frac{i\alpha_1^{1/2}}{2K(1 - \frac{\beta_1}{\alpha_1})} &
\end{aligned} \tag{3.183}$$

and finally we can calculate Ψ

$$\begin{aligned}\Psi_1 &= -\int_0^{\alpha_1} d\lambda \frac{p_i}{\lambda^{1/2}(\lambda-\alpha_1)^{1/2}(\lambda-\beta_1)^{1/2}} \\ &= i\frac{\alpha_1^{1/2}K(\frac{\alpha_1}{\beta_1})}{\beta_1^{1/2}K(1-\frac{\beta_1}{\alpha_1})}\end{aligned} \tag{3.184}$$

We have now described the mechanical steps from [7] needed to construct the solution to the KdV equation in the small dispersion limit, and developed the equations for the phase before breaking β_0 and one additional phase (α_1, β_1). If it is sufficient with these two phases we have a complete asymptotic solution($\epsilon \to 0$) to the KdV equation (3.1). To summarise, the solution before breaking $t < t^*$ is given by

$$u(x,t) \sim \begin{cases}\beta_0(x,t), \ x \in [-s,s] \\ 0 \ o.w.\end{cases} \tag{3.185}$$

and after breaking $t > t^*$ the solution is

$$u(x,t) \sim \begin{cases}\beta_0(x,t), \ x \in (x_0,s) \\ \alpha_1(x,t)+\beta_1(x,t)+2q_0-2\epsilon^2\partial_{xx}\log(\Theta(\frac{\Omega_1}{2\pi\epsilon},\Phi_1)), \ x \in (x_1,x_0) \\ 0 \ o.w.\end{cases} \tag{3.186}$$

where β_0 is the upper branch of β_0 before breaking. To obtain an actual solution the remaining integrals need to be calculated and this is in general a numerical task. In addition the middle term in (3.186) must be treated numerically after the phase (α_1, β_1) is obtained. Numerical implementations and results of this will be described in chapter (4), in the remaining two sections of this chapter we will examine if it is sufficient with only using the two phases we have derived in this section and bringing up a possible weakness with the theory.

3.4 Investigating the possibility of a new phase $N = 2$

In section 3.3 we introduced the phase function g and through a series of simplifications and assumptions it was shown that to find the solution to the KdV we needed to find the phase function for all space x and time t. Further we discussed the three simplest cases $(N = 0, \beta_0 = 0)$, $(N = 0, \beta_0 \neq 0)$ and $(N = 1, \beta_0 = 0)$, each valid in a (x, t) region, by developing general equations

to determine β_0 for the second case and (α_1, β_1) for the third. The first case is the trivial solution and corresponds to the regions in space and time where the solution is zero. An important question, for potentials $u_0(x)$ that satisfies the requirements in definition (1), are if these three cases enough to find solutions to the KdV equation for all (x, t)? The case $(N = 0, \beta_0 \neq 0)$ is valid for times before the KdV equation breaks down, either valid for all x or for a finite region, determined if u_0 has compact or non-compact support. The trivial solution is only applicable for potentials with compact support. In the solution process the time and space variables are parameters and the eigenvalue λ is the independent variable, we now ask if it is possible to solve the system (3.187)-(3.188), determining the phase $(N = 1, \beta_0 = 0), \forall \lambda \in (0, 1)$? As a reminder, the equations derived in the previous section is as follows

$$6t(\alpha_1 + \beta_2) + x = f_1(\alpha_1, \beta_1) \tag{3.187}$$

$$12t\beta_1^{3/2} s(\frac{\alpha_1}{\beta_1}) + \beta_1 f_2(\alpha_1, \beta_1) = 2\tau(\alpha_1) \tag{3.188}$$

where

$$\begin{aligned} 0 \leq \alpha_1, \beta_1 \leq 1 \\ \alpha_1 < \beta_1 \end{aligned} \tag{3.189}$$

and $s(\gamma)$ is defined in equation (3.146) and f_2 are from (3.155)

$$f_2 = \beta_1 \int_0^\gamma d\eta G(\eta, \gamma)\tau'(\beta_1\eta) - \beta_1 \int_\gamma^1 d\eta H(\eta, \gamma)\rho'(\beta_1\eta) \tag{3.190}$$

where G are defined in (3.150) and H in (3.153). The quantity f_1 in (3.187) are

$$\begin{aligned} f_1 &= -\frac{\pi}{2}\int_0^{\alpha_1} d\mu \frac{\mu^{1/2}\tau'(\mu)}{(\alpha_1 - \mu)^{1/2}(\beta_1 - \mu)^{1/2}} + \frac{\pi}{2}\int_{\alpha_1}^{\beta_1} d\mu \frac{\mu^{1/2}\rho'(\mu)}{(\mu - \alpha_1)^{1/2}(\beta_1 - \mu)^{1/2}} \\ &= -\frac{\pi}{2}\int_0^{\alpha_1} d\mu k_1(\alpha_1, \beta_1; \mu)\tau'(\mu) + \frac{\pi}{2}\int_{\alpha_1}^{\beta_1} d\mu k_2(\alpha_1, \beta_1; \mu)\rho'(\mu) \\ &= f_{1a} + f_{1b} \end{aligned} \tag{3.191}$$

Equations (3.187) and (3.191) are of main interest in the following calculations, but the whole system is included for completeness. We are now interesting in answering for which (α_1, β_1) there can exist a solution for (3.187), and specifically if there can exist solutions where $\alpha_1 \to \beta_1$. From the conditions on (α_1, β_1) we will look for a solution in a triangle domain, illustrated in figure (3.4). Further, the KdV equation defined with a negative nonlinear term dictates a left moving solution, meaning that in the region $x \in [x_0, x_1]$ where this phase is valid the space variable x is always negative, thus $x < 0$. Also, since time is always positive we have $6t(\alpha_1 + \beta_1) > 0$. Using this we know something about

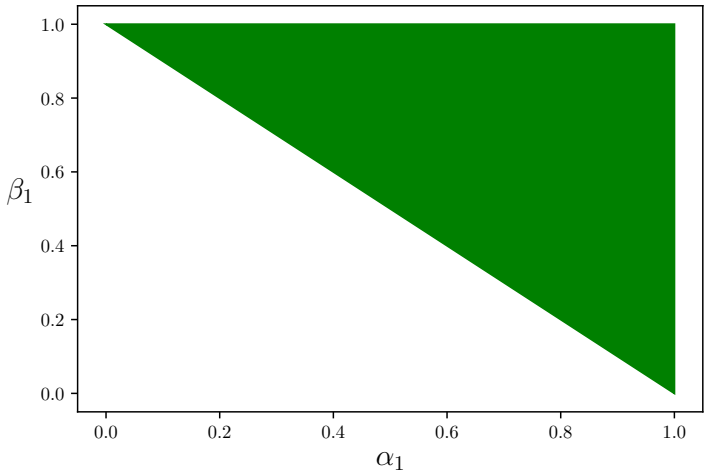

Figure 3.4: Solution space(coloured region) for system (3.187)-(3.188)

the LHS of equation (3.187) and inspired by this let us examine the RHS. Let us for the moment discard τ' and ρ' in (3.191) and compute

$$K_1(\alpha_1, \beta_1) = \int_0^{\alpha_1} d\mu k_1(\alpha_1, \beta_1; \mu) = 2\sqrt{\beta_1}\left[K(\frac{\alpha_1}{\beta_1}) - E(\frac{\alpha_1}{\beta_1})\right] \tag{3.192}$$

and

$$K_2(\alpha_1, \beta_1) = \int_{\alpha_1}^{\beta_1} d\mu k_2(\alpha_1, \beta_1; \mu) = 2\sqrt{\alpha_1}E(1 - \frac{\alpha_1}{\beta_1}) \tag{3.193}$$

We now take the limit as $\alpha_1 \longrightarrow \beta_1, \alpha_1, \beta_1 \neq 0$ for both K_1 and K_2

$$\lim_{\alpha_1 \to \beta_1} K_1 = \infty \tag{3.194}$$

$$\lim_{\alpha_1 \to \beta_1} K_2 = \pi\sqrt{\beta_1} \tag{3.195}$$

Since (3.194) diverges as $\alpha_1 \longrightarrow \beta_1$, the integral f_{1a} also diverge unless the quantity τ' counters this i.g. $\lim_{\alpha_1 \to \beta_1} \tau' = 0$. Similarly, the integral f_{1b} does not diverge unless ρ' displays some singular behaviour in the limit. We are interested in finding, in the limit $\alpha_1 \longrightarrow \beta_1$ whether f_1 converges or diverges, and it it diverges we want to know it goes to positive or negative infinity. The following possibilities exists

- The divergent term K_1 (3.194) dominates, causing f_1 to approach $\pm\infty$, depending on the sign of τ'
- τ' is zero in the limit, cancelling the divergent term (3.194)

- ρ' is zero in the limit
- ρ' can make f_{1b} divergent,causing f_1 to either converge or diverge, depending on signs and factors compared to f_{1a}.
- A consistent combination of the options above

These possibilities will now be examined. As a reminder, the functions τ and ρ are defined as

$$\rho(\mu) = x_+\mu^{1/2} + \int_{x_+}^{s} dx \left[\mu^{1/2} - (\mu - u_0(x))^{1/2}\right] \tag{3.196}$$

$$\tau(\mu) = 2\int_0^{x_+} dx(u_0(x) - \mu)^{1/2} \tag{3.197}$$

where s is the support of u_0. Since the integrals in system (3.187)-(3.188) is integrated over μ, we let $\lambda \to \mu$, but the two variables represents the same. Differentiating under the integral sign [12] gives

$$\rho' = \frac{x_+(\mu)}{2\sqrt{\mu}} + \frac{1}{2}\int_{x_+(\mu)}^{s} dx \left[\frac{1}{\sqrt{\mu}} - \frac{1}{\sqrt{\mu - u_0(x)}}\right] \tag{3.198}$$

$$\tau' = -\int_0^{x_+} dx \frac{1}{\sqrt{u_0(x) - \mu}} \tag{3.199}$$

The function u_0 is the potential and satisfies (1). The function $x_+(\mu)$ are defined $x_+ = u_0^{-1}(\mu)$ and is continuous since u_0 is continuous. Further, using the definition of τ and x_+ we must have

$$\begin{aligned} \tau(\mu) &\geq 0 \\ \tau'(\mu) &\leq 0, \forall \mu \in (0,1) \end{aligned} \tag{3.200}$$

By looking at the definition of τ (3.197) and x_+ it is clear that $u_0 > \mu$ in the entire region of integration, see figure (3.5). Similarly, τ must have a maximum point when $\mu = 0$, corresponding to $x_+ \to s$, and decreases monotonically to zero when $\mu \to 1$. As a consequence τ' can only be zero in the limit $\mu \to 1$. From this we obtain our first result

- Since $\tau' \leq 0$ and $K_1(\alpha_1, \beta_1) \leq 0$, f_{1a} must either be zero or positive. Thus, as $\alpha_1 \to \beta_1$, provided $\tau' \neq 0$, f_{1a} diverges to positive infinity, if $\tau' = 0$, f_{1a} can converge.

Limits of ρ' and τ' as $\mu \to 1$

Let us first examine if τ' can be zero at $\mu = 1$. In the limit $x \to 0^{\pm}$ we have from definition (1) that we can approximate the potential as $u_0(x) \sim 1 - a|x|^n$

Figure 3.5: Coloured region illustrates the integral (3.196) from 0 to $u_0(x) = \mu$, a region where $u_0 \geq \mu$

where $n = 1, 2$. The turning point x_+ is computed by

$$\begin{aligned} 1 - a|x|^n &\approx \mu \\ x_+ &\sim \left(\frac{1-\mu}{a}\right)^{1/n} \end{aligned} \tag{3.201}$$

Let us make asymptotic calculations of tau as $\mu \longrightarrow 1$, first the linear case $n = 1$

$$\begin{aligned} \tau &\sim 2\int_0^{\frac{1-\mu}{a}} dx(1 - ax - \mu)^{1/2} \\ &= \frac{4}{3a}(1-\mu)^{3/2}, x \longrightarrow 0^+ \end{aligned} \tag{3.202}$$

and the derivative for this case is

$$\tau' \sim -\frac{2}{a}(1-\mu)^{1/2} \tag{3.203}$$

Taking the limit as $\mu \longrightarrow 1$ does not pose any problems for either τ or τ'

$$\begin{aligned} \lim_{\mu \to 1} \frac{4}{3a}(1-\mu)^{3/2} &= 0 \\ \lim_{\mu \to 1} -\frac{2}{a}(1-\mu)^{1/2} &= 0 \end{aligned} \tag{3.204}$$

Indicating that for potentials that are linear as $x \longrightarrow 0$ gives exactly the result that $\tau'(1) = 0$, the only point where this is possible. Repeating the process for

the parabolic case $n = 2$ we find τ and τ'

$$\begin{aligned}\tau(\mu) &\sim \frac{\pi}{2\sqrt{a}}(1-\mu)\\ \tau'(\mu) &\sim -\frac{\pi}{2\sqrt{a}},\ x \to 0\end{aligned} \tag{3.205}$$

The limit for the derivative now is not zero, it is in fact constant and can only be zero if $a \to \infty$. Thus, for the case of a potential that are asymptotic to a parabolic it is not possible that $\tau' = 0$ for any value of μ. This leads us to the following results

- For a potential satisfying a linear asymptotic condition $u_0 \sim 1-a|x|, x \to 0$ we have $\lim_{\mu\to 1}\tau'(x) = 0$. This means that f_{1a} can converge, but only in the limit $(\alpha_1, \beta_1) \to (1, 1)$.

- For a potential satisfying a parabolic asymptotic condition $u_0 \sim 1 - ax^2, x \to 0$ it is not possible for τ' to be zero for any value $\mu \in (0, 1)$ and f_{1a} can not converge.

Next we ask if ρ' can behave in such a way that f_{1b} diverges. Computing the integral for ρ' is more demanding since we have to integrate over the entire domain $[0, \infty]$. Write ρ' generically as

$$\begin{aligned}\rho' &= \frac{x_+}{2\sqrt{\mu}} + \frac{1}{2}A\\ &= \frac{x_+}{2\sqrt{\mu}} + \frac{1}{2}\left[A_1 + A_2 + A_3\right]\end{aligned} \tag{3.206}$$

Where we split up the integral in (3.199) into three pieces (x_+, ϵ), (ϵ, δ) and (δ, ∞) for A_1, A_2 and A_3 respectively, see figure (3.6). The idea now is to match the asymptotic requirements to each of the three regions examine if they contain any singularities. The first term in (3.206) gives

$$\lim_{\mu\to 1}\frac{x_+}{2\sqrt{\mu}} = \frac{0}{2\sqrt{1}} = 0 \tag{3.207}$$

For the middle region II we have the first term in

$$\begin{aligned}A_2 &= \int_\epsilon^\delta dx\left[\frac{1}{\sqrt{\mu}} - \frac{1}{\sqrt{\mu - u_0(x)}}\right]\\ &\sim \int_\epsilon^\delta dx\left[1 - \frac{1}{\sqrt{1-u_0(x)}}\right], \mu \to 1\end{aligned} \tag{3.208}$$

here $u_0 < 1$ and is integrated over a finite domain. In addition, u_0 does not contain any singularities for any $x \in (-\infty, \infty)$ and we conclude that A_2 is finite

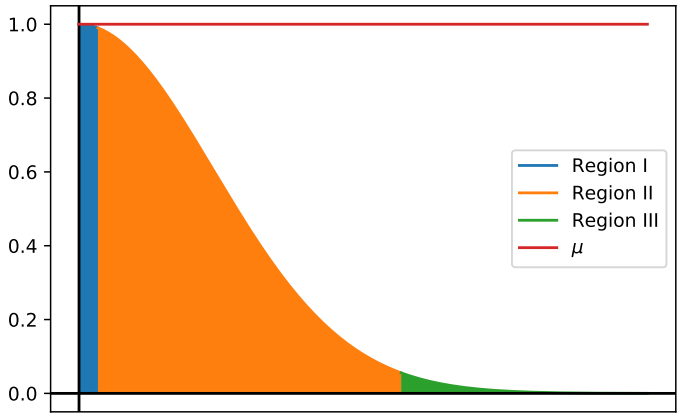

Figure 3.6: Three regions $I \in (x_+, \epsilon)$, $II \in (\epsilon, \delta)$ and $III \in (\delta, \infty)$

as $\mu \to 1$. Region III must be treated differently depending on the support of u_0. For non-compact we support set $u_0(x) \sim x^{-p}$, the quantity A_3 can be approximated

$$\begin{aligned} A_3 &= \int_\delta^\infty dx \left[\frac{1}{\sqrt{\mu}} - \frac{1}{\sqrt{\mu - u_0(x)}} \right] \\ &\sim \int_\delta^\infty dx \left[\frac{1}{\sqrt{\mu}} - \frac{1}{\sqrt{\mu - x^{-p}}} \right] \\ &= \delta \left[-1 + {}_2F_1(\frac{1}{1}, -\frac{1}{p}, \frac{-1+p}{p}, \delta^{-p}) \right] \end{aligned} \tag{3.209}$$

where ${}_2F_1$ are the hypergeometrical function as defined in [4]. δ is just some number, only required to be greater than zero, and all we need to know if A_3 converges or diverges. If we set $\delta = 1$ and it converges in this case setting a larger δ would not change this, using Gauss theorem [4] for ${}_2F_1$ gives us then

$$\begin{aligned} f(p) &= \left[-1 + {}_2F_1(\frac{1}{1}, -\frac{1}{p}, \frac{-1+p}{p}, 1) \right] \\ &= -1 + \frac{\sqrt{\pi}\Gamma(\frac{-1+p}{p})}{\Gamma(\frac{1}{2} - \frac{1}{p})} \end{aligned} \tag{3.210}$$

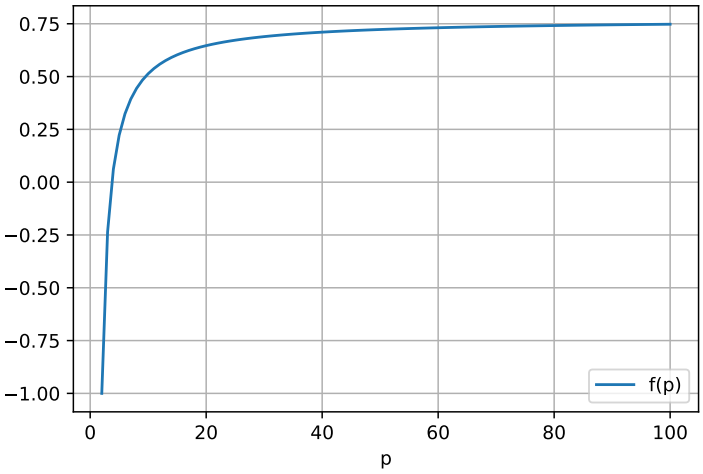

Figure 3.7: $f(p)$

where Γ the Euler Gamma function and $p \geq 2$. The arguments to the two gamma functions in $f(p)$ are

$$\begin{aligned} \frac{1}{2} \leq 1 - \frac{1}{p} < 1 \\ 0 < \frac{1}{2} - \frac{1}{p} < \frac{1}{2} \end{aligned} \tag{3.211}$$

The function $f(p)$ are plotted in figure (3.7) and bounded $-1 \leq f(p) \leq \frac{3}{4}$. Thus, if we choose $\delta \geq 1$ for region III we have $f(p) \geq A_3$ and A_3 does not diverge as $\mu \longrightarrow 1$ when the potential have non-compact support. For potentials with compact support the derivative of u_0 is not zero and we can linearise using Taylor at this point $u_0(s + x) = u_0(s) + u_0'(s)x$. The quantity $u_0(s)$ is zero and we are left with

$$\begin{aligned} A_3 &= \int_\delta^\infty dx \left[\frac{1}{\sqrt{\mu}} - \frac{1}{\sqrt{\mu - u_0(x)}} \right] \\ &\sim \int_\delta^0 dx \left[\frac{1}{\sqrt{\mu}} - \frac{1}{\sqrt{\mu - u_0'(s)x}} \right] \end{aligned} \tag{3.212}$$

This integral contains integrable square root terms that will give a finite quantities, meaning that the integral A_3 in region III will not produce any singularities for either compact or non-compact support. Last we have region I, using the asymptotic condition we have

$$A_1 \sim \int_{x_+}^\epsilon dx \left[\frac{1}{\sqrt{\mu}} - \frac{1}{\sqrt{\mu - 1 + a|x|^n}} \right], x \longrightarrow 0 \tag{3.213}$$

The first term in the above equation

$$\int_{x_+}^{\epsilon} dx \left[\frac{1}{\sqrt{\mu}}\right] = \frac{1}{\sqrt{\mu}} x\Big|_{x_+}^{\epsilon} = \frac{1}{\sqrt{\mu}}\left[\left(\epsilon - \frac{1-\mu}{a}\right)^{1/n}\right] \tag{3.214}$$

is finite in the limit $\mu \to 1$ so we concentrate on the second term in (3.213). First consider the linear case $n = 1$

$$\int_{\frac{1-\mu}{a}}^{\epsilon} dx \left[-\frac{1}{\sqrt{\mu - 1 + ax}}\right] = -\frac{2}{a}\sqrt{\mu - 1 + a\epsilon} \tag{3.215}$$

Also finite as $\mu \to 1$. The last quantity we must check is the second term for a parabolic potential

$$\lim_{\mu\to 1} \int_{\sqrt{\frac{1-\mu}{a}}}^{\epsilon} dx \left[-\frac{1}{\sqrt{\mu - 1 + ax^2}}\right] = -\frac{1}{\sqrt{a}}\log(2a\epsilon) + \frac{1}{\sqrt{a}}\log(\sqrt{a}) \tag{3.216}$$

$$+ \lim_{\mu\to 1} \frac{1}{2\sqrt{a}}\log((1-\mu)) \tag{3.217}$$

where the last term diverges to negative infinity.

Limits of ρ' as $\mu \to 0$

The limit $\mu \to 0$ for ρ' is simpler to examine since we do not need to split the integral into pieces, only check the two cases. For compact support we have

$$\begin{aligned} u_0(s) &= 0 \\ s &= u_0^{-1}(0) \neq 0 \vee \pm\infty \end{aligned} \tag{3.218}$$

thus the first term in (3.198)

$$\lim_{\mu\to 0} \frac{x_+}{\sqrt{\mu}} = \infty \tag{3.219}$$

The second part

$$\int_{x_+}^{s} dx \left[\frac{1}{\sqrt{\mu}} - \frac{1}{\sqrt{\mu - u_0(x)}}\right] \tag{3.220}$$

It is clear that

$$\int_{x_+}^{s} dx \frac{1}{\sqrt{\mu}} \geq 0 \tag{3.221}$$

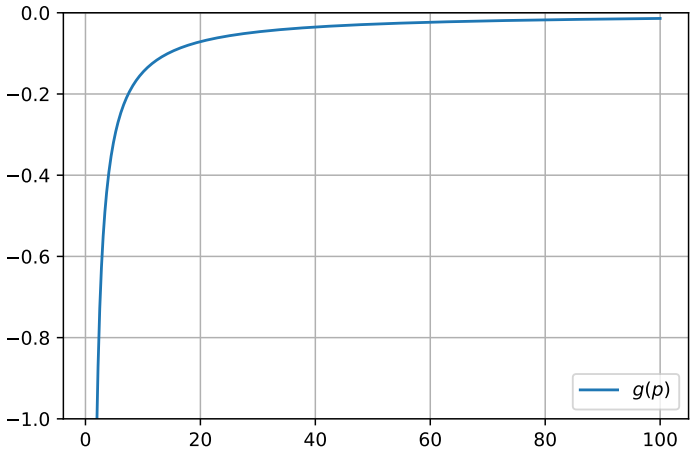

Figure 3.8: $g(p)$

and since $\mu \geq u_0$

$$\int_{x_+}^{s} dx \frac{1}{\sqrt{\mu - u_0(x)}} \geq 0 \tag{3.222}$$

Since the potential u_0 has compact support, its first derivative is not zero at $x = s$ and can be to first order be approximated linearly and thus goes nice to zero as $x \longrightarrow s$, therefore

$$\lim_{\mu \to 0} \int_{x_+}^{s} dx \left[\frac{1}{\sqrt{\mu}} - \frac{1}{\sqrt{\mu - u_0(x)}} \right] = 0 \tag{3.223}$$

For potentials with non-compact support we approximate $u_0 \sim x^{-p}, x \longrightarrow \pm\infty$ where $p \geq 2$. We calculate ρ'

$$\rho' = \frac{x_+(\mu)}{2\sqrt{\mu}} + \frac{1}{2} \int_{x_+(\mu)}^{s} dx \left[\frac{1}{\sqrt{\mu}} - \frac{1}{\sqrt{\mu - x^{-p}}} \right] \tag{3.224}$$

$$= \frac{1}{2} \frac{1}{\mu^{\frac{1}{2}+\frac{1}{p}}} \left[1 + \frac{-\Gamma(\frac{1}{2} - \frac{1}{p}) + \sqrt{\pi}\Gamma(\frac{p-1}{p})}{\Gamma(\frac{1}{2} - \frac{1}{p})} \right]$$

$$= \frac{1}{2} \frac{1}{\mu^{\frac{1}{2}+\frac{1}{p}}} \left[1 + g(\frac{1}{2} - \frac{1}{p}) \right] \tag{3.225}$$

The function $g(p)$ is bounded $-1 \geq g(p) \geq 0$ and plotted in figure (3.8). For all $p \geq 2$ we have the result that ρ' diverges to positive infinite since $1 \geq g$ here. The special case $p = 2$ we get $\rho' =$ but since this is an asymptotic it is more

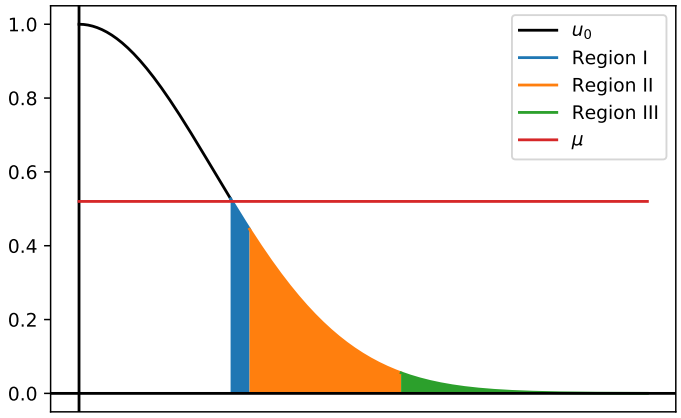

Figure 3.9: Three regions $I \in (x_+, \epsilon)$, $II \in (\epsilon, \delta)$ and $III \in (\delta, \infty)$

correct to interpret this as an indication that ρ' is finite. Now we have found results for ρ' near the points $\mu = 0$ and $\mu = 1$, but what about $0 < \mu < 1$, is it possible for ρ' diverge here? Inspired by the method we used to examine the limit $\mu \to 1$ we divide the region of integration into the same three regions, but now μ an arbitrary value between 0 and 1, see figure (3.9). Regions II and III can use exactly the same argument as before and we must only check if the region I can produce singularities. When deriving the formulas for ρ and τ using the WKB-approximation we linearised the potential u_0 at the points $x_\pm$ so let us do this for region I

$$u_0(x_+ + x') \approx u_0(x_+) + u_0'(x_+)x' \tag{3.226}$$

We can now compute the integral needed for region I

$$\lim_{\epsilon \to x_+} \int_0^{\epsilon - x_+} dx' \frac{1}{\sqrt{u_0'(x_+)x'}} = \lim_{\epsilon \to x_+} \frac{2}{\sqrt{u_0'(x_+)}} \sqrt{x'} \Big|_0^{\epsilon - x_+} = 0 \tag{3.227}$$

Now all cases we need have been examined, let us summarise the results

- $\tau \geq 0$ and $\tau' \leq 0$, valid in region $0 < \mu < 1$. The situation $\tau' = 0$ is only possible in the limit $\mu \to 1$ and u_0 approaches this limit linearly.
- In the limit $\mu \to 0$, ρ' diverges to positive infinity for all potentials, except in the special case where u_0 decays algebraically, $u_0 \sim x^{-2}, x \to \pm\infty$
- In the limit $\mu \to 1$ the behaviour of ρ' depends on how u_0 behaves as $x \to 0^\pm$. For potentials that approach linearly ρ' is finite, for potentials

approaching parabolic $u_0 \sim 1 - x^2, x \to 0$, ρ' diverges to negative infinity.

Our original question and the reason why we examined all these cases where ultimately to examine for which (α_1, β_1) the system (3.187)-(3.187) has solutions. By looking at the integral kernels k_1 and k_2 in (3.191) we found conditions on τ' and ρ' needed be able to satisfy equation (3.187) in the limit $\alpha_1 \to \beta_1$. Finding such a solution corresponds to ending the phase in the RH problem and no more subintervals are needed. Let us use the results and discuss the consequences. As a reminder, we need to answer two questions; can we have $\tau'(1) = 0$ and whether the behaviour of ρ' can compensate for the divergent K_2 term (3.194). The first question can be answered immediately, the limit $\lim_{\mu\to 1} \tau'(\mu)$ can only (and is) be zero if the potential u_0 behaves linear as $x \to 0^{\pm}$. Further we found that in the limit $\mu \to 0$, ρ' is either finite or diverges to positive infinity, neither of these cases can compensate for the divergent($\to \infty$) f_{1a} term. We also examined ρ' and τ' for cases where μ is not near the endpoints 0 or 1, showing that the two does not contain any singularities in this region. What remains is to discuss $\rho', \mu \to 1$. The case for a potential with linear asymptotic behaviour we saw that ρ' is finite. We also have the result that τ' can be zero in this limit and by combining these two results leads us to the conclusion that it is possible to satisfy equation (3.187) with a solution on the form $\alpha_1 \to \beta_1$, and if this is the case no new phase is needed.

When the potential behaves parabolic asymptotically as $\mu \to 1$ we have the following; $\tau' < 0$ and $\lim_{\mu\to 1} \rho' = -\infty$. This combination is exactly what we can not have to make a conclusion without further investigation since in this case we have

$$\begin{aligned} \lim_{\mu\to 1} f_{1a} &= \infty \\ \lim_{\mu\to 1} f_{1b} &= -\infty \end{aligned} \tag{3.228}$$

To proceed we need to compare the numerical factors on the two terms f_{1a} and f_{1b}. Starting with f_{1a} and using the asymptotic expression for τ' (3.205)

$$\begin{aligned} f_{1a} &\sim \frac{1}{\sqrt{a}} \int_0^{\alpha_1} d\mu \frac{\mu^{1/2}}{(\alpha_1 - \mu)^{1/2}(\beta_1 - \mu)^{1/2}} \\ &= \frac{2}{\sqrt{a}} \sqrt{\beta_1} \left[K(\frac{\alpha_1}{\beta_1}) - E(\frac{\alpha_1}{\beta_1}) \right] \end{aligned} \tag{3.229}$$

For f_{1b} we use the term from (3.216) causing to ρ' diverge, and picking up a factor of $\frac{1}{2}$ that we omitted from (3.198) in the calculation of (3.216)

$$f_{1b} \sim \frac{\pi}{8\sqrt{a}} \int_{\alpha_1}^{\beta_1} d\mu \frac{\mu^{1/2} \log(1 - \mu)}{(\mu - \alpha_1)^{1/2}(\beta_1 - \mu)^{1/2}} \tag{3.230}$$

In this region the term $\mu^{1/2}$ behaves nice, $\lim_{\mu\to 1}\mu^{1/2}=1$, not approaching zero or infinity. Let us then approximate the integral by moving the $\mu^{1/2}$ out of the integrand

$$\frac{\pi}{8\sqrt{a}}\int_{\alpha_1}^{\beta_1} d\mu \frac{\mu^{1/2}\log(1-\mu)}{(\mu-\alpha_1)^{1/2}(\beta_1-\mu)^{1/2}} \sim \delta^{1/2}\frac{\pi}{8\sqrt{a}}\int_{\alpha_1}^{\beta_1} d\mu \frac{\log(1-\mu)}{(\mu-\alpha_1)^{1/2}(\beta_1-\mu)^{1/2}} \tag{3.231}$$

this approximation is only valid when integrating over a small region as $\alpha_1 \to \beta_1$ and we are not near $\mu = 0$. The number δ is this a point near the small region we integrate over. We can compute the above integral exact

$$\int_{\alpha_1}^{\beta_1} d\mu \frac{\log(1-\mu)}{(\mu-\alpha_1)^{1/2}(\beta_1-\mu)^{1/2}} = -\pi\left[\log(\frac{4}{1-\alpha_1}) - 2\log\left(1+\sqrt{\frac{\beta_1-1}{\alpha_1-1}}\right)\right] \tag{3.232}$$

Taking the limit $\alpha_1 \to \beta_1$

$$\lim_{\alpha_1\to\beta_1} -\pi\left[\log(-\frac{4}{\alpha_1-1}) - 2\log\left(1+\sqrt{\frac{\beta_1-1}{\alpha_1-1}}\right)\right] = -\pi\log(\frac{1}{1-\beta_1}) \tag{3.233}$$

and as expected $\lim_{\beta_1\to 1} -\pi\log(\frac{1}{1-\beta_1}) = -\infty$. From this we have that f_{1a} goes to positive infinity and f_{1b} goes to negative infinity as $(\alpha_1,\beta_1)\to(1,1)$. In order to analyse which of these quantities that dominate we must collect and compare numerical factors, for f_{1a} (3.191) we have the divergent term from (3.192) and the asymptotic approximation of τ' (3.205)

$$(-\frac{2}{\pi})(2\sqrt{\beta_1})(-\frac{\pi}{2\sqrt{a}}) = \frac{2}{\sqrt{a}} \tag{3.234}$$

as $\beta_1 \to 1$. For f_{1b} we use the factors from (3.231) and (3.233)

$$(\delta^{1/2}\frac{\pi}{8\sqrt{a}})(-\pi) = -\frac{\pi^2}{8\sqrt{a}} \tag{3.235}$$

in the limit $\delta \to 1$. Clearly

$$|\frac{2}{\sqrt{a}}| > |\frac{\pi^2}{8\sqrt{a}}| \tag{3.236}$$

thus, f_{1a} dominates over f_{1b} as $(\alpha_1,\beta_1)\to(1,1)$. All cases have now been examined and for potentials with asymptotic behaviour $u_0(x)\sim 1-ax^2, x\to 0$ the function (3.191) diverges to positive infinity as $\alpha_1\to\beta_1$.

What consequences does the results of the above analysis give in terms of the system of equations (3.187)-(3.188)? We have established that

$$6t(\alpha_1 + \beta_2) + x = f_1(\alpha_1, \beta_1) \tag{3.237}$$

Let us fix an $t = t^* > 0$, meaning that the maximum of $6t^*(\alpha_1 + \beta_2)$ is $12t^*$. In section 3.2 we found, after solving Burgers equation using the method of characteristics, that the solution to the KdV equation is moving to the left, meaning that phase $N = 1, (\alpha_1, \beta_1)$ that occurs after breaking is in a region of $x \in (x_1, x_0)$ where $x < 0$. This means that x in (3.237) is always negative and $6t(\alpha_1 + \beta_2)$ is always positive. The problem is as follows, the term x is not bounded, it can become an arbitrary negative number smaller than x_0, but the term containing t is bounded, it has a maximum positive value for a fixed t. It follows that the LHS of (3.237) will become negative when $x < 6t(\alpha_1 + \beta_1)$. Further, we have established for both types of potentials(linear and parabolic behaviour when $x \to 0$) that

$$\lim_{\alpha_1 \to \beta_1} f_1 = \infty, \beta_1 \neq 1 \tag{3.238}$$

In the limit $(\alpha_1, \beta_1) \to (1, 1)$ we carefully examined both potentials and found the following, for the linear case

$$\lim_{\alpha_1 \to \beta_1} f_1 = c_0, \beta_1 \to 1 \tag{3.239}$$

where c_0 is a finite positive number. For the parabolic case

$$\lim_{\alpha_1 \to \beta_1} f_1 = \infty, \beta_1 \to 1 \tag{3.240}$$

The results indicates that along the diagonal $\alpha_1 = \beta_1$ in (3.4) f_1 is infinite, except for the special case $\alpha_1 = \beta_1 = 1$ for linear potentials, where a perfect cancellation occurs in f_{1a} as $(1 - \mu)^{1/2}$ in τ' cancels the term $(\beta_1 - \mu)^{1/2}$. We make the following conclusions based on this

- For a potential with asymptotic behaviour $1 - a|x|, x \to 0$ we can not discard the possibility of solutions of the system (3.187)-(3.188) where $\alpha_1 \to \beta_1$, but such a solution can only happen as $\mu \to 1$.

- For potentials with asymptotic behaviour $1 - a|x|^2, x \to 0$ we, based on asymptotic calculations of equation (3.187), discard the existence of solutions of the system where $\alpha_1 \to \beta_1$.

- The two above statements are independent of the asymptotic behaviour for large $|x|$ (compact/non-compact), as long as they satisfy the requirements for u_0 in definition (1)

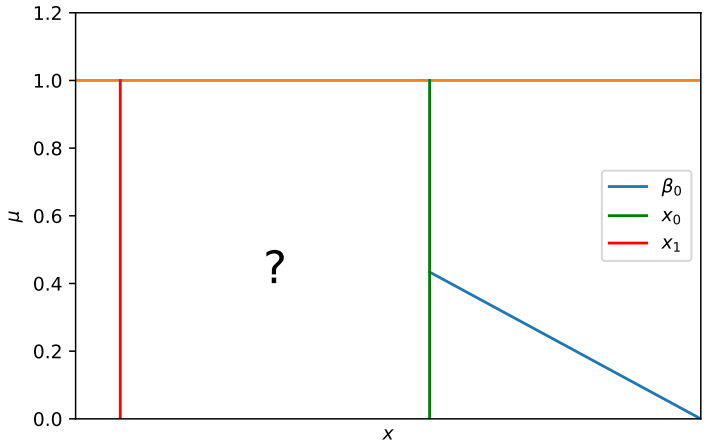

Figure 3.10: How can (α_1, β_1) behave between (x_1, x_0)?

Since we have not examined the second equation (3.188) in detail we can not make stronger statements. However, numerical calculations indicate that the second equation is not behaving in a way that invalidates these results, this will be discussed in a later section.

What does this mean for the behaviour of the solution to the system of equations, how can (α_1, β_1) behave in the region between (x_1, x_0)(see figure (3.10))? From [7], we have that $\lim_{x\to x_0} \alpha_1 = 0$ and that

$$\begin{aligned} \lim_{x\to x_0^+} \beta_0 &= \lim_{x\to x_0^-} \beta_1 \\ \lim_{x\to x_0^+} \beta_0' &= \lim_{x\to x_0^-} \beta_1' \end{aligned} \tag{3.241}$$

These conditions combined with the analysis done in this section leads us to two possible suggestions for how solutions to the system (3.187)-(3.188) might look like, for a linear see figure (3.11) and for parabolic see figure (3.12). A third possibility is a solution on a more arbitrary from as illustrated in figure (3.13). We can not discard solutions of this form, but is it for example possible to have solutions on the form (3.13) where $x_1 \to -\infty$? We know that α_1 can never meet β_1, consequently they can not cross each other. Further we know that (α_1, β_1) is bounded between 0 and 1. Bolzano-Weierstrass theorem [12] states that every bounded sequence in $\mathbb{R}^n$ has a convergent subsequence, and this combined with the fact that the LHS of (3.187) is becoming more and more negative as $x \to -\infty$ leads to a contradiction. Thus, even if there exists solutions on form (3.13) has to have some finite $x^* < 0$ where it is no longer possible to satisfy (3.187). This argument is also valid for solutions where

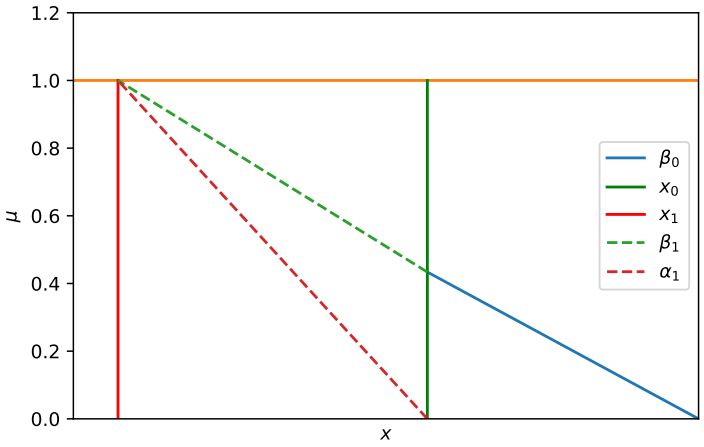

Figure 3.11: A possible form of solution for potentials $u_0(x) \sim 1 - a|x|, x \to 0$, but not for potentials $u_0(x) \sim 1 - a|x|^2, x \to 0$

α_1 and/or β_1 approaches a constant. For completeness, solutions where both $\alpha_1 = \beta_1 = 0$ is not possible since $f_1 \geq 0$ and $6t(0 + 0) + x = x < 0$, which is a contradiction. The last case is the limit $t \to \infty$, but this is of little practical interest as one of the requirements in the theory of integrable systems [1] is that $\lim_{t\to\infty} u(x, t) = 0$. For curiosity, one can observe that this case would lead to infinities on both sides of equation (3.187), the equation is satisfied for every point x and $\alpha_1 = \beta_1$,all consistent with theory. The conclusion in this section is as follows

- For potentials u_0 that satisfies the requirements in definition (1) and where $n = 1$, corresponding to approaching $x \to 0$ linearly, we can not discard solutions where $\alpha_1 \to \beta_1 \to 1$.
- For potentials with $n = 2$, there can not exist such solutions.
- The region (x_1, x_0) where the phase is valid is always finite, except when $t \to \infty$.

We also make the following conjectures based on the calculations in this section

- For potentials with $n = 1$, the solution has the form seen in figure (3.11), α_1 meets β_1 in $\mu = 1$ and the phase ends and no additional phases is needed.

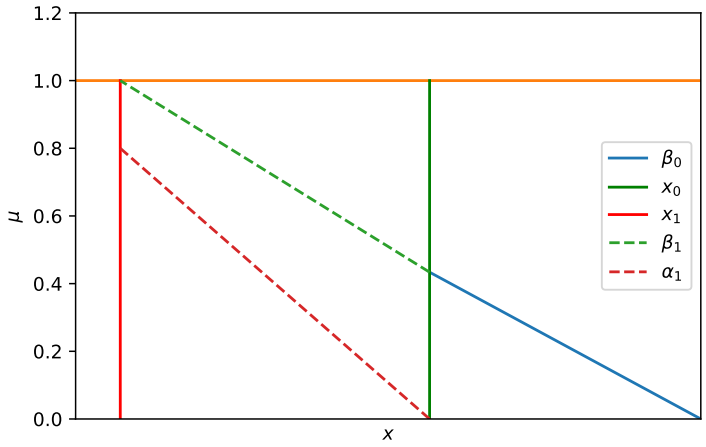

Figure 3.12: A possible form of solution for potentials $u_0(x) \sim 1 - ax^2, x \longrightarrow 0$

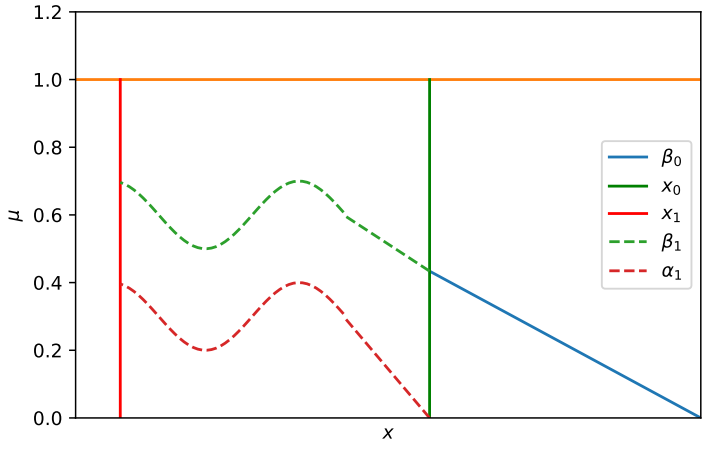

Figure 3.13: Third possible form of solution to system (3.187)-(3.188)

- For potentials with $n = 2$, the solution takes the form seen in figure (3.12), α_1 can never meet β_1 for any μ and as a consequence another phase e.g $N = 2, (\alpha_2, \beta_2)$ must occur at some finite x and the new phase occurs exactly as $\beta_1 \longrightarrow 1$.

This ends our discussion of the possibility of a new phase for now, but we will return to the question in later sections where we discuss the above statements.

3.5 Scattering of the peak of a potential

In section 3.1 we derived the WKB-approximation for a Schrödinger two turning point problem needed in the forward scattering step. In the previous section we saw that if the phase $N = 1$ could be sufficient the critical behaviour is how the potential u_0 behaves as it approaches $x \longrightarrow 0^{\pm}$. For the potentials that behaves linearly we found that the phase can end and that this can only happen exactly in $\mu = 1$. A different result was found for the potentials with parabolic behaviour, here a new phase $N = 2$ must occur. Both these situations seems to be closely related to the limit $\mu \longrightarrow 1$, which leads us into examining this limit further in order to understand what exactly happens here. When deriving the connection formulas and calculating the reflection and transmission coefficient using the WKB-approximation we linearised the potentials x_0 at the singular points $u_0(x_{\pm})$, but doing this in the limit $x \longrightarrow 0^{\pm}$ is simply not valid as the derivative of u_0 is zero for potentials $u_0 \sim 1 - ax^2, x \longrightarrow 0$, see figure (3.14). In our calculations in the previous section we did split up the potential u_0 to account that it is not valid to linearise it everywhere. The problem is that we used the quantities τ' and ρ' in the same calculations, these being directly obtained from the WKB approximation where we did not treat the limit $\mu \longrightarrow 1$ in any special manner. Thus we first ask if it is valid to use the two turning point WKB approximation at the peak $\mu = 1$, see figure (3.14). The short answer to this question is no - if the scattering problem is solved as a single turning point problem and instead of linearising around the singular points we use $u_0 \sim 1 - ax^2, x \longrightarrow 0$ we arrive at different expressions for the reflection and transmission coefficients. Instead of going through all the details we simply cite the results from [5]

$$\begin{aligned} R &= \frac{1}{2} \\ T &= \frac{1}{2} \end{aligned} \tag{3.242}$$

This is a very different result than if we use expressions (3.66) and (3.67), where we would find $R = 1$ and $T = 1$, a nonsensical physical result, everything can

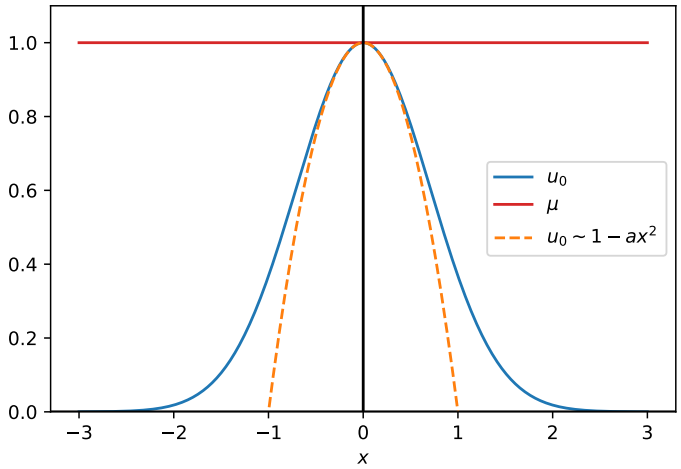

Figure 3.14: Scattering problem at the peak $u_0(x) = 1$

not be transmitted and reflected at the same time. In figure (3.15) the point is illustrated, plot (a) is the two turning point WKB approximation and plot (b) is a qualitative example of how we expect the shape of exact solutions to look like. As ϵ get smaller the overlapping region around $\mu = 1$ gets steeper, but there will always be an error at $\mu = 1$. These findings raises a few questions not considered(not mentioned, at least) in the original article [7]. First, we know that potentials of this kind always leads to a new phase $N = 2$ when the WKB approximation proposed is used, but can the above result indicate that the new phase is not necessarily a property emerging from the potential u_0 itself, rather a result of the non-validity of the approximation in this limit? One should note that the WKB approximation for potentials of type $1 - a|x|, x \longrightarrow 0$ is not valid at the point $\mu = 1$ either, the derivate is not even defined at this point. A natural question is what justification was made when not considering the point $\mu = 1$ in the solution process, but rather dividing up into regions $(-\infty, 0)$, $(0, 1)$ and $(1, \infty)$? We will not attempt to answer this, as it requires us to first derive the WKB approximation valid for the peak, then insert the new expressions for R and T into the scattering matrix (3.78), and then go through a full analysis for the new RH problem we get. Further, it is not clear that it is possible to solve the corresponding RH since the original method makes use of properties from the expressions for ρ and τ obtained from the two turning point WKB approximation. An additional difficulty, if it is correct that this point need special care, is that it is likely the two solutions must be patched together and how to do this is not clear.

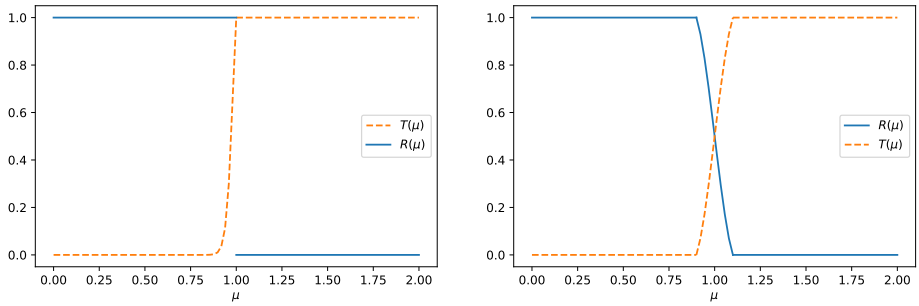

(a) WKB-approximation **(b)** Qualitative example

Figure 3.15: Shapes of reflection and transmission coefficients

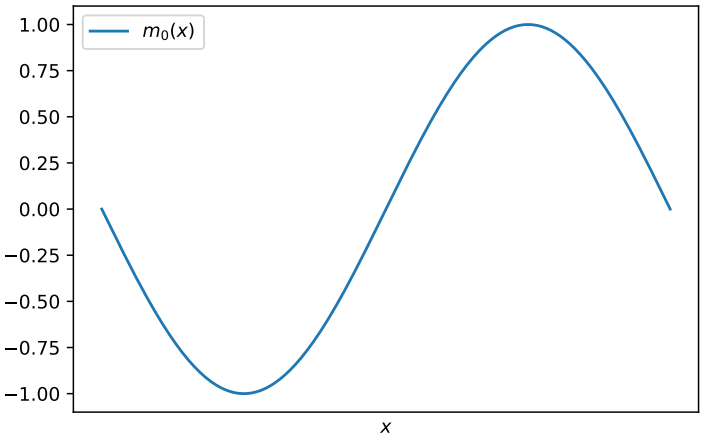

Figure 3.16: Full cycle potential $m_0(x)$

3.6 More general potentials

From a physical perspective it might be more interesting to study initial potentials that consists of a full period(or full cycle) as illustrated on figure (3.16). Thus one ask if it is possible to solve the KdV equation using the method described in section 3.3 for a potential of this kind. While it might mathematically be of interest to derive the WKB approximation for a full cycle potential, insert the result into the scattering matrix (3.78) and examine if the method can be used, it might not be the correct approach in our context. The model equation derived in chapter 2 was the mKdV, hence the initial potentials for the KdV should originate from the mKdV and is transformed using the Miura transformation $u = m^2 + \epsilon m_x$. Thus we should ask what kind of initial potential should

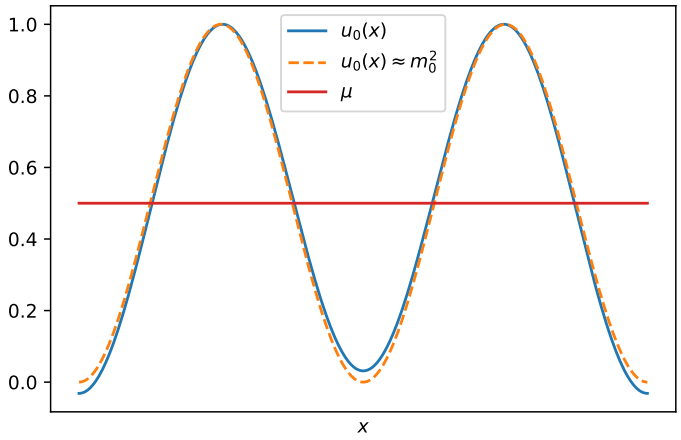

Figure 3.17: Potential $u_0(x)$ when using the Miura transformation on full cycle potential, see figure (3.16), $\epsilon = 0.01$.

we solve the KdV equation for if we have a full cycle initial potential for the mKdV equation, rather than solve the KdV equation with a full cycle potential. For potentials that satisfies definition (1) this is not an issue as the properties of m_0 is preserved to u_0 in the transformation $u_0 \approx m_0^2$ (as $\epsilon \to 0$). This is not the case for a full cycle potential, here the properties is not preserved, as m_0 is odd and the transformation would give an u_0 that is even. Let us consider an example, make the potential m_0 for the mKdV equation

$$m_0 = \begin{cases} \sin(\pi x), & -1 < x < 1 \\ 0 \ o.w. \end{cases} \tag{3.243}$$

resulting in a shape seen in figure (3.16). Employing the transformation give

$$u_0 = \begin{cases} \sin^2(\pi x) + \epsilon\pi \cos(\pi x), & -1 < x < 1 \\ 0 \ o.w. \end{cases} \tag{3.244}$$

and as $\epsilon \to 0$ we have

$$u_0 \approx \begin{cases} \sin^2(\pi x), & -1 < x < 1 \\ 0 \ o.w. \end{cases} \tag{3.245}$$

For any potential m_0 with the characteristics similar to the above, the corresponding potential u_0 would result to somehing similar to figure (3.17). For sufficient small ϵ we can approximate with a potential that is positive and share many of the properties we had for a half cycle potential. To examine if

the RH method can be extended the WKB approximation for the reflection and transmission coefficient for the four point turning problem seen in figure (3.17) must be solved. Then all steps in the RH procedure must be checked with the new expressions to see if the conditions allowing for the method holds.

4

Numerical procedures and a worked example

In chapter 3 we explained and expanded on the procedure proposed in [7] for solving the KdV equation as a Riemann-Hilbert problem, resulting in a number of quantities that are needed in the solution process. While we could compute, either partially or full, some of these quantities analytically it is necessary to develop numerical methods to obtain what remains. We will in this chapter propose algorithms needed, the results using these and present a full example calculation of the KdV equation. Originally we wanted to use a Gaussian shaped initial condition $u_0(x) = \exp(-\gamma x^2)$ as a prototype calculation, but doe to the findings in section 3.4 this idea was discarded as we can not use the method without developing equations for additions phase(s). Here we saw that a potential of this shape would require at least one addition phase, and perhaps even more severe is from the discussion in section 3.5 we do not know if the new phase is strictly necessary or an artefact of using the WKB approximation. Therefore we have chosen the triangle shaped potential (4.1), illustrated on figure (4.1).

$$u_0(x) = \begin{cases} 1 - |x| & \text{if } |x| \leq 1 \\ 0 & \text{if } |x| > 1 \end{cases} \tag{4.1}$$

Using this potential has some additional advantages, many of the unknown quantities can be calculated exact, enabling us to compare numerical and analytical solutions. A disadvantage is that this example is not likely to be very

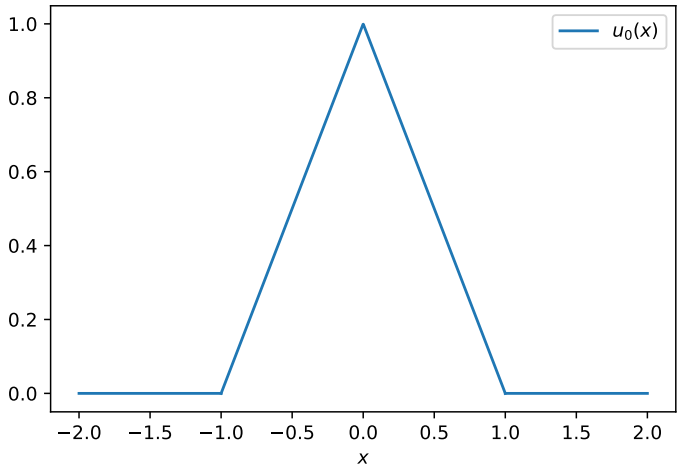

Figure 4.1: Triangle potential defined in equation (4.1)

realistic from a physical point of view and mathematically it is very special. Another disadvantage is that computing the solution using a purely numerical method to the KdV equation is difficult and in the dispersionless limit where the solution, as we will see, both displays a near vertical profile in the transfer region between the two phases and have a rapid oscillating solution in the second phase. Combined with the triangle potential, while simple analytically is actually numerically challenging, we have not been able to implement a numerical solver that are able to go beyond breaking time. However, by exploiting the existence of an infinite number of conservation laws for the KdV equation [1]. These conservation laws can be used to check the obtained solution, but it does require to have a solution for all x. Therefore choosing the the triangle potential, where no additional phase(s) is needed, as a test problem means that we can test the solution using the corresponding conservation laws for the KdV equation.

The main quantities we need to calculate we have from chapter 3

- The turning points $x_\pm$ for the WKB-approximation, section 3.1
- $\rho(\lambda)$,$\tau(\lambda)$ and their derivatives, section 3.1
- β_0, the phase before breaking time t^*, section 3.3
- The values of (α_1, β_1), the first phase after breaking t^*, section 3.3

In addition to the triangle potential we will compare and test the accuracy of

numerical solutions to exact calculations for some potentials where we are able to do exact calculations. These additional potentials are the parabolic (D.14), the algebraic (D.33), secant (D.46). See the appendix section D for definitions and calculations of exact quantities. The numerical procedures in the following sections are implemented in Python, mainly by the use of the SciPy library [17]. Since we use numerical methods from this library we will mainly give high level descriptions of the algorithms.

4.1 Turning points $x_\pm$

The turning points are calculated by inverting u_0

$$\begin{aligned} u_0(x) &= \lambda \\ x_\pm &= \pm|u_0^{-1}(\lambda)| \end{aligned} \tag{4.2}$$

Since $x_- = -x_+$ we only need to calculate x_+. One possible method would be to compute the root of $u_0(x) - \lambda = 0$, but since λ is a straight line we instead propose the following method

$$u_0^{-1}(\lambda) = (u_0(x), x) \tag{4.3}$$

If we create numerical arrays of x the above method is trivial to implement. The two types of support the potential can have requires us to treat the two cases slightly different. For potentials with compact support we simply stop at $x = s$, where s is the support of u_0. Potentials with non-compact support would in theory require a numerical array from $[0, \infty)$, but in practice this is not necessary since it is required that u_0 decays sufficiently fast as $x \longrightarrow \pm\infty$. Instead we set a cut-off point $u_0(x^*) < \delta$ and create a numerical array $x = [0, x^*]$. Finally we create an interpolating function u_0^{-1} with input $(u_0(x), x)$, see algorithm

(1)

Data: $u_0(x)$,s,δ,n
Result: interpolating function $u_0^{-1}(\lambda)$
if *support is compact* **then**
  $x^* = s$;
else
  start = 0;
  while $u_0(start) > \delta$ **do**
    start += step ;
  end
  x^* = start ;
end
x = linear spaced array from 0 to x^* with n number of points ;
u_0^{-1} = create interpolating function from input $(u_0(x), x)$;
return $u_0^{-1}(\lambda)$;

Algorithm 1: Computing interpolating function for u_0^{-1}

We can examine the accuracy of this method for any potential by calculating $u_0(u_0^{-1}(\lambda)) - \lambda$, which for exact calculations should be zero. For numerical calculations the accuracy depends on the number n of points in the x array, how small δ is chosen and which interpolating method is used, we use a spline interpolation of third order. Figures (4.2) and (4.3) plots the accuracy for two potentials with compact support and two with non-compact support. For the first case even a very small number of grid points gives a accurate results with errors of size 10^{-3} and when setting the number of grid points to $n = 10000$ the errors are for both the triangle and parabolic potential of order 10^{-15}. For potentials with non-compact support more grid points are needed to get accurate results, setting $n = 1000$ or $n = 10000$ gives decent results with errors of order 10^{-4} and 10^{-11}, respectively. Calculating the turning points using this method gives accurate results and is computational efficient since it mostly consist of a few array manipulations.

4.2 ρ, τ and their derivatives

Numerical calculations of ρ (3.68) and τ (3.69) mainly consist of computing many integrals for discrete values of $\lambda \in (0, 1)$. For a particular potential u_0 we either integrate over x from zero to the support of u_0 or to infinity. Determine the number of discrete points λ should be divided into and calculate all these integrals to gives an array for ρ and τ for each λ. Using these two arrays we create an interpolating function for the two functions, and these functions

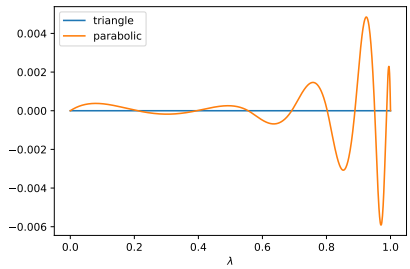

(a) $n = 10$

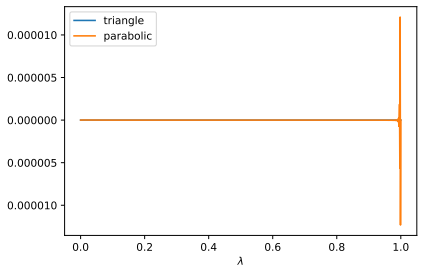

(b) $n = 100$

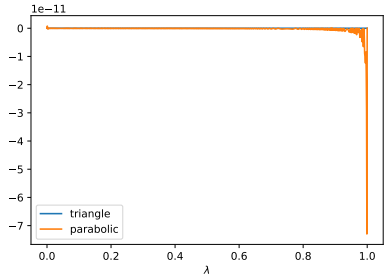

(c) $n = 1000$

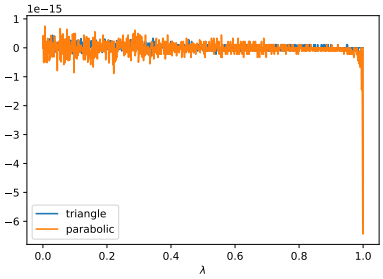

(d) $n = 10000$

Figure 4.2: Error estimates using algorithm (1) to compute x_+ for two potentials with compact support. Here n denotes the number of linear spaced points from 0 to s. Estimates calculated using $u_0(u_0^{-1}(\lambda)) - \lambda$

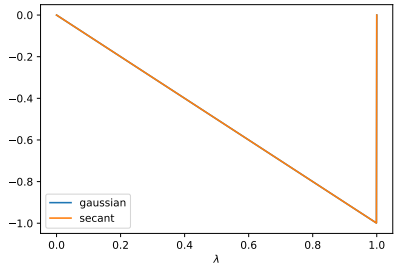

(a) $n = 10$

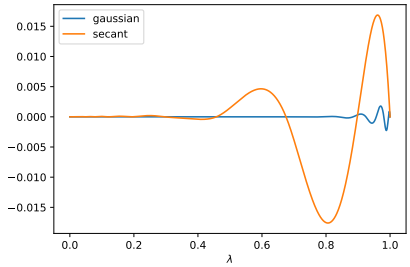

(b) $n = 100$

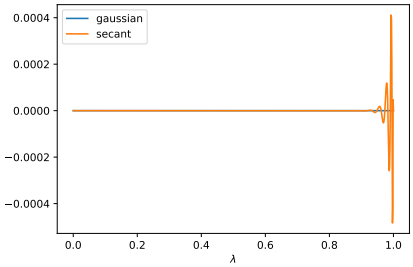

(c) $n = 1000$

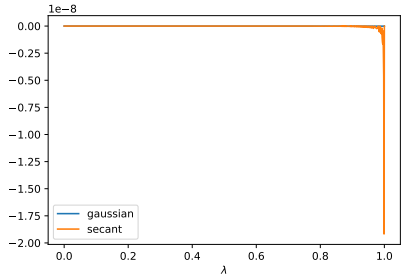

(d) $n = 10000$

Figure 4.3: Error estimates using algorithm (1) to compute x_+ for two potentials with non-compact support. Here n denotes the number of linear spaced points from 0 to x^*. Estimates calculated using $u_0(u_0^{-1}(\lambda)) - \lambda$

can again be differentiated to give ρ' and τ'. To obtain sufficient accurate results a high number of integrals must be computed, but all these integrals are independent i.e they can all be computed without any interaction between each other. Thus this is what is known as an embarrassingly parallel problem, where no extra effort is needed to run this algorithm in parallel. Using algorithm (1) to calculate the turning points we propose the procedure described in algorithm (2). Note that in the description of the algorithm we use i as both an index for the arrays and as the value for a specific λ, this is not correct in an actual implementation of the algorithm. For increased computationally efficiency the algorithm should be split in two, one for computing ρ and one for τ, in order to take advantage of memory caching and compiler optimizations. The variable 'workers' in algorithm (2) denotes the number of workers that should work simultaneously on the main loop, setting it to 1 corresponds to running in serial and for integer values greater than 1 corresponds to parallel execution.

Data: $u_0(x)$,s,n,workers
Result: interpolating functions for ρ, τ, ρ' and τ'
if *support is compact* **then**
  $x^* = s$;
else
  $x^* = \infty$
end
λ = linear spaced array from $[0, 1]$ with n number of grid points;
R,T = initialize two empty arrays with n grid points, to hold calculated values;
for all $i \in \lambda$ **in parallel do**
  $x_+ = u_0^{-1}(i)$;
  R[i] = integrate $\sqrt{i} - \sqrt{i - u_0(x)}$ over x from x_+ to x^* ;
  R[i] = R[i] + $x_+\sqrt{\lambda}$;
  T[i] = integrate $2\sqrt{u_0(x) - i}$ over x from 0 to x^* ;
end
ρ = create interpolating function using λ and R[i] as input ;
τ = create interpolating function using λ and T[i] as input ;
ρ' = differentiate the interpolating function ρ ;
τ' = differentiate the interpolating function τ ;
return ρ, τ, ρ' and τ' ;

Algorithm 2: Computing interpolating functions for ρ, τ, ρ' and τ'

Let us compare the numerical solutions to the exact quantities calculated in (D). Figures (4.4), (4.6), (4.8) and (4.10) shows that the shapes of analytical and numerical calculations are similar for all the potentials. In addition, all potentials behave asymptotically as we predicted in section 3.4, supporting our calculations.

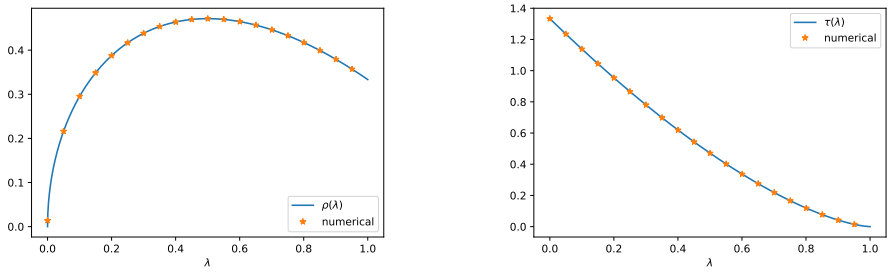

(a) $\rho(\lambda)$ **(b)** $\tau(\lambda)$

Figure 4.4: Comparison of numerical and analytical solutions ρ and τ for the triangle potential (4.1). Numerical solution computed using algorithm (2) and analytical solutions computed in section D. Here the number of grid points $n = 1000$ and the numerical solution is sampled every 50 points

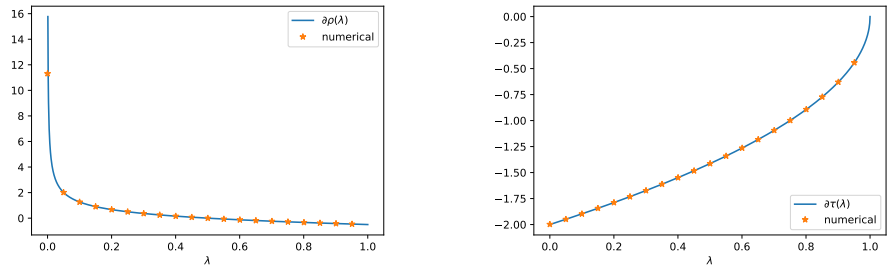

(a) $\partial\rho(\lambda)$ **(b)** $\partial\tau(\lambda)$

Figure 4.5: Comparison of numerical and analytical solutions ρ' and τ' for the triangle potential (4.1). Numerical solution computed using algorithm (2) and analytical solutions computed in section D. Here the number of grid points $n = 1000$ and the numerical solution is sampled every 50 points

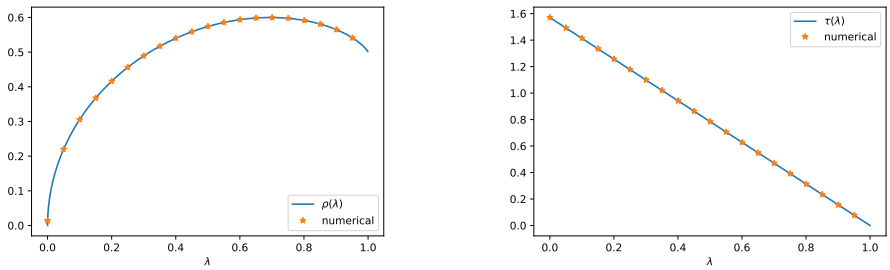

(a) $\rho(\lambda)$ **(b)** $\tau(\lambda)$

Figure 4.6: Comparison of numerical and analytical solutions ρ and τ for the parabolic potential (D.14). Numerical solution computed using algorithm (2) and analytical solutions computed in section D. Here the number of grid points $n = 1000$ and the numerical solution is sampled every 50 points

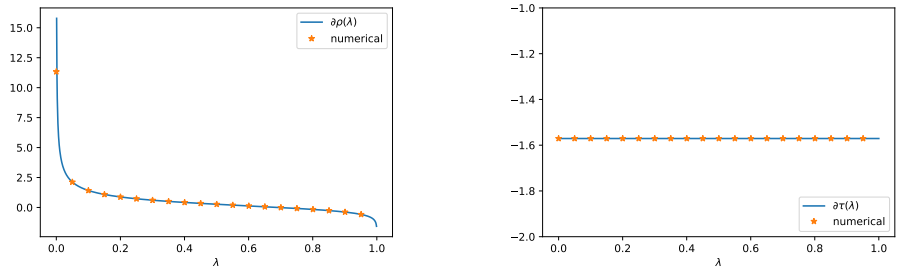

(a) $\partial\rho(\lambda)$ **(b)** $\partial\tau(\lambda)$

Figure 4.7: Comparison of numerical and analytical solutions ρ' and τ' for the parabolic potential (D.14). Numerical solution computed using algorithm (2) and analytical solutions computed in section D. Here the number of grid points $n = 1000$ and the numerical solution is sampled every 50 points

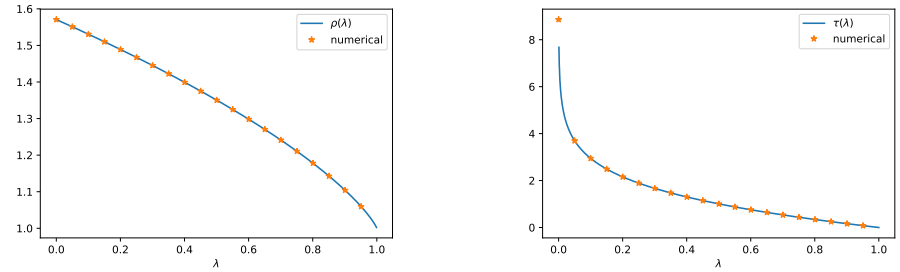

(a) $\rho(\lambda)$ **(b)** $\tau(\lambda)$

Figure 4.8: Comparison of numerical and analytical solutions ρ and τ for the algebraic potential (D.33). Numerical solution computed using algorithm (2) and analytical solutions computed in section D. Here the number of grid points $n = 1000$ and the numerical solution is sampled every 50 points

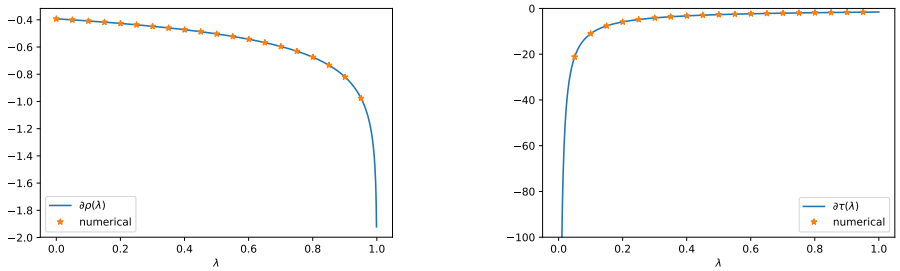

(a) $\partial\rho(\lambda)$ **(b)** $\partial\tau(\lambda)$

Figure 4.9: Comparison of numerical and analytical solutions ρ' and τ' for the algebraic potential (D.33). Numerical solution computed using algorithm (2) and analytical solutions computed in section D. Here the number of grid points $n = 1000$ and the numerical solution is sampled every 50 points

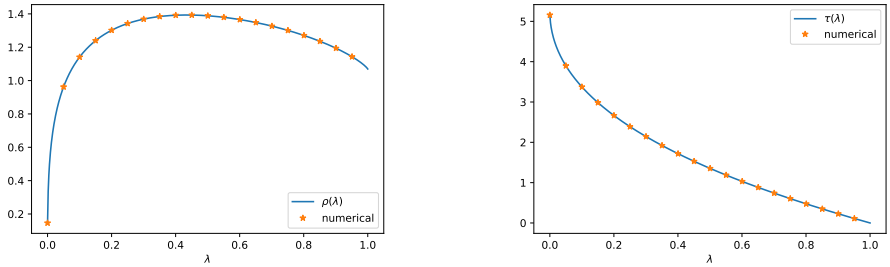

(a) $\rho(\lambda)$ **(b)** $\tau(\lambda)$

Figure 4.10: Comparison of numerical and analytical solutions ρ and τ for the secant potential (D.46). Numerical solution computed using algorithm (2) and analytical solutions computed in section D. Here the number of grid points $n = 1000$ and the numerical solution is sampled every 50 points

The proposed algorithm can run in parallel and we will now examine if is necessary in practice. We run the algorithm in serial and in parallel using 2, 4, 8 and 12 workers(cores). We divide λ into n number of discrete grid points and for each n we set the serial performance equal to 1. Then a measured speedup when running in parallel can be found and the results are plotted in figure (4.12) and (4.13), for a algebraic and a parabolic potential. When the number of grid points are small, $n < 10^3$, there is little to gain to run with multiple workers. In this region the computation time is short and parallelization mostly increase computational cost due to having to initialise the workers. For the region $n > 10^3$ the speedup is notable, for example $n = 10^4$ there is a increase in performance with a factor ≈ 8 when executing with 12 workers. A natural question is how many grid points is actually necessary to create sufficient accurate functions for τ and ρ. For a parabolic potential we calculate $|\partial\rho(\lambda) - \partial\rho^i(\lambda)|$ and plot the results in figure (4.14). Near the endpoints $\lambda \approx 0$ and $\lambda \approx 1$ the errors are high and to obtain sufficiently accurate results we do need a large number of grid points, thus justifying the extra complexity parallelisation brings. Another option would be to have dynamic grid, where the points near $\lambda = 1$ and $\lambda = 0$ is closer than in the middle region.

Since the most intensive and time consuming parts of computing the quantities β_0 and the phase (α_1, β_1) is exactly to compute many independent integrals we will not go through the same analysis for the these. We expect a similar picture as seen in figures (4.12) and (4.13) to hold, this is exactly what we experience when running the algorithms.

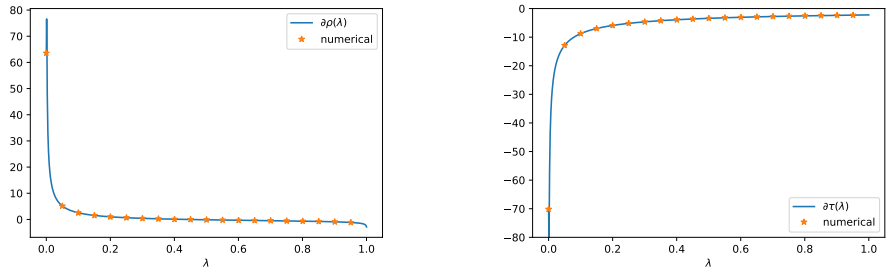

(a) $\partial\rho(\lambda)$ **(b)** $\partial\tau(\lambda)$

Figure 4.11: Comparison of numerical and analytical solutions ρ' and τ' for the secant potential (D.46). Numerical solution computed using algorithm (2) and analytical solutions computed in section D. Here the number of grid points $n = 1000$ and the numerical solution is sampled every 50 points

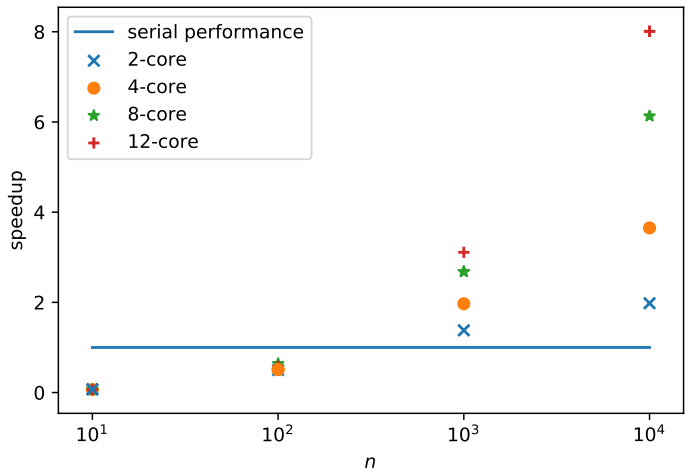

Figure 4.12: Measured speedup when running algorithm (2) in parallel, algebraic potential. For each $n = 10, 10^2, 10^3, 10^4$ the algorithm ran 10 times and the mean taken. Serial performance is set to 1 for each n.

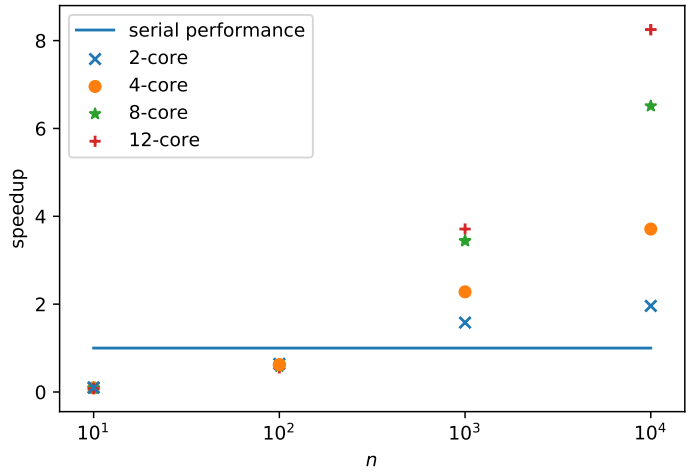

Figure 4.13: Measured speedup when running algorithm (2) in parallel, parabolic potential. For each $n = 10, 10^2, 10^3, 10^4$ the algorithm ran 10 times and the mean taken. Serial performance is set to 1 for each n.

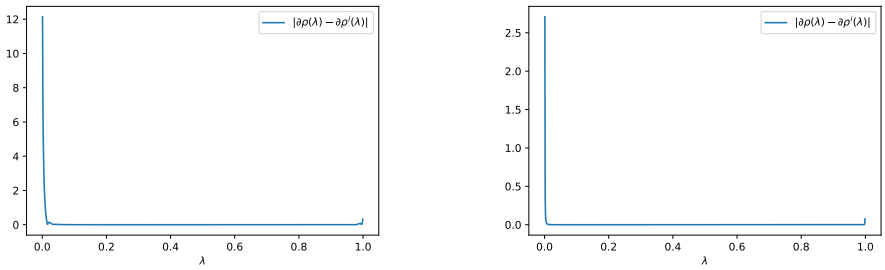

(a) $n = 10^2$ **(b)** $n = 10^3$

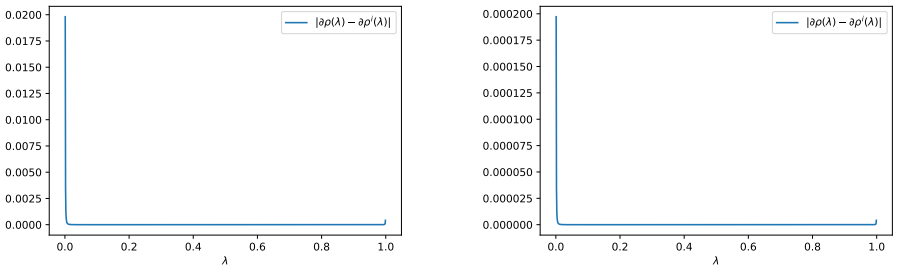

(c) $n = 10^4$ **(d)** $n = 10^5$

Figure 4.14: Error estimates for $\partial\rho$ using algorithm (2) for a parabolic potential. Here n denotes the number of linear spaced points from 0 to 1. Estimates calculated using $|\partial\rho(\lambda) - \partial\rho^i(\lambda)|$, where $\partial\rho$ denotes the exact solution and $\partial\rho^i$ denotes the numerical interpolating function.

4.3 Breaking time t^*

To numerically find the breaking time t^* we use equation (3.75)

$$t^* = -\frac{1}{min_{\eta \in \mathcal{R}} 6u_0'(\eta)}, \eta \in [0, s] \tag{4.4}$$

where s is the support of u_0, possibly $s \longrightarrow \infty$. We can find t^* by first numerically differentiate u_0 and then differentiate the whole expression with respect to η and find its minimum for $\eta \in [0, s]$. Specifically, we need to minimize

$$\frac{d}{d\eta} \frac{1}{6u_0'(\eta)} \tag{4.5}$$

It is not guaranteed that there exist a root to the above equation so to find its minimum a suitable numerical minimizer must be used. Algorithm (3) describes the steps. Note that if the support of u_0 is infinite we must cut of and set it to some finite x^*, however this is not a problem in practice since the minimal point can not be at $\eta \longrightarrow \infty$ and we except that it be at a small finite number.

Data: $u_0(x)$,s,n
Result: breaking time t^*
x^n = linear spaced array from $[0, s]$ with n number of grid points;
u_0' = numerically differentiate u_0 for values $x \in [0, s]$;
$g(x)$ = numerically differentiate $\frac{1}{6u_0'(x)}$ for values $x \in [0, s]$;
r = result when minimizing $g(x)$, where $x \in [0, s]$;
$t^* = \frac{1}{6u_0'(r)}$;
return t^* ;

Algorithm 3: Numerical algorithm for calculating t^*

Using this method gives us t^*, the maximum time where the phase β_0 is still valid. After this we must examine the next phase $N = 1, (\alpha_1, \beta_1)$. For the triangle potential with derivative $u_0' = \pm 1$ we have

$$t^* = \frac{1}{6} \tag{4.6}$$

4.4 Phase before breaking $N = 0, \beta_0 \neq 0$

In section 3.3 we found analytical equations determining β_0, the phase that gives the solution to the KdV equation before breaking time t^*, to be

$$6t\pi\beta_0 + x\pi = C(\beta_0), x > x^* \tag{4.7}$$
$$6t\pi\beta_0 + x\pi = C(\beta_0) - D(\beta_0), x < x^* \tag{4.8}$$

where

$$C(\beta_0) = \int_0^{\beta_0} d\lambda \frac{2\rho'(\lambda)}{(\beta_0 - \lambda)^{1/2}} \tag{4.9}$$
$$D(\beta_0) = \int_{\beta_0}^{1} d\lambda \frac{-2\tau'}{(\lambda - \beta_0)^{1/2}} \tag{4.10}$$

where $x^* = -6t$. The aim is to solve the system (4.7)-(4.8) when $t < t^*$. Since $C(\beta_0)$ and $D(\beta_0)$ are independent of x and t we first compute these quantities and then solve the system for a given x and t. For the triangle potential we can solve C and D exact, using the calculated expressions for τ' and ρ' in section D.

$$\begin{aligned} C(\beta_0) &= \int_0^{\beta_0} d\lambda \frac{1}{\lambda^{1/2}(\beta_0 - \lambda)^{1/2}} - 2\int_0^{\beta_0} d\lambda \frac{\lambda^{1/2}}{(\beta_0 - \lambda)^{1/2}} \\ &= \pi - \pi\beta_0 \\ D(\beta_0) &= -4\int_{\beta_0}^{1} d\lambda \frac{(1-\lambda)^{1/2}}{(\lambda - \beta_0)^{1/2}} = -2\pi(\beta_0 - 1) \end{aligned} \tag{4.11}$$

this gives us

$$6t\beta_0 + x = 1 - \beta_0, x > x^* \tag{4.12}$$
$$6t\beta_0 + x = \beta_0 - 1, x < x^* \tag{4.13}$$

Thus, for the triangle case the phase β_0 is

$$\beta_0 = \begin{cases} \frac{1+x}{1-6t}, x^* < x < 1 \\ \frac{1-x}{1+6t}, -1 < x < x^* \\ 0 \ o.w \end{cases} \tag{4.14}$$

The result that β_0 has support $x \in [-1, 1]$ is due to the support of the triangle potential. To compute C and D numerically the point $\lambda = \beta_0$ must be considered, as (4.9) and (4.10) are singular here. One option forward would be to analyse the integrands and make asymptotic approximations for the singular points, however this would require us to make assumptions about ρ and τ. Instead we use a special purpose numerical integrator that can handle these kinds of

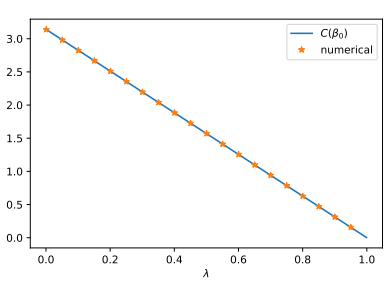

(a) $C(\beta_0)$

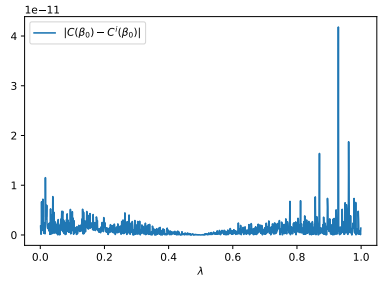

(b) $|C(\beta_0) - C^i(\beta_0)|$

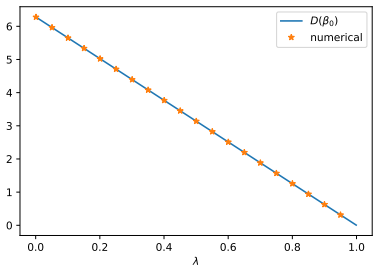

(c) $D(\beta_0)$

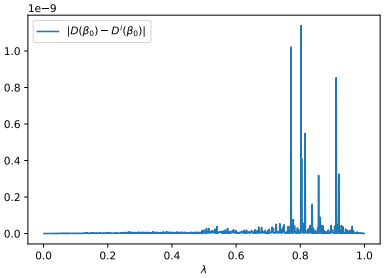

(d) $|D(\beta_0) - D^i(\beta_0)|$

Figure 4.15: Triangle potential, Exact and numerical versions of $C(\beta_0)$ eqn (4.9), $D(\beta_0)$ eqn (4.10) and corresponding error estimates. Here the number of grid points is $n = 1000$, and C^i and D^i denotes the numerical interpolating functions.

singularities and numerically integrate directly. However, due to not knowing the exact formulas for ρ' and τ', the results of the numerical integration should be examined carefully. In addition to the triangle potential it is possible to compute $C(\beta_0)$ and $D(\beta_0)$ for the parabolic potential, see the appendix (D), and we can compare numerical solutions for both these potentials. Figures (4.15) and (4.16) illustrates the results where is $n = 1000$ and the errors are all in the range $10^{-9} - 10^{-11}$.

After C and D are computed the quantity β_0 can be computed by numerically solving the system (4.7)-(4.8). This is implemented using an appropriate non-linear root finder. Note that the equations (4.7)-(4.8) are independent of each other and can be solved as two separate problems. Thus, we propose algorithm (4) as a complete procedure for obtaining β_0 for a particular time t. For this case we only parallelise the first for loop, as for the last two loops we are doing a root search and while it is trivial to parallelise these loops also, it is much more efficient to compute the roots in serial and giving the result from one iteration to next, as this will be close to the next solution. As for the speed

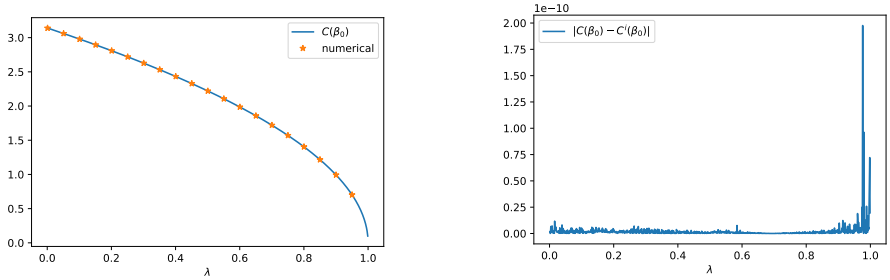

(a) $C(\beta_0)$ **(b)** $|C(\beta_0) - C^i(\beta_0)|$

(c) $D(\beta_0)$ **(d)** $|D(\beta_0) - D^i(\beta_0)|$

Figure 4.16: Parabolic potential, Exact and numerical versions of $C(\beta_0)$ eqn (4.9), $D(\beta_0)$ eqn (4.10) and corresponding error estimates. Here the number of grid points is $n = 1000$, and C^i and D^i denotes the numerical interpolating functions.

up and necessity of the parallel loop the discussion and results from (4.2) are valid for this case also, as the computational task are almost identical.

Data: t,ρ',τ',n,workers
Result: interpolating function for β_0^i
β_0^n = linear spaced array from $[\frac{1}{n}, 1 - \frac{1}{n}]$, with n grid points ;
C^n, D^n = initialize two empty arrays with n grid points, to hold calculated values;
$\ker_C = \frac{2\rho'}{(\beta_0 - \lambda)^{1/2}}$;
$\ker_D = \frac{-2\tau'}{(\lambda - \beta_0)^{1/2}}$;
for all $j \in \beta_0^n$ **in parallel do**
  $C^n[j]$ = integrate $\ker_C$ from $\frac{1}{n}$ to $\beta_0^n[i]$;
  $D^n[j]$ = integrate $\ker_D$ from $\beta_0^n[j]$ to $1 - \frac{1}{n}$;
end
$C(\beta_0)^i$ = create interpolating function using β_0^n and C^n as input ;
$D(\beta_0)^i$ = create interpolating function using β_0^n and D^n as input ;
$x^* = -6t$;
x^r = linear spaced array for the right branch, from x^* to s^r, with n grid points ;
x^l = linear spaced array for the left branch, from x^* to s^l, with n grid points ;
β_0^l, β_0^r = initialize two empty arrays with n grid points, to hold calculated values;
guess = 1 ;
forall $j \in x^r$ **do**
  guess = root find the equation $6t\pi + x_l[j]\pi - C^i[j] = 0$ and place result into $\beta_0^r[j]$, with guess as initial starting point ;
end
guess = 1 ;
forall $j \in x^l$ **do**
  guess = root find the equation $6t\pi + x_l[j]\pi - C^i[j] + D^i[j] = 0$ and place result into $\beta_0^l[j]$, with guess as initial starting point ;
end
β_0^i = create interpolating function using (x^r, β_0^r) and (x^l, β_0^l)
return β_0^i ;

Algorithm 4: Computing interpolating function β_0^i

Let us use algorithm (4) to compute β_0 and compare with exact calculations. While it is possible to compute C and D for the parabolic potential, inverting the equations (4.7)-(4.8) to give an explicit answer for β_0 in terms of (x, t) is not trivial, and perhaps not even possible. We therefore only compare the numerical and analytical solutions for the triangle potential, see figure (4.17).

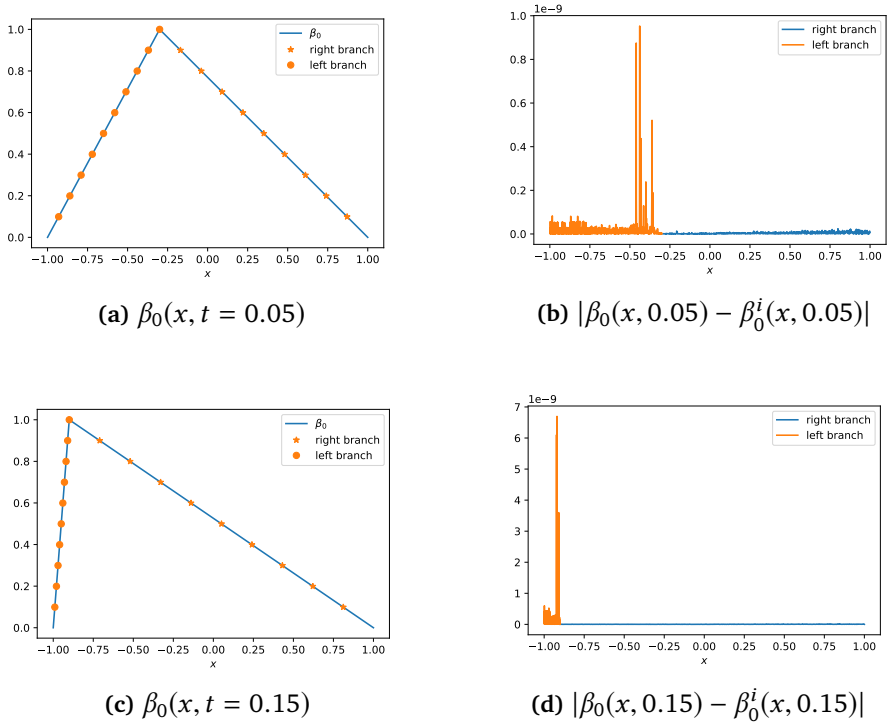

(a) $\beta_0(x, t = 0.05)$

(b) $|\beta_0(x, 0.05) - \beta_0^i(x, 0.05)|$

(c) $\beta_0(x, t = 0.15)$

(d) $|\beta_0(x, 0.15) - \beta_0^i(x, 0.15)|$

Figure 4.17: Triangle potential, Exact and numerical versions of β_0 and corresponding error estimates. Here the number of grid points is $n = 1000$, and β_0^i denotes the numerical interpolating functions.

The results are of same order $\approx 10^{-9}$ as the calculations for C and D. The left branch contains bigger errors that the right branch, which is not surprising since there are two quantities that are computed numerically and due to the interval is shrinking. A numerical solution for β_0 for the parabolic potential can be seen in figure (4.18). The breaking time is $t^* = \frac{1}{12} \approx 0.83$, and we see that when approaching the breaking point the solution becomes vertical and the phase ends. The same phenomena happens for the triangle case (4.17) with breaking time $t^* = \frac{1}{6} \approx 0.166$.

4.5 Second phase $N = 1, (\alpha_1, \beta_1)$

We developed equations for the first phase after breaking in section 3.3, consisting of solving a $2x2$ system of nonlinear equations. Explicit analytical solutions of this system is unlikely to find, for any initial potential. This means that the system must be solved numerically to obtain α_1 and β_1. The method we will take is the same as for calculating β_0, except now we have to solve a system

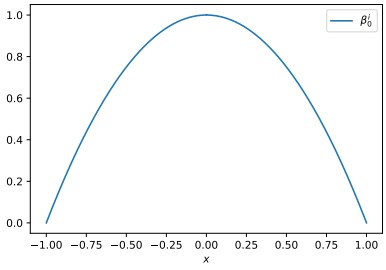

(a) $\beta_0(x, t = 0.0)$

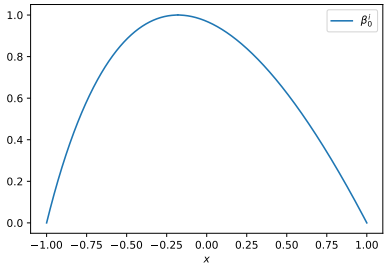

(b) $\beta_0(x, t = 0.03)$

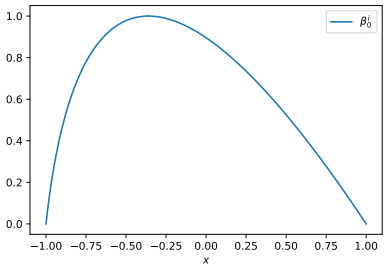

(c) $\beta_0(x, t = 0.06)$

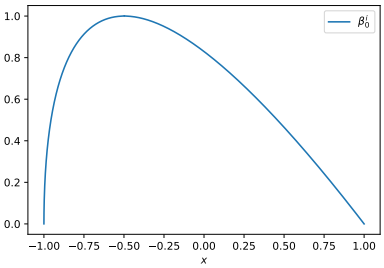

(d) $\beta_0(x, t = 0.083)$

Figure 4.18: Parabolic potential, numerical calculation of β_0.

two nonlinear equations. As a reminder, the actual system we are interested in is on the form

$$6t\pi(\alpha_1 + \beta_1) + \pi x = F_1(\alpha_1, \beta_1) + F_2(\alpha_1, \beta_1) \quad (4.15)$$

$$12t\beta_1^{3/2} S(\gamma) + \beta_1 G_1(\alpha_1, \beta_1) - \beta_1 G_2(\alpha_1, \beta_1) = 2\tau(\alpha_1) \quad (4.16)$$

where $\gamma = \frac{\alpha_1}{\beta_1}$ and F_1, F_2, G_1 and G_2 [1] are as defined in (3.3). The quantities F_1, F_2, G_1 and G_2 all contain integrals that must be evaluated before the above system can be solved. The first step is therefore to evaluate these four quantities over a triangular domain $0 < \alpha_1 < \beta_1 < 1$. This requires computing four double integrals for many discrete points of α_1, β_1. Thus this being a large numerical task this should also be parallelised, computing all four double integrals with a reasonable number of grid points is simply unfeasible to do in serial. When these four quantities is obtained we proceed to solve the system (4.15)-(4.16). We expect to be able to find solutions for all t after breaking, but we do not except to be able to find solutions for all x. From the calculations in section 3.4 we expect it to be a finite interval $x \in (x_1, x_0), x_1 < x_0$ for which we can find solutions to (4.15)-(4.16). Can we, for a particular time $t' \leq t^*$, numerically find the region (x_1, x_0) for which we can solve the system? To find x_0 we use the fact that $\beta_0(x_0, t') = \beta_1(x_0, t')$, if we have equations for F_1, F_2 and for C (4.9) we can numerically find x_0. The results from section 3.4 showed when it is possible to solve the above system where $\alpha_1 \to \beta_1$, and that this can only happen when the initial potential u_0 has asymptotic behaviour $u_0 \sim 1 - a|x|, x \to 0$. Based on this and from numerical results we make the following proposal how to find x_1

- For potentials with behaviour $u_0 \sim 1 - a|x|, x \to 0$ we set $\alpha_1 = 1$ and $\beta_1 = 1$ in (4.15) and solve for x
- For potentials with behaviour $u_0 \sim 1 - ax^2, x \to 0$ we set $\beta_1 = 1$ and solve for the largest α_1 that can satisfy (4.15)

For the triangle potential we can compute x_1 and x_0 exact by setting $\beta_1 = 1$ in (4.15) and using the exact expressions for τ' (D.12) and ρ' (D.10)

$$\begin{aligned} F_1 &= -2\int_0^{\alpha_1} d\mu \frac{\tau'(\mu)\mu^{1/2}}{(\alpha_1 - \mu)^{1/2}(1-\mu)^{1/2}} + 2\int_{\alpha_1}^{1} d\mu \frac{\rho'(\mu)\mu^{1/2}}{(\mu - \alpha_1)^{1/2}(1-\mu)^{1/2}} \\ &= 2\pi\alpha_1 - \pi\alpha_1 \end{aligned} \quad (4.17)$$

Setting $\alpha_1 = 1$ and using (4.15) gives us $x_1 = 1 - 12t$. Similar we set $\alpha_1 = 0$ and in addition use (4.16) and we get $x_0 = 1 - (4(1 + 6t))^{1/3}$. After x_0 and

1. The integrals G_1 and G_2 contains the complete elliptic integral of third kind Π. At the time of writing this these no numerical efficient implementation of this function exists that are usable in Python. See the appendix C.2 for further details.

x_1 is computed we can solve the system (4.15)-(4.16) for a given time t'. This is done be using a numerical root finder, with initial guess $(\alpha_1, \beta_1) = (0, \beta_0(x_0, t')$, then by iterating through an array of $x \in (x_1, x_0)$ using the solution to the previous iteration as initial guess. The whole procedure is described in algorithm (5).

Data: t,ρ',τ',n,workers
Result: interpolating functions (α_1^i, β_1^i)
α_1^n = linear spaced array from $[\frac{1}{n}, 1 - \frac{1}{n}]$, with n grid points ;
β_1^n = linear spaced array from $[\frac{1}{n}, 1 - \frac{1}{n}]$, with n grid points ;
D = outer product of α_1^n and β_1^n ;
F_1, F_2, G_1, G_2 = initialize four empty arrays with $n \times n$ grid points, to hold calculated values ;
for all $j, k \in D$ **in parallel do**
    Integrate $\ker_{F_1}, \ker_{F_2}, \ker_{G_1}$ and $\ker_{G_2}$ over triangular domain D ;
    Fill F_1, F_2, G_1, G_2 with values from above step ;
end
$F^i(\alpha_1, \beta_1)$ = 2-dimensional interpolating function using $(\alpha_1^n, \beta_1^n, F_1)$ and $(\alpha_1^n, \beta_1^n, F_2)$ as input ;
$G^i(\alpha_1, \beta_1)$ = 2-dimensional interpolating function using $(\alpha_1^n, \beta_1^n, G_1)$ and $(\alpha_1^n, \beta_1^n, G_2)$ as input ;
x_0, x_1 = numerically compute the starting point x_0 and end point x_1, for a given t ;
X = linear spaced array from x_0 to x_1 with n elements ;
$g = (0, x_0)$;
while $X \geq x_1$ **do**
    g = numerically solve system (4.15)-(4.16) with g as initial guess ;
    $(\alpha_1^n, \beta_1^n) = g$
end
α_1^i = create interpolating function using X and α_1^n ;
β_1^i = create interpolating function using X and β_1^n ;
return (α_1^i, β_1^i) ;

Algorithm 5: Computing interpolating function (α_1^i, β_1^i)

When implementing algorithm (5) one first compute F_1, F_2, G_1 and G_2 and construct the interpolating functions F^i and G^i . These need only be calculated one time and after they can be used to solve for arbitrary $t > t^*$. It is not necessary to use a square grid $n \times n$ as described in (5), a more reasonable approach could for example be to use more points for β_1 than α_1.

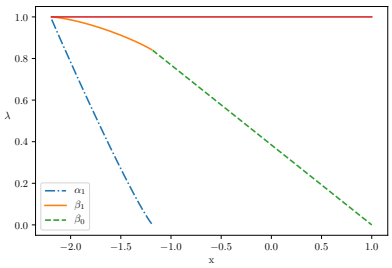

(a) $t = \frac{1}{6} + \frac{1}{10}$

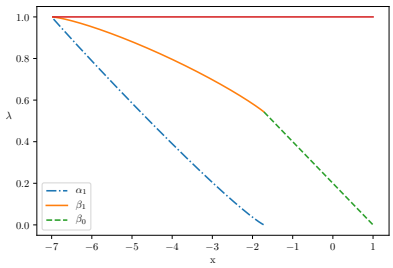

(b) $t = \frac{1}{6} + \frac{1}{2}$

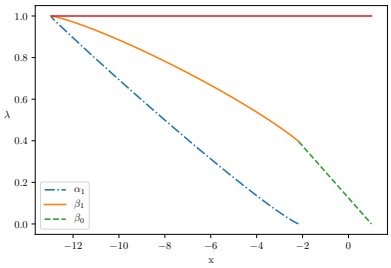

(c) $t = \frac{1}{6} + 1$

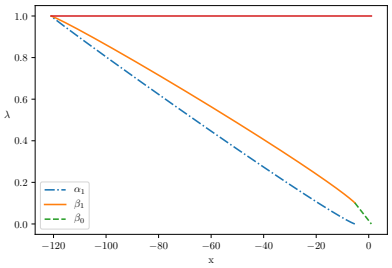

(d) $t = \frac{1}{6} + 10$

Figure 4.19: Numerical calculations of (α_1, β_1) from system (4.15)-(4.16), triangle potential

4.6 Numerical results for (α_1, β_1) for some initial potentials

Now that numerical procedures for calculating ρ', τ' and the phase (α_1, β_1) has been developed we can examine if the numerical results agree with the conclusions made in section 3.4. The main conclusion was that for potentials $1 - ax^2, x \to 0$ additional phase(s) is always needed and for potentials $1 - a|x|, x \to 0$ it is possible that only one phase is sufficient. In addition we made predictions on asymptotic behaviour of ρ' and τ' in the two limits $\lambda \to 0$ and $\lambda \to 1$. We identified that if $\lim_{\lambda \to 1} \tau' = 0$, then the phase can end and that this can only happen for potentials that approached this limit linearly. Starting with our main example, the triangle potential (4.1), we see on figure (4.5) that exactly this is what happens. Further, solving for the phase for various times $t > t^*$ we see from the plots in figure (4.19) that the solutions take the form $\alpha_1 \to \beta_1$ exactly at $x = x_1$, ending the phase. This agrees with predictions made in section 3.4. Analytical and numerical calculations of ρ' and τ' for the other potentials we consider is plotted in figures (4.7), (4.9) and (4.11). These three potentials behave parabolic as $x \to 0$ and does behave as predicted. For example we have for all that $\tau > 0$ and $\tau' < 0$ for $\lambda \in (0, 1)$. All three have behaviour

$$\lim_{\lambda \to 1} \rho'(\lambda) = -\infty \tag{4.18}$$

also as predicted. The other limit $\lambda \to 0$, we have for the parabolic and secant potential

$$\lim_{\lambda \to 0} \rho'(\lambda) = \infty \tag{4.19}$$

The algebraic potential is the special case that decays $u_0 \sim x^{-2}, x \to \pm\infty$, and we predicted that $\lim_{\lambda \to 0} \rho'(\lambda) = C_0$, where C_0 is a finite number, see figure (4.9). Thus the exact calculations for ρ' and τ' completely agrees with our predictions. This means that when we solve for (α_1, β_1) we do not expect that the solutions takes the same shape as for the triangle potential, but that it ends for some finite x_1 where α_1 is not arbitrary close to β_1. Let us examine this numerically, using algorithm (5) first to solving for the phase for the parabolic and the algebraic potential, setting time $t = 1$. The results are plotted in figures (4.20) and (4.21), and what happens numerically is exactly as $\beta_1 \to 1$ the equations for (α_1, β_1) can no longer be satisfied and here α_1 is not arbitrary near β_1. This picture is the same for any $t^* < t < \infty$, and we can not find solutions to the KdV equation for all time t and space x using only one phase after breaking for this class of potentials. Another prediction we made in (3.4) was that for the potentials that behave linear as $x \to 0$. As seen for the triangle potential this leads to solutions where the phase ends as $\alpha_1 \to \beta_1$, but can we

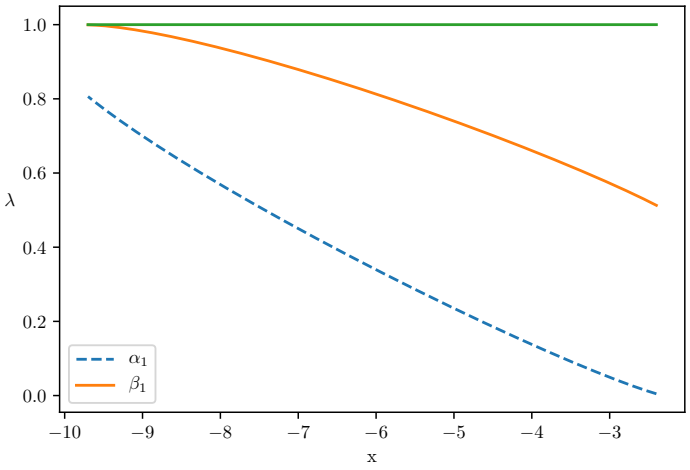

Figure 4.20: Phase (α_1, β_1) for parabolic potential for time $t = 1$

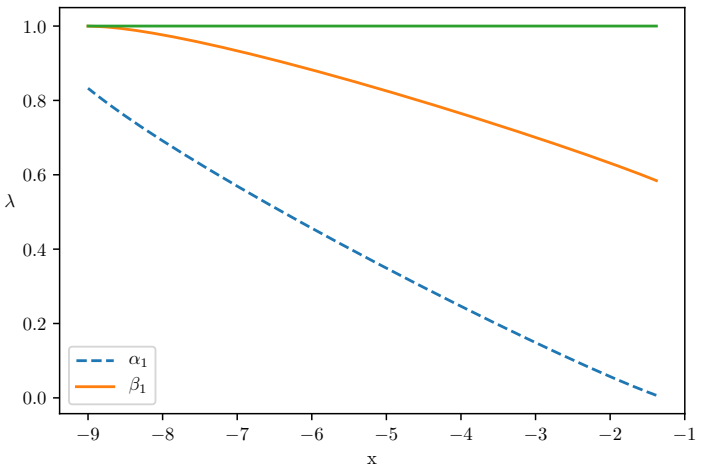

Figure 4.21: Phase (α_1, β_1) for algebraic potential for time $t = 1$

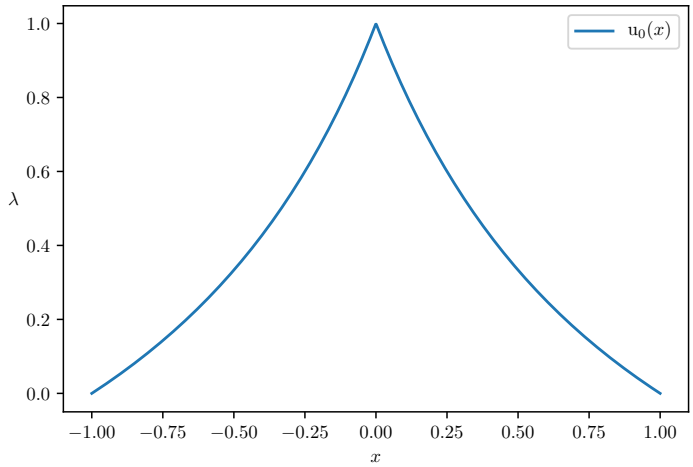

Figure 4.22: Potential defined in (4.20)

examine other potentials of this kind? Let us make the following somewhat artificial potential

$$u_0(x) = \frac{2}{1+|x|} - 1 \tag{4.20}$$

with support $x \in [-1,1]$, see figure (4.22). If our predictions are correct then $\lim_{\lambda\to 1} \tau'(\lambda) = 0$, and a solution to the phase similar to the triangle potential should be possible. From the numerics we get the picture shown in figure (4.23) for ρ' and τ', and their asymptotic ($\lim_{\lambda\to 1 \vee 0}$) characteristics is identical to that of the triangle potential. Next is the question whether this means that the characteristics for the solution of phase is the same also, solving for (α_1, β_1) using the numerical ρ' and τ' give solutions on form seen in (4.24).

The main point by this is, while we have not formally proven that potentials of kind leads to solutions similar to that seen on figures (4.19) and (4.24), it is what we see numerically and what the asymptotic calculations suggests. For the class of parabolic potentials, the numerics suggests that the solutions can no longer exist as $\beta_1 \longrightarrow 1$(figures (4.20)-(4.21)), supporting the statements we made in section 3.4.

4.7 Constructing the solution $u(x,t)$

In chapter 3 we postulated that for the triangle potential the whole solution could be computed using two phases. In the previous section numerical calcula-

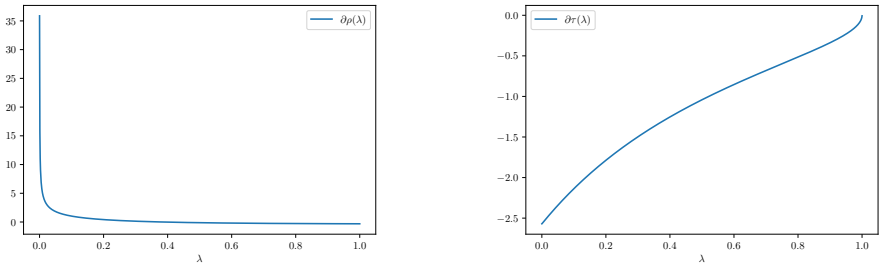

(a) $\partial\rho(\lambda)$ **(b)** $\partial\tau(\lambda)$

Figure 4.23: Numerical calculations of ρ' and τ' for potential (4.20)

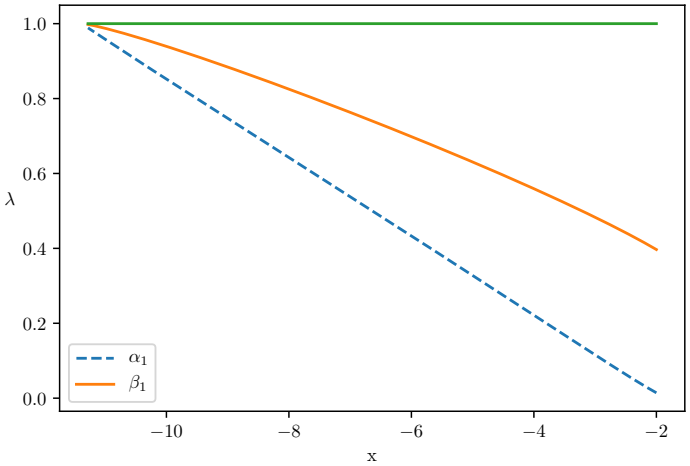

Figure 4.24: Phase (α_1, β_1) for linear potential (4.20), time $t = 1$

tions supported this, see for example (4.19), here the phase $N = 1$ is computed and we have $\alpha_1 \longrightarrow \beta_1 \longrightarrow 1$. Thus we have everything we need to construct the solution $u(x,t)$ in this particular case. For times $t < t^*$ the solution is simply β_0. For times after breaking we must pick a specific time $t = t' > t^*$ and use the numerical expressions for F_1, F_2, G_1 and G_2 to solve the system (4.15)-(4.16) for (α_1, β_1), $x \in (x_1, x_0)$. We use the solution to calculate the remaining quantities needed to construct $u(x,t'), x \in (x_1, x_0)$. Note that after F^i and G^i are computed they can be used to solve for an arbitrary $t > t^*$ and $\epsilon << 1$, allowing us to calculate $u(x,t)$ at a relatively low cost(seconds) as the most intensive calculation consists of computing F_i and G_i(minutes/hours). For the triangle potential, using the results from chapter 3.3 the solution is given by equations (3.185) and (3.186). As a reminder we write down the solution after breaking

$$u(x,t) \sim \begin{cases} \beta_0(x,t), \ x \in (x_0, s) \\ \alpha_1(x,t) + \beta_1(x,t) + 2q_0 - 2\epsilon^2 \partial_{xx} \log(\Theta(\frac{\Omega_1}{2\pi\epsilon}, \Phi_1)), \ x \in (x_1, x_0) \\ 0 \ o.w. \end{cases} \tag{4.21}$$

where we now assume that (α_1, β_1) is known through algorithm (5). Analytical expressions for q_0 and Φ_1 was found in section 3.3, the quantity Ω_1 must be numerically determined using (α_1, β_1) and equation (3.176). What remains is to insert the pieces into (4.21). The Riemann-Theta function Θ is implemented in Python using the package openRT [6], a derivative work of Abelfunctions [26]. Combining all the pieces we can finally obtain a solution to the KdV equation, where we must numerically compute the second derivative of Θ. We set $\epsilon = 0.1$ and plot the solution for times $0 < t < \frac{1}{6} + 0.8$, see figure (4.25).

Before breaking the solution shifts to the left and exactly at $t = \frac{1}{6}$ a vertical slope has been developed. For the Burger's equation ($\epsilon = 0$) this is exactly where the solution becomes multivalued. Since our model describes light behaviour we do not expect multivalued solutions and it is also known that the KdV equation does not, instead it starts rapid oscillations that regularise the shock. Observe that after breaking, in the region around $x \approx x_0(t)$ where the solution shifts from the first phase determined by β_0 to the second phase determined by (α_1, β_1), there is a discontinuity in u'. This is a numerical phenomena and would not be present if we could compute everything analytically. As the solution evolves it exhibits a near vertical profile for $x \approx x_0$, perhaps partly explaining the challenge of implementing purely numerical solvers that preserves the correct solution after breaking.

An advantage using the RH approach is the ability to find a solution for a specific time $t = t'$ without having to calculate the solutions for all previous

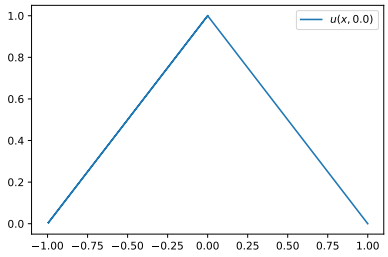

(a) $u(x, 0)$

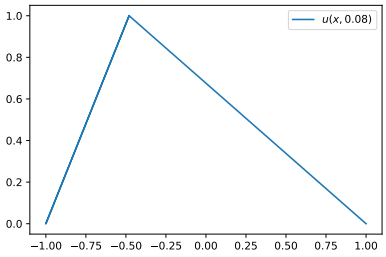

(b) $u(x, 0.08)$

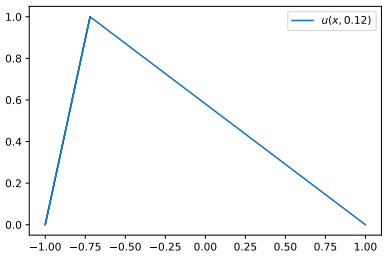

(c) $u(x, 0.12)$

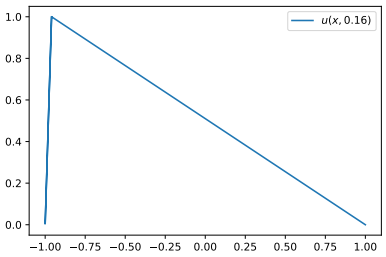

(d) $u(x, 0.16)$

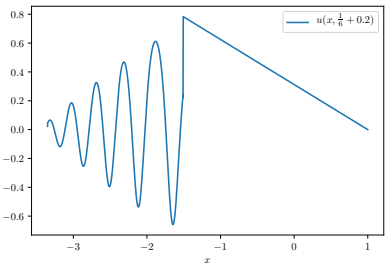

(e) $u(x, \frac{1}{6} + 0.2)$

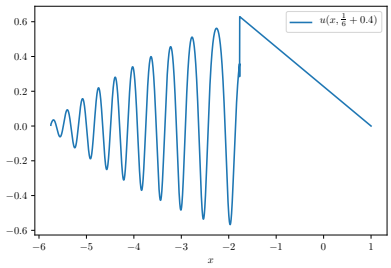

(f) $u(x, \frac{1}{6} + 0.4)$

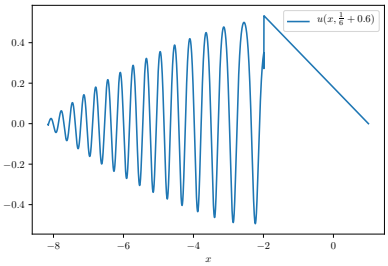

(g) $u(x, \frac{1}{6} + 0.6)$

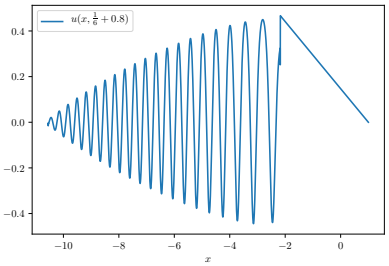

(h) $u(x, \frac{1}{6} + 0.8)$

Figure 4.25: Numerical solution $u(x, t)$ of the KdV equation with $\epsilon = 0.1$ using the Riemann-Hilbert method, before and after breaking time $t^* = \frac{1}{6}$

times, as the case would be if a standard numerical method is used. Additionally the numerical errors propagating from one time step to the next is avoided, as the phase equations are used to find the solution.

As we have not succeeded in implementing a numerical scheme able to go beyond breaking(at a reasonable use of time and resources) we do not have a second solution we can use to compare the RH solution seen in figure (4.25). Though the solution we have obtained looks reasonable, concluding that it is correct purely using this as a qualitative argument is not sufficient. Fortunately there some more quantitative test we can employ to examine the solution, this will be the topic of the next section.

4.8 Conservation laws and examining the solution

The KdV equation has an infinite number of conservation laws, here meaning that there exists an infinite number of properties of $u(x,t)$ that are time invariant. In the appendix section A.1 we introduce the concept in more technical terms and derive the first three conservation laws, these being

$$\begin{aligned} d_0 &= u \\ d_1 &= u_x \\ d_2 &= u_{xx} + u^2 \end{aligned}$$

and the conserved quantity u implies that $d_3 = u^2$ is also conserved. Since $u(x,0)$ is known, we can use the conservation laws by integrating over all x for times $t > 0$ to test the numerically calculated solution, in theory testing as many quantities we want. While this at first might seem simple to utilise, in practice it is not due to numerical issues, this will be discussed in more detail later. For now let us use $u_0(x)$ to calculate the three conserved quantities d_0, d_1 and d_3

$$\begin{aligned} d_0 &= \int_{-\infty}^{\infty} dx u_0(x) \\ &= 2\int_0^1 dx(1-x) \\ &= 1 \end{aligned} \tag{4.22}$$

and for d_3

$$\begin{aligned} d_3 &= \int_{-1}^{1} dx(x^2 - 2x + 1) \\ &= \frac{2}{3} \end{aligned} \tag{4.23}$$

The derivative of u_0 is

$$u_0' = \begin{cases} 1, x < 0 \\ -1, x > 0 \end{cases} \tag{4.24}$$

which we can use to compute d_1

$$\begin{aligned} d_1 &= \int_{-1}^{1} dx u_0' \\ &= \int_{-1}^{0} dx + \int_{0}^{1} dx(-1) = 0 \end{aligned} \tag{4.25}$$

Using these results we compute for times $t > 0$ by subtracting the numerical results from equations (4.22),(4.25) and (4.23) e.g. $\delta d_0 = 1 - \int_{-\infty}^{\infty} dx u(x, t')$. The results of these calculations can be seen in figures (4.26), (4.27) and (4.28). Perhaps unsurprising, the errors before breaking is very small ($< 10^{-5}$) compared to the errors after breaking. After $t = t^* = \frac{1}{6}$ we see a jump in the computed error, but the errors are not very large ($\approx 10^{-1} - 10^{-3}$). For times immediately after breaking the largest error occur for all the three quantities, before we see a trend that the error decays as the time increases.

The problem employing more of the conserved quantities for $u(x, t)$ is the loss the numerical operations introduce. Looking at the oscillatory shape of solution on figure (4.25) it is clear that first having to numerically compute high derivatives and then integrate is demanding. Already at $d_2 = u^2 + u_{xx}$ the errors in the numerical operations is too large to use the calculations in a meaningful way.

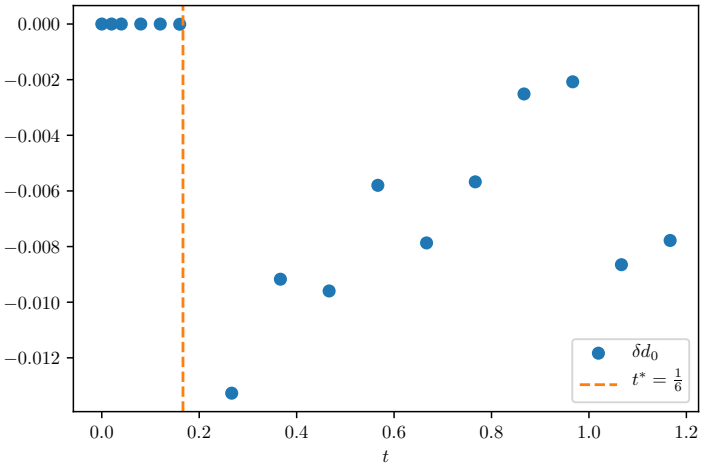

Figure 4.26: Numerical error for the conservation law $d_0 = u$. Computed by subtracting the integral $\int_{-\infty}^{\infty} dx u(x,t)$ from the reference $\int_{-\infty}^{\infty} dx u(x,0)$

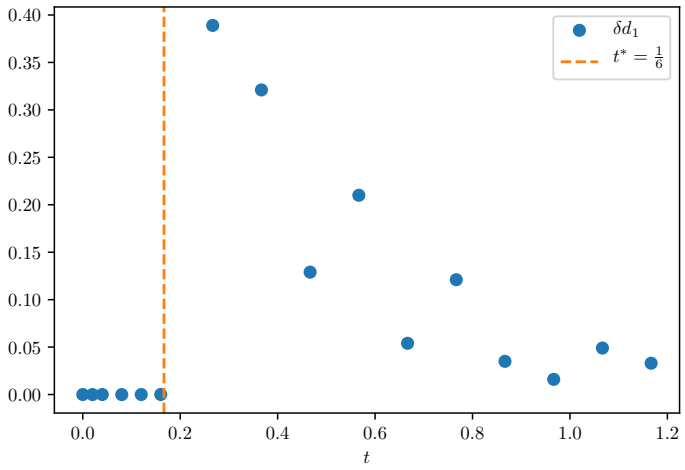

Figure 4.27: Numerical error for the conservation law $d_1 = u_x$. Computed by subtracting the integral $\int_{-\infty}^{\infty} dx u_x(x,t)$ from the reference $\int_{-\infty}^{\infty} dx u_x(x,0)$

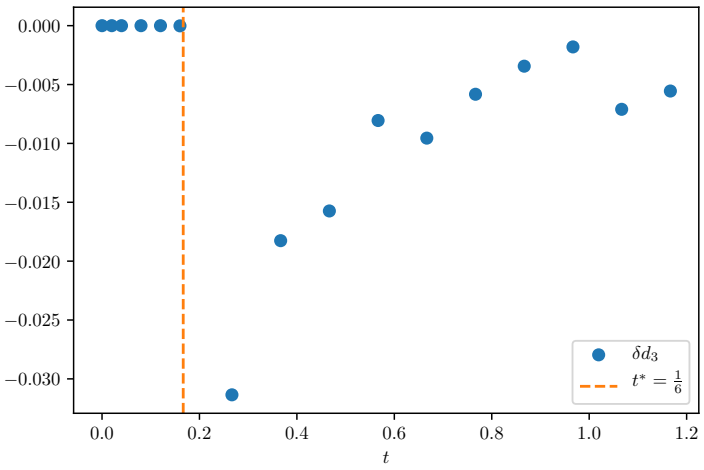

Figure 4.28: Numerical error for the conservation law $d_3 = u^2$. Computed by subtracting the integral $\int_{-\infty}^{\infty} dx u^2(x,t)$ from the reference $\int_{-\infty}^{\infty} dx u^2(x,0)$

5

Conclusion

In this chapter we summarise and discuss our findings from chapters 2, 3 and 4. Advantages and disadvantages using the proposed methods are discussed and some topics for further work is proposed.

5.1 Summary and discussion

5.1.1 Proposing a mathematical model

In chapter 2 we proposed a mathematical model for high intensity laser pulse propagation in air. This was derived by starting with Maxwell's equations, proceeding by making standard physical assumptions and mathematical simplifications in nonlinear optics, then employing a multiple scale perturbation hierarchy. From this we could write down equations for each perturbation order ϵ^n, giving conditions for the solvability at each order. Expanding up to order two we obtained a system of partial differential equations, where additional physical assumptions had to be made to further simplify the equation. By assuming linear polarization and that most of the activity stays on the propagation axis, thus disregarding radial effects, we could proceed. The last step was not a well justified step, but rather an assumption we believe to hold for some cases and thus especially open to be criticised. After some addition algebra we arrived at the modified Korteweg-de Vries equation, a known partial differential equation describing phenomena with both dispersive and

nonlinear behaviour and this is the the equation we propose as a qualitative model describing laser pulse propagation in air. Since air is a weakly dispersive medium for the wavelengths we consider, the dispersive term in the equation is small. Through the Miura transformation solutions to the mKdV equation could be found by solving the simpler KdV equation.

5.1.2 The Riemann-Hilbert approach for solving the KdV equation

After arriving at the mKdV equation as a model, in practice considering the KdV equation trough the Miura transformation, the remaining part of the thesis focused on solving this equation. Though being solvable using the inverse scattering transform, due to the smallness of the dispersive term a simplification could be made by solving the equation asymptotically. Using a method proposed by Deift et al. [7] the equation could be solved in the dispersionless limit as a Riemann-Hilbert problem. We presented the necessary steps in the solution process and made some explicit calculations, minimum of what is needed if the method is to be used in a practical way. While many of the mathematical details behind the procedure are complicated, the actual mechanical steps, in principle, fairly straight forward. An essential idea is to find equations for the different phases developed by the KdV equation, where each is valid for a unique interval in time and space. Instead of going through the steps for a specific initial condition we took a more crude approach where we simply developed equations for the two simplest phases $N = 0, \beta_0 \neq 0$ and $N = 1, (\alpha_1, \beta_1)$ and then later asked if these could be sufficient for the class of initial conditions we consider.

Developing equations for the first phase $N = 0$ did not pose any great difficulties and resulted in a single equation determining the unknown β_0. For the next phase $N = 1$ developing the correct equations was possible, but not trivial and resulted in a system of 2×2 equations containing unevaluated integrals. To be able to solve the two systems the integrals must be computed and this is mostly a numerical task. The difficulty calculating the phase $N = 1$ illustrates one of the key challenge using this method, if many phases are needed the algebra and the following numerical work gets complex and intensive. If we have to go beyond these two phases e.g. set $N = 2$, it is not likely that we will be able to do much analytically. This will result in having to solve a system of 3×3 equations, likely determined by integrals we can not simplify much, resulting in a complex numerical task. After (numerical) expressions for the phases are obtained the work is essentially done, constructing the solution $u(x, t)$ was fairly straight forward.

It is important to realise if we use this asymptotic method to solve the mKdV

equation then the dispersion term should be small. This is due to the transformation $u = m^2 + \epsilon m_x$, where we want to approximate the initial potential $u_0 \approx m_0^2$. If we can not do this the corresponding potential u_0 we use as initial condition for the KdV equation is not in a form suitable to solve using the method we have followed. Therefore, before attempting to solve the mKdV it should be verified that the potential m_0 and the desired ϵ allows approximating u_0 by disregarding the ϵm_{0x} term.

5.1.3 Possibility of a new phase

After equations for the phases $N = 0, \beta_0 \neq 0$ and $N = 1, (\alpha_1, \beta_1)$ was developed, we wanted to know if these two phases(in addition to the trivial $N = 0, \beta_0 = 0$) is sufficient to calculate the solution $\forall(x, t)$ for the types of potentials we consider(satisfies definition (1)). While we could not rigorously prove when the two phases are sufficient, we could identify the critical behaviour of the potentials determining if they could be enough or if more phases must be added. From our calculations we identified the key characteristic of the potentials to how they behave in the limit $\lambda \longrightarrow 1$ or equivalently $x \longrightarrow 0^{\pm}$. By asymptotic calculations we found that in the limit $\lim_{x \to 0^{\pm}}$, if the potential behaves linearly

$$u_0(x) \sim 1 - a|x| \tag{5.1}$$

then the two phases could be sufficient and a solution $\alpha_1 \longrightarrow \beta_1$ could exist. If such a solution exist for a potential of this type we also found that this has to happen as $\alpha_1, \beta_1 \longrightarrow 1$. On the other hand, if the potential behaves asymptotically

$$u_0(x) \sim 1 - ax^2 \tag{5.2}$$

then such solutions can not exist, we found that there can be no solution where $\alpha_1 \longrightarrow \beta_1$ for $\lambda \in (0, 1)$. From a practical viewpoint this result is not optimal. It means that the only kind of potentials where we can hope to find solutions without having to add more phases are of type (5.1). Potentials of this type is likely to be of limited practical use, and due to having discontinuous derivative at $x = 0$ these potentials must be artificially constructed to have this behaviour. In addition, these potentials are likely to be of less realistic from a physical perspective. More common is potentials of type (5.2) and as we have seen that at least one addition phase must be added, increasing the complexity of obtaining a solution.

5.1.4 A possible weakness of the theory

An interesting question that emerged during this thesis was the importance of the limit $\lambda \to 1$. In the original article that describes the solution process this limit is not mentioned, rather the the three regions $\lambda \in (-\infty, 0)$, $\lambda \in (0, 1)$ and $\lambda \in (1, \infty)$ is considered. However in our analysis there are indications that this limit should be considered, it is the limit where the WKB approximation becomes invalid, it is the top of the potential and where we observe the phases to end, either entirely $\alpha_1, \beta_1 \to 1$ or a new phase must start $\beta_1 \to 1, \alpha_1 \neq 1$. What is not clear is if the authors in [7] considered this limit and concluded that is not essential or if they simply disregarded the limit as special. If the latter is the case, it is not trivial to understand the justification. From calculations we found two distinct behaviours directly linked to the properties of the initial potential as $\lambda \to 1$. While we have not done enough analysis to claim that disregarding this limit is an error in the proposed procedure it is our view that it at least should have been mentioned if considered. If not considered, it should be.

5.1.5 Numerical results

After the analytical work in chapter 3 the remaining work mostly consisted of implementing and obtaining numerical results for the quantities not possible to find analytically, ultimately to calculate a full example for the problem. Originally the idea was to use a Gaussian $\exp(-\gamma x^2)$ as initial potential, however the result that we could not find the full solution using only two phases changed this idea, being effectively limited to the triangle potential(or similar) to be able to use the procedure to calculate the solution $u(x, t)$. However, all the numerical algorithms developed can be reused if equations for more phases are added.

In chapter 4 the numerical algorithms needed was proposed and the results from the implementation of these was presented. The numerical calculation of the quantities $x_\pm$,breakdown time t^*, ρ, τ and their derivatives did not pose any problems to implement and analytical and numerical results agreed with high accuracy. Calculations of the phases β_0 and (α_1, β_1) was more demanding, both from a purely numerical perspective and due to the lack of exact calculations for comparison. The equations determining the phases must be computed by integrating expressions with singular endpoints, causing numerical challenges if not handled correctly. Additionally the computational work, especially for (α_1, β_1), is intensive and calculating in serial is not really a viable option if high accuracy results for the phases are needed.

For many of the quantities needed to be calculated we suggested that they could be partially computed in parallel. For the most part this means computing

a large number of integrals that are independent of each other. In addition we examined in detail if there was any practical gain by parallelising the calculations for ρ and τ, and we found that for high accuracy calculations we achieved an increase in performance compared to running in serial. We did not analyse this in detail for the other quantities, but since the main computation for all these are numerical calculations of integrals we expect to find the same results for these and this is also what we experienced in practice. For example, to calculate the quantities needed for the phase $N = 1$ was not reasonable to do in serial due to the large number of integrals needed to be calculated.

Since the solution method involves many moving parts - asymptotic approximations, dividing the solution process into multiple partitions, integral transform and so fourth - an example calculation to verify if the obtained solution actually has anything to do with the solution to the KdV equation was performed. Qualitative and by using conservation laws the solution does not immediately seem to be wrong. Due to numerical uncertainty we could not use as many conservation laws as wanted to verify the solution, the errors in the numerical operations becomes a problem on its own due to the rapid oscillations of the solution $u(x, t)$.

In section 3.4 we examined the system of equations determining the phase $N = 1$. Predictions about the behaviour of the system and the implications for the phase was made. Numerical results supported the findings, agreeing with our predictions. Prior to the analysis performed in this thesis the difficulty calculating the phase (α_1, β_1) for potentials $u_0 \sim 1 - ax^2, x \longrightarrow 0$ beyond a point $x < x'$ when $\beta_1 \approx 1, \alpha_1 \neq 1$ was assumed to be a purely numerical issue. However, based on the analytical and numerical results we now claim it is not possible to go beyond x' for any potentials that behave parabolic at the peak.

5.2 Further work

From the authors perspective there are two main branches of further work, where one being investigation of the proposed model while the second is to examine the RH problem solution method.

To either support our model or to invalidate it more work should go into analysing it. For example by comparing it against other methods from where we can obtain insight into the physical situation. Unfortunately there does not seem to be any simple methods to achieve this. One obvious way would be to conduct experiments and somehow compare the critical behaviour from the theoretical model and the experiment. While this being an obvious way, it is

not necessarily a reasonable approach, performing experiments requires both expertise and resources. It would also need to resolve how to interpret and compare results from both methods. Another method, perhaps more realistic, but still challenging would be to calculate Maxwell's equations directly using the same physical assumptions. This is not a trivial task either as there is a reason that solutions to these equations are not normally calculated directly. Computing the solution from Maxwell's equations must therefore mainly be done numerically, which also is challenging as it requires both knowledge and computational power.

A second route would be to examine the Riemann-Hilbert solution process and some interesting questions have come up during this work. It is the authors view that the most important question to answer is if and why it is valid to ignore the seemingly special point $\lambda = 1$. This is the limit where the WKB approximation is not valid and the critical limit where the final phase must end. If this limit must be treated differently then to investigate if is possible to incorporate this into the existing procedure would be important, perhaps by patching solutions together. On the other hand if it is valid to treat the limit without any modifications to the procedure, then equations for a phase $N = 2$ must be developed. It is unclear how much more can be done analytically, as we saw already at $N = 1$ that the algebra involved is complicated. Looking into full cycle potentials for the mKdV equation and try to solve the KdV equation using corresponding potential using the Riemann-Hilbert method could also be interesting.

5.3 Final remarks

We started this thesis by proposing a model for laser pulses and proceeded to make an attempt to solve the corresponding equation. While progress has been made on both work still remains. As we have seen to use the proposed solution method is challenging both analytically and numerically. Before further attempts are made to use the method we suggest that the question if the limit $\lambda \to 1$ must be treated in a special manner is resolved.

Appendices

A

Conservation laws for the KdV equation

One property of the KdV equation is the existence of infinite many conservation laws [1]. The existence of the conservation laws was important in developing the inverse scattering transform as a general solution method to the KdV equation, but can also be used as a tool for checking numerical solutions to the equation. The simplest conservation law for the KdV equation is conservation of mass, meaning that the mass at $t = 0$ is the same as a later time t^*. A simple test for correctness would be to compute the start mass using the initial data and verify if the mass at t^* obtained from the numerical solution agrees. Since there exists an infinite many conservation laws, checking many of these give more and more indications on the validity(or non-validity) of the numerical solution. The KdV have independent variables x and t and partial derivatives of these and a conservation law for an equation of this type is

$$\partial_t T_n(x, t; u) + \partial_x X_n(x, t; u) = 0 \tag{A.1}$$

where u is the solution to the equation and T_n are called the conserved density and X_n is the associated flux. If we integrate this equation over all space

$$\frac{d}{dt}\int_{-\infty}^{\infty} dx T_n = -\frac{d}{dx}\int_{-\infty}^{\infty} dx X_n \tag{A.2}$$

It is required that the solution $u \to 0$ as $x \to \pm\infty$ for the following to hold, a requirement which is also necessary for the KdV to be solvable using the IST,

therefore no real restrictions for our purposes. The RHS of the above equation is therefore zero

$$\begin{aligned} \frac{d}{dt}\int_{-\infty}^{\infty} dx T_n &= 0 \\ \int_{-\infty}^{\infty} dx T_n &= d_n \end{aligned} \tag{A.3}$$

This means that the quantity d_n is conserved in time. Write

$$\begin{aligned} \partial_t(u) + \partial_x(\pm 3u^2 + \partial_x^2 u) &= u_t + 3uu_x + 3u_x u + u_{xxx} \\ &= u_t \pm 6uu_x + u_{xxx} \end{aligned} \tag{A.4}$$

This equation is written in the form (A.1) and is identical to the KdV equation and this is the first conservation law for the KdV equation

$$\int_{-\infty}^{\infty} dx u = d_0 \tag{A.5}$$

and thus u is a conserved quantity. In physics terms we can say it corresponds to conservation of mass or momentum. Is it possible to find more conservation laws? Introduce a more general form of the Miura transform seen in chapter 2, $u = m - \epsilon m_x - \epsilon^2 m^2$

$$u_t + 6uu_x + u_{xxx} = (1 - \epsilon\partial_x - 2\epsilon^2 m)(m_t + 6(m - \epsilon^2 m^2)m_x + m_{xxx}) \tag{A.6}$$

For u to be a solution of the KdV equation we must have

$$(m_t + 6(m - \epsilon^2 m^2)m_x + m_{xxx}) = 0 \tag{A.7}$$

Written in the form (A.1)

$$\partial_t m + \partial_x(3m^2 - 2m^3 + m_{xx}) = 0 \tag{A.8}$$

Formally we write m as a power series

$$m = \sum_{n=0}^{\infty} m_n(x,t)\epsilon^n \tag{A.9}$$

Since (A.8) is written in a conserved form we should also have

$$\int_{-\infty}^{\infty} dx m(x,t;\epsilon) = d \tag{A.10}$$

Due to the fact that u does not depend on ϵ

$$\int_{-\infty}^{\infty} dx m_n(x,t;\epsilon) = d_n \tag{A.11}$$

then by uniqueness of a power series expansion implies

$$u = \sum_{n=0}^{\infty} m_n(x,t)\epsilon^n - \epsilon\partial_x \sum_{n=0}^{\infty} m_n(x,t)\epsilon^n - \epsilon^2 \left[\sum_{n=0}^{\infty} m_n(x,t)\epsilon^n\right]^2 \tag{A.12}$$

We now equate terms of powers in ϵ

$$\begin{aligned} u &= d_0 \\ 0 &= d_1 - \partial_x d_0 \\ 0 &= d_2 - \partial_x d_1 - d_0^2 \end{aligned} \tag{A.13}$$

Solving these recursively gives the first three conserved quantities

$$\begin{aligned} d_0 &= u \\ d_1 &= u_x \\ d_2 &= u_{xx} + u^2 \end{aligned}$$

There is no reason to stop here, it can be continued for as many powers of ϵ needed and provides an infinite number of conserved quantities.

B

Riemann-Hilbert problems

There is a number of problems in physics and mathematics that can be expressed as Riemann-Hilbert problems. We will give a short introduction to how they will be used in the context of solving the KdV-equation. For a more detailed and general description, see for example [20]. We will consider the complex plane with a curve C that consists of the entire real axis, cutting it in two, the upper and lower half plane. We then denote $Im(z) > 0$ as the $\oplus$ region and $Im(z) < 0$ as the $\ominus$ region, illustrated in (B.1). In general the curve C does not need to be the entire real axis, but can be an arbitrary number of open or closed curves in the complex plane. In its simplest form, a scalar Riemann-Hilbert problem consist of finding a sectionally analytic function $\Phi(z)$ that satisfies a specific jump condition when approaching the real axis from $\oplus$ and $\ominus$. We denote these two limits for the function $\Phi(z)$ as Φ^+ and Φ^-. We now state the scalar RH problem as

$$\Phi^+(t) = g(t)\Phi^-(t) + f(t), t \in C \tag{B.1}$$

where $g(t)$ is the jump condition on C, for our case we have $C \in \mathbb{R}$. If $f(t) = 0$, equation (B.1) is a scalar homogeneous RH problem. Is it possible to find a

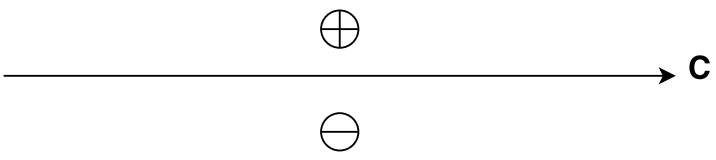

Figure B.1: Illustration of a curve C dividing the complex plane

general solution to these kind of problems? We first look at the homogeneous case and demand that $g(t)$ satisfy a Hölder condition on C, meaning that for any two points t and t_1 on L the following holds

$$|g(t) - g(t_1)| \leq \Lambda |t - t_1|^{\lambda}, \Lambda > 0, 0 < \lambda \leq 1 \tag{B.2}$$

If this condition is met we can take the logarithm of (B.1)

$$\varphi^{+}(t) - \varphi^{-}(t) = \phi(t), t \in \mathbb{R} \tag{B.3}$$

Consider a Cauchy type integral

$$\Phi(z) = \frac{1}{2\pi i} \int_C \frac{\phi(t)}{t - z} \tag{B.4}$$

Since z is on C, the integral (B.4) is ambiguous, the answer depends on the way the singularity $t = z$ is approached. Specifically, if we include the singularity from the $\oplus$ side might give a different answer than if it is included from the $\ominus$ side and we will see that this is connected to the solution to the RH problem (B.1). If we include the singular point from the $\oplus$ side means that when we approach from the point $t = z$ from the left we must deform the path using a half circle of radius ϵ and go around but still keep the point in $\oplus$, then take the limit $\epsilon \longrightarrow 0$. We split the domain of integration into three pieces, $(-\infty, z + \epsilon)$ and $(z + \epsilon, \infty)$, the third region is the small circle around the singularity. If we imagine walking along C from the left we see that when we approach $t = z$ the starting angle must be $-\pi$ for $\oplus$ and π for $\ominus$. We can calculate the Cauchy integral for both Φ^{+} and Φ^{-}

$$\begin{aligned}
\Phi^{+}(z) &= P.V \frac{1}{2\pi i} \int_{-\infty}^{\infty} dt \frac{\phi(t)}{t - z} + \lim_{\epsilon \to 0} \frac{1}{2\pi i} \int_{-\pi}^{0} d\theta \frac{i\epsilon\phi(z + \epsilon \exp(i\theta))}{z + \epsilon \exp(i\theta) - z} \\
&= P.V \frac{1}{2\pi i} \int_{-\infty}^{\infty} dt \frac{\phi(t)}{t - z} + \frac{1}{2}\phi(z) \qquad \text{(B.5)} \\
\Phi^{-}(z) &= P.V \frac{1}{2\pi i} \int_{-\infty}^{\infty} dt \frac{\phi(t)}{t - z} + \lim_{\epsilon \to 0} \frac{1}{2\pi i} \int_{\pi}^{0} d\theta \frac{i\epsilon\phi(z + \epsilon \exp(i\theta))}{z + \epsilon \exp(i\theta) - z} \\
&= P.V \frac{1}{2\pi i} \int_{-\infty}^{\infty} dt \frac{\phi(t)}{t - z} - \frac{1}{2}\phi(z) \qquad \text{(B.6)}
\end{aligned}$$

If we subtract these two expressions

$$\begin{aligned}
\Phi^{+}(z) - \Phi^{-}(z) &= P.V \frac{1}{2\pi i} \int_{-\infty}^{\infty} dt \frac{\phi(t)}{t - z} + \frac{1}{2}\phi(z) - \left[P.V \frac{1}{2\pi i} \int_{-\infty}^{\infty} dt \frac{\phi(t)}{t - z} - \frac{1}{2}\phi(z) \right] \\
&= \phi(z) \qquad \text{(B.7)}
\end{aligned}$$

We also have

$$\Phi^{+}(z) + \Phi^{-}(z) = \frac{1}{\pi i} P.V \int_{-\infty}^{\infty} dt \frac{\phi(t)}{t - z} \tag{B.8}$$

These results are exactly equation (B.3) and can be used to solve the scalar Riemann-Hilbert problem (B.1), with $f = 0$. Equations (B.5), (B.6) are the Sokhoski-Plemelj formula. Denote the solution to the homogeneous problem given by the formula as $X(z)$, with corresponding limiting functions as $X^+(z)$ and $X^-(z)$. We then rewrite the jump condition $g(t)$ in terms of $X(z)$

$$g(z) = \frac{X^+(z)}{X^-(z)} \tag{B.9}$$

If we insert this into the inhomogeneous RH problem

$$\begin{aligned} \Phi^+(z) &= \frac{X^+(z)}{X^-(z)}\Phi^-(z) + f(z) \\ \frac{\Phi^+}{X^+} - \frac{\Phi^-}{X^-} &= \frac{f}{X^+} \end{aligned} \tag{B.10}$$

This is a new homogeneous problem on the form seen in (B.3) and can be solved with the Sokhoski-Plemelj formula

$$\begin{aligned} \frac{\Phi(z)}{X^+(z)} &= \frac{1}{2\pi i}\int_{-\infty}^{\infty} dt \frac{\frac{f(t)}{X^+(t)}}{t-z} \\ &= \frac{1}{2\pi i}\int_{-\infty}^{\infty} dt \frac{f(t)}{X^+(t)(t-z)} \end{aligned} \tag{B.11}$$

Let us now consider two simple examples, we have a jump function

$$g(t) = \begin{cases} -1, & \text{if } t < 0 \\ 1, & \text{if } t > 0 \end{cases} \tag{B.12}$$

We see that for $t > 0$ there are no jump, meaning that the limits from $\oplus$, $\ominus$ are equal. This means that the problem consist of finding a function with these properties as we approach the negative real axis. If we take the branch cut $(-\infty, 0]$ we know from complex analysis that the square root function has a jump of this kind when we approach the cut from the two sided, specifically

$$\lim_{\theta\to\pi} \sqrt{r}\exp(i\frac{\theta}{2}) = -\lim_{\theta\to-\pi} \sqrt{r}\exp(i\frac{\theta}{2}) \tag{B.13}$$

In addition to this a translated square root function would satisfy a translated jump function $g(t+\delta)$. Finally we see that the solution is not unique since analytical functions(across the branch cut) does not contain a jump. Thus, we can always multiply the solution with an arbitrary analytical function $P(z)$ and still have a valid solution. This gives the general solution to the RH problem (B.1)

$$\varphi(z) = X(z)\left[\int_{-\infty}^{\infty} dt \frac{1}{2\pi i}\frac{h(t)}{X^+(t)(t-z)} + P(z)\right] \tag{B.14}$$

where $X(z)$ are the solution to the homogeneous problem

$$X(z) = \frac{1}{2\pi i} \int_{-\infty}^{\infty} dt \frac{\phi(t)}{t - z} \tag{B.15}$$

C

Special Functions

C.1 Airy Function

The Airy functions are solutions to the differential equation

$$\frac{d^2u}{dz^2} + zu = 0$$
$$u = c_0 Ai(z) + c_1 Bi(z) \tag{C.1}$$

The Airy functions has the following asymptotic expansions for large arguments

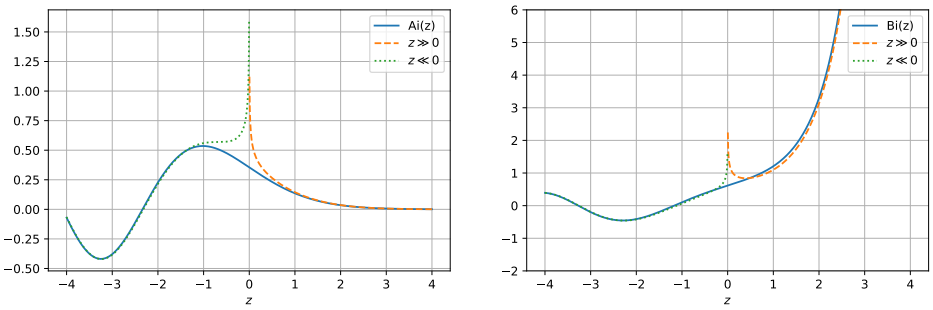

(a) Ai(z)

(b) Bi(z)

Figure C.1: Airy functions $Ai(z)$ and $Bi(z)$ with asymptotic expansions (C.2)-(C.5)

[3].

$$Ai(z) \sim \frac{1}{2\sqrt{\pi}z^{1/4}} \exp(-\frac{2}{3}z^{3/2}), \qquad z \to \infty \tag{C.2}$$

$$Bi(z) \sim \frac{1}{\sqrt{\pi}z^{1/4}} \exp(\frac{2}{3}z^{3/2}), \qquad z \to \infty \tag{C.3}$$

For small arguments we have

$$Ai(z) \sim \frac{1}{\sqrt{\pi}|z|^{1/4}} \sin(\frac{2}{3}|z|^{3/2} + \frac{\pi}{4}), \qquad z \to -\infty \tag{C.4}$$

$$Bi(z) \sim \frac{1}{\sqrt{\pi}|z|^{1/4}} \cos(\frac{2}{3}|z|^{3/2} + \frac{\pi}{4}), \qquad z \to -\infty \tag{C.5}$$

C.2 Elliptic Integrals

The elliptic integrals are integrals originally emerged when trying to calculate arc lengths of ellipses. In this thesis we are interested in the complete elliptic integrals of first $K(k)$,second $E(k)$ and third kind $\Pi(n, k)$. That an elliptic integral is complete means that the domain of integration is $[0, \frac{\pi}{2}]$. They are defined as follows

$$K(k) = \int_0^{\frac{\pi}{2}} d\theta \frac{1}{\sqrt{1 - k^2 \sin^2(\theta)}} \tag{C.6}$$

$$E(k) = \int_0^{\frac{\pi}{2}} d\theta \sqrt{1 - k^2 \sin^2(\theta)} \tag{C.7}$$

$$\Pi(n, k) = \int_0^{\frac{\pi}{2}} d\theta \frac{1}{(1 - n \sin^2(\theta))\sqrt{1 - k^2 \sin^2(\theta)}} \tag{C.8}$$

At the time of writing this thesis the only Python implementation of the elliptic integral of third kind Π in the form (C.8) was in the library mpmath [16]. This library is not suitable for large scale numerical calculations as it is for arbitrary precision math and not optimized for fast numerical operations. As a solution to this we use the iteration scheme for (C.8) found in [10] and implemented this algorithm in C++ and compiled as a shared library that could be imported into Python. The iteration scheme is valid for $k < 1$ and $n < 1$ and implemented

as described by algorithm (6).

Data: k,n,$tolerance = 1e{-}15$,$maxIterations = 50$
Result: $\Pi(n, k)$
$i = 0$;
$k' = \sqrt{1-k}$;
$a_0 = 1$;
$g_0 = k'$;
$\zeta_0 = 0$;
$\delta_n = \frac{1-n}{k'}$;
$\epsilon_n = \frac{n}{1-n}$;
$\zeta_n = \zeta_0$;
$a_n = a_0$;
$g_n = g_0$;
while $i < maxIterations \wedge [|a_n - g_n| > tolerance \vee |\delta_n| > tolerance]$ **do**
  $\zeta_0 = \frac{\epsilon_n+\zeta_n}{2}$;
  $\epsilon_n = \frac{\delta_n\epsilon_n+\zeta_n}{1+\delta_n}$;
  $\zeta_n = \zeta_0$;
  $a_0 = \frac{a_n+g_n}{2}$;
  $g_0 = \sqrt{a_n g_n}$;
  $a_n = a_0$;
  $g_n = g_0$;
  $\delta_n = \frac{g_n(2+\delta_n+\frac{1}{\delta_n})}{4a_n}$;
  $i = i + 1$;
end
return $\frac{\pi(1+\zeta_n)}{2a_n}$;

Algorithm 6: Complete Elliptic Integral of Third Kind

The implementation has been thoroughly tested against the implementations in mpmath [16] and Mathematica [13]. An example from these calculations is given in figure (C.2) and the results is representable for other calculations. The difference between our implementation and mpmath is for all test cases of order 10^{-14}, when using double precision arithmetic. We need this function when numerically solving the integrals for (α_1, β_1) in section 4.5, but does our implementation speed up the calculations? Let us perform the integral

$$\int_{-1}^{1} dx \Pi(x, 0.6) \approx 5.862094705674906 \tag{C.9}$$

Both implementations give the numerical result, to the same number of decimals, seen in the equation above. However, execution time when computing the integral using the two implementations is not comparable, running 10 times

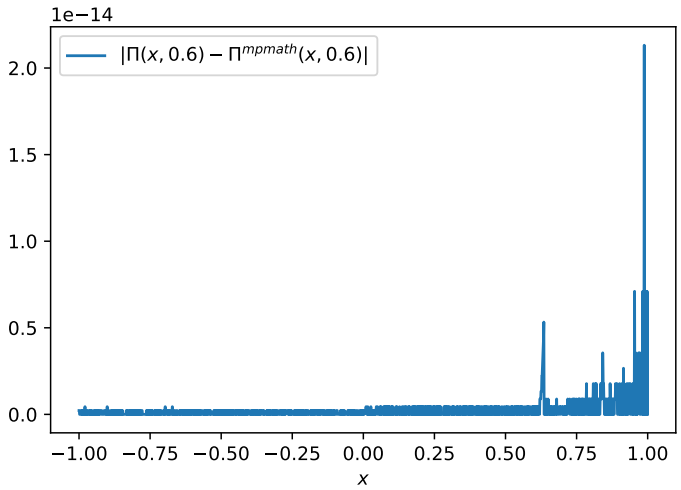

Figure C.2: Difference between Π using algorithm (6) and Π from mpmath [16]

and averaging gives $t \approx 900ms$ when using mpmath and $t \approx 200\mu s$ when using algorithm (6). This difference is of order 10^3 and for practical calculations when the integrals contains other terms in addition to Π the difference has been seen to be even greater. Thus, using Π^{mpmath} for a reasonable grid size of 1000×1000 is simply not practical. For example, let us say that each integral containing Π takes one second, then $1000^2 s$ is close to 280 hours. Using algorithm (6) we can compute the same number of integrals in a matter of minutes.

D

Exact calculations for specific potentials

In chapter 3 we derived approximations for the reflection and transmission coefficients associated with the forward scattering using the WKB-approximation. This resulted in having to solve the two integrals

$$\rho(\lambda) = \lambda^{1/2} x_+(\lambda) + \int_{x_-}^{\infty} d\eta(\lambda^{1/2} - \sqrt{\lambda^{1/2} - u_0(\eta)}) \tag{D.1}$$

$$\tau(\lambda) = \int_{x_-}^{x_+} d\eta \sqrt{u_0(\eta) - \lambda} \tag{D.2}$$

In addition, we found the breakdown time t^* for the Burgers equation

$$t^* = -\frac{1}{min_{\eta \in \mathcal{R}} 6u_0'(\eta)} \tag{D.3}$$

We will in this section examine this for a few specific potentials u_0 where exact calculations of these three quantities are possible.

D.1 Triangle

$$u_0(x) = \begin{cases} 1 - |x| & \text{if } |x| \leq 1 \\ 0 & \text{if } |x| > 1 \end{cases} \tag{D.4}$$

First we need to calculate the singular turning points $x_\pm$

$$\begin{aligned} 1 - x &= \lambda \\ x &= 1 - \lambda \end{aligned} \tag{D.5}$$

This gives $x_+ = 1 - \lambda$ and

$$\begin{aligned} x_- &= -x_+ \\ &= \lambda - 1 \end{aligned} \tag{D.6}$$

Now use (D.1) and the support of u_0

$$\rho(\lambda) = \lambda^{1/2} x_+ + \int_{x_+}^{1} dx(\lambda^{1/2} - \sqrt{\lambda^{1/2} - 1 + x}) \tag{D.7}$$

$$= \lambda^{1/2}(1 - \lambda) + \int_{1-\lambda}^{1} dx(\lambda^{1/2} - \sqrt{\lambda^{1/2} - 1 + x}) \tag{D.8}$$

$$\begin{aligned} &= \lambda^{1/2}(1 - \lambda) + \left[x\sqrt{\lambda} - \frac{2}{3}(\lambda + x - 1) \right]_{1-\lambda}^{1} \\ &= \lambda^{1/2} - \frac{2}{3}(1 - \lambda)^{3/2} \end{aligned} \tag{D.9}$$

computing the derivative of ρ gives

$$\rho'(\lambda) = \frac{1}{2\lambda^{1/2}} - \lambda^{1/2} \tag{D.10}$$

Repeating the process for τ using (D.2)

$$\begin{aligned} \tau(\lambda) &= 2 \int_0^{x_+} dx(1 - x - \lambda)^{1/2} \\ &= -\frac{4}{3}(1 - x - \lambda)^{3/2} \Big|_0^{1-\lambda} \\ &= \frac{4}{3}(1 - \lambda)^{3/2} \end{aligned} \tag{D.11}$$

with derivative

$$\tau'(\lambda) = -2(1 - \lambda)^{1/2} \tag{D.12}$$

To find the breakdown time t^* for a triangle potential we use equation (D.3)

$$\begin{aligned} t^* &= \frac{1}{min_{x \in [0,1]} 6x} \\ &= \frac{1}{6} \end{aligned} \tag{D.13}$$

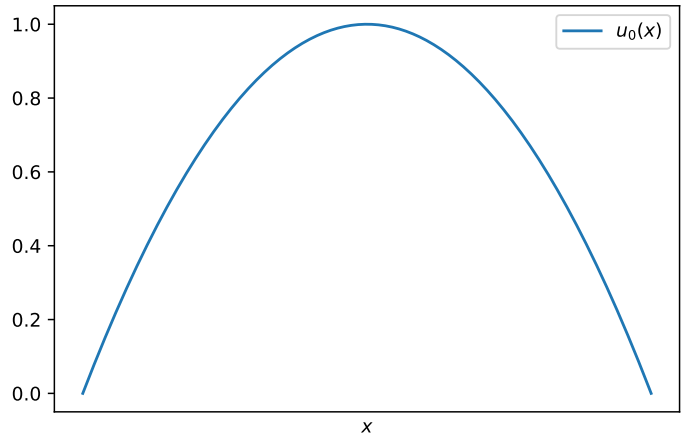

Figure D.1: Shape of parabolic potential function $u_0(x)$ defined in (D.14).

D.2 Parabolic

We have the parabolic potential, see figure (D.1)

$$u_0(x) = \begin{cases} 1 - ax^2 & \text{if } |x| \leq \frac{1}{\sqrt{a}} \\ 0 & \text{if } |x| > \frac{1}{\sqrt{a}} \end{cases} \tag{D.14}$$

First we calculate $x_\pm$

$$\begin{aligned} x_\pm &= u_0^{-1}(\lambda) \\ &= \pm\sqrt{\frac{1-\lambda}{a}} \end{aligned} \tag{D.15}$$

Since u_0 have support $x \in [-\frac{1}{\sqrt{a}}, \frac{1}{\sqrt{a}}]$ we integrate from x_+ to $x^* = \frac{1}{\sqrt{a}}$ in (D.1)

$$\begin{aligned} \rho(\lambda) &= \lambda^{1/2} x_+(\lambda) + \int_{x_-}^{x^*} dx(\lambda^{1/2} - \sqrt{\lambda^{1/2} - 1 - ax^2}) \\ &= \lambda^{1/2} x_+(\lambda) + \int_{x_-}^{x^*} dx \left[\lambda^{1/2} - (1-\lambda)^{1/2}(\frac{a}{1-\lambda}x^2 - 1)^{1/2}\right] \\ &= \lambda^{1/2} x_+(\lambda) + \int_{x_-}^{x^*} dx \left[\lambda^{1/2} - (1-\lambda)^{1/2}((\frac{x}{x_+})^2 - 1)^{1/2}\right] \end{aligned} \tag{D.16}$$

Make the change of variable $\eta = \frac{x}{x_+}$ and $d\eta = \frac{1}{x_+}dx$

$$\begin{aligned}
\rho(\lambda) &= \lambda^{1/2}x_+ + x_+\int_1^{\frac{1}{\sqrt{1-\lambda}}} d\eta \left[\lambda^{1/2} - (1-\lambda)^{1/2}(\eta^2-1)^{1/2}\right] \\
&= \lambda^{1/2}x_+ + x_+\lambda^{1/2}\int_1^{\frac{1}{\sqrt{1-\lambda}}} d\eta - x_+(1-\lambda)^{1/2}\int_1^{\frac{1}{\sqrt{1-\lambda}}} d\eta(\eta^2-1)^{1/2} \\
&= \lambda^{1/2}x_+ + \frac{x_+\lambda^{1/2}}{(1-\lambda)^{1/2}} - \lambda^{1/2}x_+ - x_+(1-\lambda)^{1/2}\int_1^{\frac{1}{\sqrt{1-\lambda}}} d\eta(\eta^2-1)^{1/2} \\
&= \frac{x_+\lambda^{1/2}}{(1-\lambda)^{1/2}} - x_+(1-\lambda)^{1/2}\frac{1}{2}\left[\frac{\lambda^{1/2}}{1-\lambda} - \log(\frac{1+\lambda^{1/2}}{(1-\lambda)^{1/2}}\right] \\
&= \frac{1}{2\sqrt{a}}\left[\lambda^{1/2} + (1-\lambda)\log(\frac{1+\lambda^{1/2}}{(1-\lambda)^{1/2}}\right] \qquad \text{(D.17)}
\end{aligned}$$

The derivative is

$$\rho'(\lambda) = \frac{1}{2\sqrt{a}}\left[\frac{1}{\lambda^{1/2}} - \log(\frac{1+\lambda^{1/2}}{(1-\lambda)^{1/2}}\right] \qquad \text{(D.18)}$$

From (D.2) we calculate τ

$$\begin{aligned}
\tau(\lambda) &= \int_{x_-}^{x_+} dx\sqrt{1-ax^2-\lambda} \\
&= 2\int_0^{x_+} dx\sqrt{1-ax^2-\lambda} \\
&= 2(1-\lambda)^{1/2}\int_0^{x_+} dx\left[1 - (\frac{\sqrt{a}}{\sqrt{1-\lambda}}x)^{1/2}\right]^{1/2} \\
&= 2(1-\lambda)^{1/2}\int_0^{x_+} dx\left[1 - (\frac{x}{x_+})^{1/2}\right]^{1/2}
\end{aligned}$$

Make the change of variable $\eta = \frac{x}{x_+}$ and $d\eta = \frac{1}{x_+}dx$

$$\begin{aligned}
\tau(\lambda) &= 2x_+(1-\lambda)^{1/2}\int_0^1 d\eta(1-\eta^2)^{1/2} \\
&= \frac{\pi}{2}x_+(1-\lambda)^{1/2} \\
&= \frac{\pi}{2\sqrt{a}}(1-\lambda) \qquad \text{(D.19)}
\end{aligned}$$

The derivative of τ is

$$\tau'(\lambda) = -\frac{\pi}{2\sqrt{a}} \qquad \text{(D.20)}$$

Finally, the breakdown time is calculated

$$\begin{aligned} t^* &= \frac{1}{min_{x\in[0,\frac{1}{\sqrt{a}}]}12ax} \\ &= \frac{1}{12\sqrt{a}} \end{aligned} \tag{D.21}$$

For the parabolic potential it is possible to calculate the integrals in the system determining β_0, using (D.18) and (D.20). For $D(\beta_0)$ we have

$$\begin{aligned} D(\beta_0) &= \int_{\beta_0}^{1} d\mu \frac{-2\tau'(\mu)}{(\mu-\beta_0)^{1/2}} \\ &= \frac{\pi}{\sqrt{a}} \int_{\beta_0}^{1} d\mu \frac{1}{(\mu-\beta_0)^{1/2}} \\ &= \frac{2\pi}{\sqrt{a}} (\mu-\beta_0)^{1/2}\Big|_{\beta_0}^{1} = \frac{2\pi}{\sqrt{a}}(1-\beta_0)^{1/2} \end{aligned} \tag{D.22}$$

$C(\beta_0)$ is determined by

$$\begin{aligned} C(\beta_0) &= \int_0^{\beta_0} d\lambda \frac{2\rho'(\lambda)}{(\beta_0-\lambda)^{1/2}} \\ &= \frac{1}{\sqrt{a}} \int_0^{\beta_0} d\mu \left[\frac{1}{\mu^{1/2}(\beta_0-\mu)^{1/2}} - \frac{1}{(\beta_0-\mu)^{1/2}} \log\left(\frac{1+\mu^{1/2}}{(1-\mu)^{1/2}}\right)\right] \\ &= \frac{1}{\sqrt{a}} [C_1 + C_2] \end{aligned} \tag{D.23}$$

We have

$$C_1 = \int_0^{\beta_0} d\mu \left[\frac{1}{\mu^{1/2}(\beta_0-\mu)^{1/2}} \right] = \pi \tag{D.24}$$

and C_2

$$-C_2 = \left[\frac{1}{(\beta_0-\mu)^{1/2}} \log\left(\frac{1+\mu^{1/2}}{(1-\mu)^{1/2}}\right)\right] \tag{D.25}$$

set $u = \log(\frac{1+\mu^{1/2}}{(1-\mu)^{1/2}}$ and $dv = \frac{d\mu}{(\beta_0-\mu)^{1/2}}$ and use integration by parts

$$-C_2 = uv\Big|_0^{\beta_0} - \int_0^{\beta_0} duv \tag{D.26}$$

we have $v = -2(\beta_0 - \mu)^{1/2}$ and

$$\begin{aligned} du &= u' d\mu \\ &= \frac{(1-\mu)^{1/2}}{1+\mu^{1/2}} \frac{\frac{1}{2\mu^{1/2}}(1-\mu)^{1/2} - (1+\mu^{1/2})(-\frac{1}{2(1-\mu)^{1/2}})}{(1-\mu)} \\ &= \frac{1}{2}\left[\frac{1}{\mu^{1/2}(1+\mu^{1/2})} + \frac{1}{1-\mu}\right] \end{aligned} \tag{D.27}$$

then

$$\begin{aligned} uv\Big|_0^{\beta_0} &= -2(\beta_0 - \mu)\log(\frac{1+\mu^{1/2}}{(1-\mu)^{1/2}}\Big|_0^{\beta_0} \\ &= 0 \end{aligned} \tag{D.28}$$

and

$$-\int_0^{\beta_0} duv = \int_0^{\beta_0} d\mu(\beta_0 - \mu)^{1/2}\left[\frac{1}{\mu^{1/2}(1+\mu^{1/2})} + \frac{1}{1-\mu}\right] \tag{D.29}$$

Both of these integrals can be calculated, the first

$$\int_0^{\beta_0} d\mu \frac{(\beta_0 - \mu)^{1/2}}{\mu^{1/2}(1+\mu^{1/2})} = \pi - 2\beta_0^{1/2} - 2(1-\beta_0)^{1/2}\cos^{-1}(\beta_0^{1/2}) \tag{D.30}$$

the second

$$\int_0^{\beta_0} d\mu \frac{(\beta_0 - \mu)^{1/2}}{1-\mu} = 2\beta_0^{1/2} - 2(1-\beta_0)^{1/2}\arctan\left[\frac{\beta_0^{1/2}}{(1-\beta_0)^{1/2}}\right] \tag{D.31}$$

combining all quantities gives us $C(\beta_0)$ for the parabolic potential

$$C(\beta_0) = \frac{2}{\sqrt{a}}(1-\beta_0)^{1/2}\left[\cos^{-1}(\beta_0^{1/2}) + \arctan\left(\frac{\beta_0^{1/2}}{(1-\beta_0)^{1/2}}\right)\right] \tag{D.32}$$

D.3 Algebraic

The algebraic potential is defined as

$$u_0(x) = \frac{1}{1+x^2} \tag{D.33}$$

and plotted in figure (D.2). For this case we have turning points

$$\begin{aligned} \frac{1}{1+x^2} &= \lambda \\ 1 + x^2 &= \frac{1}{\lambda} \\ x_\pm &= \pm(\frac{1-\lambda}{\lambda})^{1/2} \end{aligned} \tag{D.34}$$

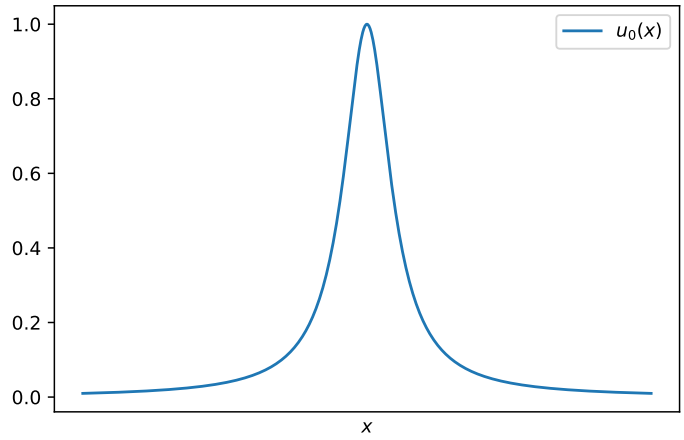

Figure D.2: Shape of algebraic potential function $u_0(x)$ defined in (D.33).

Using this in (D.1) gives us

$$\begin{aligned}
\rho(\lambda) &= \lambda^{1/2}(\frac{1-\lambda}{\lambda})^{1/2} + \int_{(\frac{1-\lambda}{\lambda})^{1/2}}^{\infty} dx \left[\lambda^{1/2} - (\lambda - \frac{1}{1+x^2})^{1/2}\right] \\
&= (1-\lambda)^{1/2} + \int_{(\frac{1-\lambda}{\lambda})^{1/2}}^{\infty} dx \left[\lambda^{1/2} - (\frac{\lambda + \lambda x^2 - 1}{1+x^2})^{1/2}\right] \\
&= (1-\lambda)^{1/2} + \int_{(\frac{1-\lambda}{\lambda})^{1/2}}^{\infty} dx \left[\frac{1}{x_+} - \left(\frac{(\frac{x}{x_+})^2 - 1}{x^2+1}\right)^{1/2}\right], \eta = \frac{x}{x_+} \\
&= (1-\lambda)^{1/2} + \int_{1}^{\infty} d\eta \left[1 - \left(\frac{\eta^2 - 1}{\eta^2 + \gamma}\right)^{1/2}\right], \gamma = \frac{1}{x_+^2} \\
&= (1-\lambda)^{1/2} E(\frac{\lambda}{\lambda - 1})
\end{aligned} \tag{D.35}$$

with derivative

$$\rho'(\lambda) = \frac{1}{2}\frac{1}{\lambda^{1/2}(1-\lambda)^{1/2}}\left[(1-\lambda)E(\frac{\lambda}{\lambda-1}) - K(\frac{\lambda}{\lambda-1})\right] \tag{D.36}$$

For τ we get

$$\begin{aligned}\tau(\lambda) &= 2\int_0^{x_+} dx \left[\frac{1}{1+x^2} - \lambda\right]^{1/2} \\ &= 2\int_0^{x_+} dx \left[\frac{1-\lambda-\lambda x^2}{1+x^2}\right]^{1/2} \\ &= 2(1-\lambda)^{1/2}\int_0^{x_+} dx \left[\frac{1-\eta^2}{\gamma+\eta^2}\right]^{1/2} \\ &= \frac{2(1-\lambda)^{1/2}}{\lambda^{1/2}} \frac{(1+\gamma)K(-\frac{1}{\gamma}) - \gamma E(-\frac{1}{\gamma})}{\gamma^{1/2}} \\ &= \frac{2}{\lambda^{1/2}}\left[K(1-\frac{1}{\lambda}) - \lambda E(1-\frac{1}{\gamma})\right] \end{aligned} \tag{D.37}$$

and

$$\tau'(\lambda) = -\frac{1}{\lambda^{1/2}} E(1-\frac{1}{\lambda}) \tag{D.38}$$

Where $K(z)$ and $E(z)$ denotes the complete elliptic integrals of first and second kind. We now calculate the breaking time t^*, we have the derivative of the potential

$$u_0'(x) = -\frac{2x}{(1+x^2)^2} \tag{D.39}$$

Time must be positive so we must have

$$u_0'(x) < 0 \iff x > 0 \tag{D.40}$$

The minimal time must then be

$$\begin{aligned} t^* &= min_{x>0}\left[\frac{(1+x^2)^2}{12x}\right] \\ &= min_{x>0} g(x) \end{aligned} \tag{D.41}$$

We have the limit

$$\lim_{x\to 0} \frac{(1+x^2)^2}{12x} = \infty \tag{D.42}$$

and

$$\lim_{x\to \infty} \frac{(1+x^2)^2}{12x} = \infty \tag{D.43}$$

Then there should exist a minimum point such that $g'(x^*) = 0, x \in (0,\infty)$

$$g'(x) = \frac{1+x^2}{12x^2}(3x^2-1) \tag{D.44}$$

This gives $x^* = \frac{1}{\sqrt{3}}$ and the breaking time is

$$t^* = g(x^*) = \frac{4\sqrt{3}}{27} \tag{D.45}$$

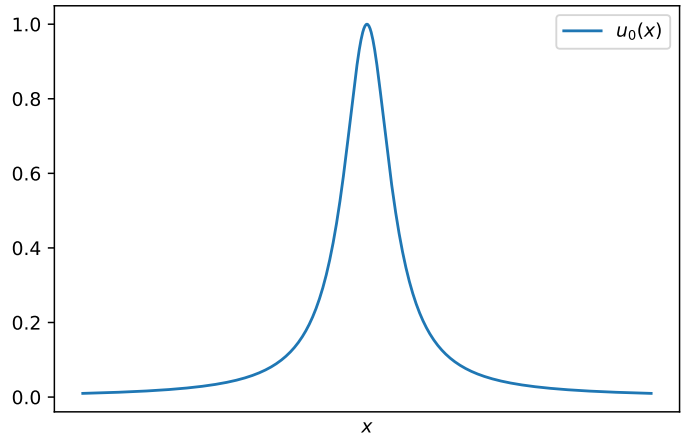

Figure D.3: Shape of secant potential function $u_0(x)$ defined in (D.46).

D.4 Secant

The secant potential is defined as

$$u_0(x) = \frac{1}{\cosh(x)} \tag{D.46}$$

We generically write the turning points as

$$x_\pm = \pm(\cosh^{-1}(x))^{-1} \tag{D.47}$$

Inserting into formula (D.1)

$$\begin{aligned}\rho(\lambda) = \lim_{\epsilon\to 0^+}\Bigg[&\lambda^{1/2}\log(\frac{1}{\epsilon}(\frac{1-\lambda}{\lambda})^{1/2} - 2i(1-\lambda)^{1/2}\Bigg(F(\sin^{-1}((1-\lambda)^{1/2}), \frac{2}{1-\lambda}) \\ &- K(\frac{2}{1-\lambda}) + \frac{\lambda}{1-\lambda}\left(\Pi(\frac{1}{1-\lambda}, \sin^{-1}((1-\lambda)^{1/2}) + \epsilon, \frac{2}{1-\lambda}\right) \\ &- \Pi(\frac{1}{1-\lambda}, \frac{2}{1-\lambda})\Bigg)\Bigg]\end{aligned} \tag{D.48}$$

where F is the incomplete integral of first kind, and Π is the elliptic integral of third kind(both complete and incomplete). The derivative is too long to write down, but it is possible to find using (D.48). For τ we have

$$\begin{aligned}\tau(\lambda) &= 2\int_0^{x_+} dx\left[\frac{1}{\cosh(x)} - \lambda\right]^{1/2} \\ &= Re\left[\frac{4}{(1-\lambda)^{1/2}}\left((1-\lambda)K(\frac{2}{1-\lambda}) + \lambda\Pi(\frac{1}{1-\lambda}, \frac{2}{1-\lambda})\right)\right]\end{aligned} \tag{D.49}$$

with derivative

$$\tau'(\lambda) = Re\left[-\frac{2}{(1-\lambda)^{1/2}}\left(K(\frac{2}{1-\lambda}) - \Pi(\frac{1}{1-\lambda}, \frac{2}{1-\lambda})\right)\right] \tag{D.50}$$

To find the breaking time we calculate $u_0' = -\frac{\sinh(x)}{\cosh(x)}$ and the condition $u_0' < 0$ gives $x > 0$. Thus

$$\begin{aligned} t^* &= min_{x>0}\left[\frac{\cosh^2(x)}{6\sinh(x)}\right] \\ &= min_{x>0} g(x) \end{aligned} \tag{D.51}$$

The limits

$$\begin{aligned} \lim_{x\to 0} g(x) &= \infty \\ \lim_{x\to\infty} g(x) &= \infty \end{aligned} \tag{D.52}$$

indicates we must have a point $g'(x^*) = 0$

$$\begin{aligned} g'(x) &= 0 \\ \cosh(x) - \frac{\cosh(x)}{\sinh(x)} &= 0 \\ x &= \sinh^{-1}(1) = x^* \end{aligned} \tag{D.53}$$

The breaking time is then

$$t^* = \frac{\cosh^2(x^*)}{6\sinh(x^*)} = \frac{1}{3} \tag{D.54}$$

Bibliography

[1] Mark J. Ablowitz. *Nonlinear Dispersive Waves: Asymptotic Analysis and Solitons*. Cambridge Texts in Applied Mathematics. Cambridge University Press, 2011.

[2] Mark J. Ablowitz, David J. Kaup, Alan C. Newell, and Harvey Segur. The inverse scattering transform-fourier analysis for nonlinear problems. *Studies in Applied Mathematics*, 53(4):249–315.

[3] M. Abramowitz and I. Stegun. *Handbook of Mathematical Functions*. Dover Publications, 1965.

[4] George E Andrews. *Special functions*, volume vol. 71 of *Encyclopedia of mathematics and its applications*. Cambridge University Press, Cambridge, 1999.

[5] S. A. Orszag C. Bender. *Advanced Mathematical Methods for Scientists and Engineers*. McGraw-Hill, Inc, 1978.

[6] Stefano Carrazza and Daniel Krefl. openRT: Open source implentation of the riemann-theta function for Python, 2017–. [https://github.com/RiemannAI/openRT].

[7] P. Deift, S. Venakides, and X. Zhou. New results in small dispersion kdv by an extension of the steepest descent method for riemann-hilbert problems. *International Mathematics Research Notices*, 1997(6):285–299, 1997.

[8] Richard P Feynman. *The Feynman lectures on physics : Vol. 3 : Quantum mechanics*, volume Vol. 3. Addison-Wesley, Reading, Mass, 1965.

[9] Clifford S. Gardner, John M. Greene, Martin D. Kruskal, and Robert M. Miura. Method for solving the korteweg-devries equation. *Phys. Rev. Lett.*, 19:1095–1097, Nov 1967.

[10] Milan Wayne Garrett. Calculation of fields, forces, and mutual induc-

tances of current systems by elliptic integrals. *Journal of Applied Physics*, 34(9):2567–2573, 1963.

[11] David J. Griffiths. *Introduction to quantum mechanics*. Pearson/Prentice Hall, Upper Saddle River, N.J, 2nd ed. edition, 2005.

[12] John K Hunter. *Applied analysis*. World Scientific, Hackensack, N.J, 2001.

[13] Wolfram Research, Inc. Mathematica, Version 11.3. Champaign, IL, 2018.

[14] P. Jakobsen. Introduction to the method of multiple scales. *ArXiv e-prints*, December 2013.

[15] P. Jakobsen and J.V. Moloney. Modelling mid-infrared optical pulse propagation using spee. *Tucson Seminar on Long Wave Optics*, 2015.

[16] Fredrik Johansson et al. mpmath: A Python library for arbitrary-precision floating-point arithmetic, 2007–. [http://mpmath.org/].

[17] Eric Jones, Travis Oliphant, Pearu Peterson, et al. SciPy: Open source scientific tools for Python, 2001–. [http://www.scipy.org/].

[18] M Kolesik and J V Moloney. Modeling and simulation techniques in extreme nonlinear optics of gaseous and condensed media. *Reports on Progress in Physics*, 77(1):016401, 2014.

[19] Dr. D. J. Korteweg and Dr. G. de Vries. Xli. on the change of form of long waves advancing in a rectangular canal, and on a new type of long stationary waves. *The London, Edinburgh, and Dublin Philosophical Magazine and Journal of Science*, 39(240):422–443, 1895.

[20] A. S. Fokas M. J. Ablowitz. *Complex Variables: Introduction and Applications*. Cambridge University Press, 1997.

[21] Robert M. Miura. Korteweg-de vries equation and generalizations. i. a remarkable explicit nonlinear transformation. 9:1202–1204, 08 1968.

[22] Alan C. Newell. The general structure of integrable evolution equations. *Proceedings of the Royal Society of London A: Mathematical, Physical and Engineering Sciences*, 365(1722):283–311, 1979.

[23] Alan C Newell. *Nonlinear optics*. Advanced topics in the interdisciplinary mathematical sciences. Addison-Wesley, Redwood City, Calif, 1992.

[24] Tenio Popmintchev, Ming-Chang Chen, Dimitar Popmintchev, Paul Arpin, Susannah Brown, Skirmantas Ališauskas, Giedrius Andriukaitis, Tadas Balčiunas, Oliver D. Mücke, Audrius Pugzlys, Andrius Baltuška, Bonggu Shim, Samuel E. Schrauth, Alexander Gaeta, Carlos Hernández-García, Luis Plaja, Andreas Becker, Agnieszka Jaron-Becker, Margaret M. Murnane, and Henry C. Kapteyn. Bright coherent ultrahigh harmonics in the kev x-ray regime from mid-infrared femtosecond lasers. *Science*, 336(6086):1287–1291, 2012.

[25] A. B. Shabat. Problems in mechanics and mathematical physics. 1976.

[26] C. Swierczewski et al. Abelfunctions: A library for computing with abelian functions, riemann surfaces, and algebraic curves, 2017. [https://github.com/abelfunctions/abelfunctions].

[27] Michael Wheeler. An introduction to riemann-hilbert problems and their applications, 2005.

[28] N. J. Zabusky and M. D. Kruskal. Interaction of "solitons" in a collisionless plasma and the recurrence of initial states. *Phys. Rev. Lett.*, 15:240–243, Aug 1965.